DOE/ER/13795--T1

DOE-DE-FG05-87ER13795

Isotopic and trace element characteristics of rhyolites from the Valles Caldera, New Mexico

Final Technical Report

Stephen Self[1], John A. Wolff, Martha L. Sykes[1] and Cherylyn E. Skuba[2]

Department of Geology
The University of Texas at Arlington
UTA Box 19049
Arlington, TX 76019

September 1991

Prepared for the U.S. Department of Energy under grant number DE-GE05-87ER13795

[1]now at: Department of Geology and Geophysics, University of Hawaii at Manoa, 2525 Correa Road, Honolulu, HI 96822

[2]now at: Department of Geology, McMaster University, 1280 Main Street West, Hamilton, Ontario L8S 4MI, Canada

Contents

List of figures

List of Tables

Preamble

This report is a summary of work supported by DOE grant #DE-FG05-87ER13795 that was completed or is still in progress; it is intended to highlight results from work published in journals and as abstracts. The stated purpose of this grant was to collect geochemical information (trace element, radiogenic isotope and stable oxygen and hydrogen isotope) on samples from core holes VC-1 and VC-2a in the Valles caldera in order to establish a consistent detailed intracaldera stratigraphy and relate this to extracaldera volcanic rock units of the Jemez Mountains. Careful stratigraphic control of the intracaldera units is necessary to evaluate models of caldera formation, ignimbrite deposition, and resurgence. Combined stable and radiogenic isotope and trace element data will also provide major insights to petrogenesis of the Bandelier magma system. The composition of non-hydrothermally altered samples from outflow units of the Bandelier Tuff and related volcanics must be known to assess isotopic variations of intracaldera ignimbrite samples.

On detailed examination of the VC-2a core samples, it became apparent that hydrothermal alteration is so extensive (e.g., Hulen et al., 1987) that no geochemical information useful for stratigraphic fingerprinting or petrogenesis could be obtained, and that correlation with other intracaldera units and extracaldera units must be made on the basis of stratigraphic position and gross lithologic characteristics. Accordingly, we emphasize geochemical data from the extracaldera Bandelier Tuffs and related units which will be useful for comparison with proposed drill hole VC-4 and for any future studies of the region. The stable isotope, radiogenic isotope and trace element data obtained from this project (summarized in this report and the appendices), combined with existing major and trace element data for volcanic rocks from this area, provide an extensive data base essential to future Continental Scientific Drilling Program projects in the Jemez Mountains of New Mexico.

Some studies were made during the time scale of this grant that follow on from a related and previously funded project on the Valles Caldera VC-1 core (DOE#DE-FG05-85ER13413, *Volcanological Investigation of the Banco Bonito Eruption and Subsurface Geology of the Ring Fracture Zone, Valles Caldera, New Mexico*). As these results are of immediate interest, they are included here as the first part of the report.

Part I. Results of studies on the VC-1 core hole and related rocks

Introduction

The volcanic section of the VC-1 core hole, located in the moat region of the Valles caldera, was originally identified as containing units as old as the Otowi Member of the Bandelier Tuff (1.51 Ma) (Gardner et al., 1986), but this was later corrected to recognize that all the units were younger than *c.* 0.5 Ma (Goff and Gardner, 1987). The latter designation of units in the VC-1 core was adopted by Self et al. (1988) in a paper interpreting the stratigraphic and volcanic significance of the cored units. However, results following publication of Self et al. (1988) and the report on our previous DOE grant (Self et al., 1987), necessitate further changes in the interpretation of the volcanic rocks of the VC-1 core hole and are summarized below. These new results have also been published in Self et al. (1991). A stratigraphic summary of the Jemez Volcanic Field is given in Table 1.

Background

Three surface-exposed units have previously been recognized as the products of the youngest phase of volcanism from the Valles Caldera in north-central New Mexico (Self et al., 1988). We proposed that the lowermost two units, the El Cajete (EC) pumice deposit and the Battleship Rock (BR) ignimbrite were erupted some time before the third unit, the Banco Bonito (BB) obsidian flow, as parts of a single lengthy eruptive episode. Reexamination of the CSDP VC-1 core (location 2 on Fig. 1), additional field data, new $^{40}Ar/^{39}Ar$ age determinations, and reinterpretation of our previously published ages for rhyolites younger than ~ 500 ka demonstrate that:

1. The Banco Bonito lava was in fact produced by a distinct eruption later than the EC-BR sequence, and the lava is underlain by a related, thin non-welded pyroclastic flow deposit in

2. Another lava flow, known only in the subsurface, the VC-1 Rhyolite (VC1R; Goff et al., 1986), was produced at the end of the EC-BR eruptive sequence.

3. The so-called VC-1 Tuffs (Goff et al., 1986; Goff and Gardner, 1987), previously thought to occur only in the subsurface, can be shown to be correlative with the BR ignimbrite.

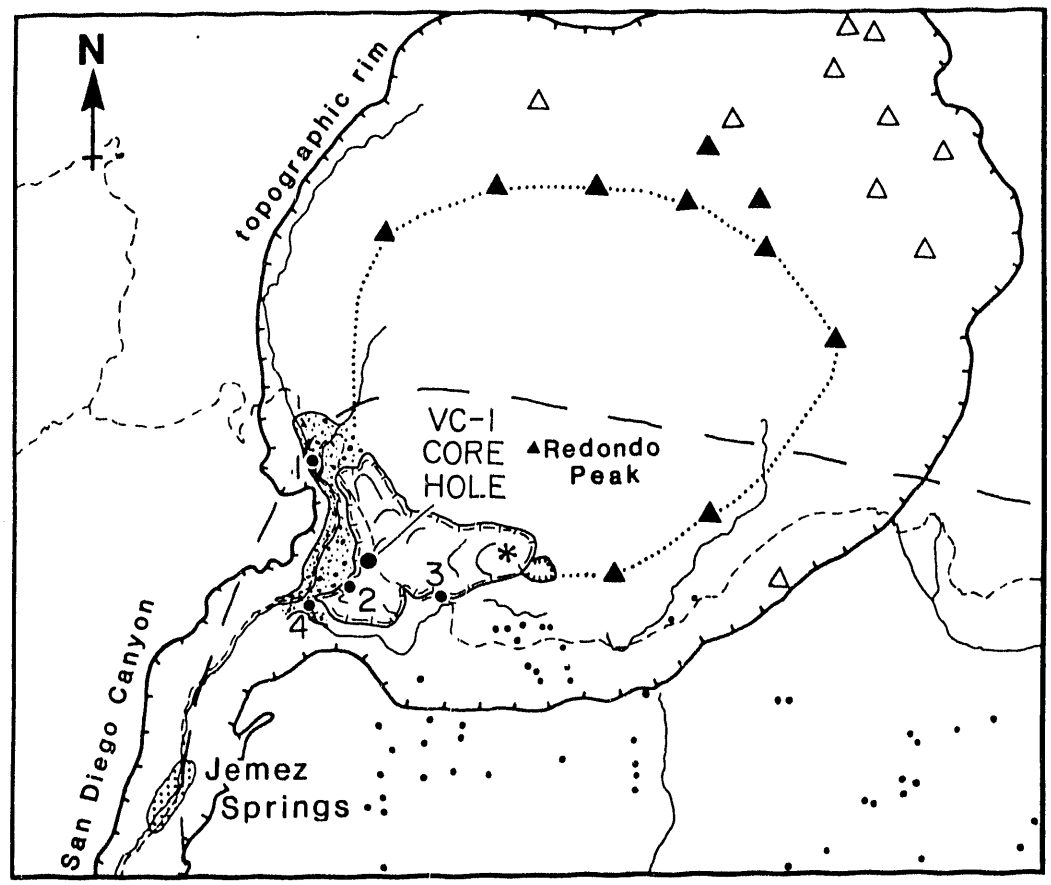

Fig. 1. Location map showing site of VC-1 and sampling localities in the SW part of the Valles Caldera and upper San Diego Canyon. Star marks vent position of Banco Bonito lava. "Pumice" ornament indicates extent of Battleship Rock ignimbrite. Dots: locations of measured sections in the El Cajete fallout deposit. Filled triangles: vent positions for Valle Grande Member rhyolite domes, which serve to locate the position of the ring fracture (dotted line). Open triangles: vent positions for Cerro Toledo rhyolite domes.

This report presents field relationships upon which the revised stratigraphy is based, new $^{40}Ar/^{39}Ar$ age data, microscopic and macroscopic descriptions of core samples, and a summary of the significance of the new finds. The stratigraphy of core hole VC-1 is presented in Fig. 2.

Stratigraphy of VC-1

Our reinterpretation of the volcanic section of the VC-1 core (Fig. 3) is based upon close inspection of hand sample textures and petrographic examination, with supporting data from new field work. A detailed log to the VC-1 core is given in Appendix 1A. Differences with respect to earlier interpretations (Goff et al., 1986; Goff and Gardner, 1987; Goff et al., 1988; Self et al., 1988) are discussed below.

Samples and depths from the VC-1 core given in this report are based on examination of the core by S. Self at the DOE Grand Junction core storage facility in May, 1988, about four years after completion of the hole. Five major discrepancies between our observations and the previously published core lithology and stratigraphy are as follows:

1. The interval from 148.8-154.0 m (488.2-505.1 ft) consists of a pumiceous breccia at the base of the BB lava conformably overlying a thin, nonwelded pyroclastic flow deposit between 154.0-158.5 m (505.1-520.0 ft). The flow deposit contains abundant pumice clasts and andesite lithics and is interpreted to be the result of explosive activity prior to or associated with effusion of the lava flow. This section of core was previously described as containing the BR ignimbrite (Gardner et al., 1987).

2. Under the pyroclastic flow deposit at 158.5 m (520.0 ft) in the core is a paleosol, which was recognized in previous studies. It overlies the pumiceous top of a glassy rhyolite lava (160.0-179.9 m; 524.8-590.1 ft), the VC-1 Rhyolite of Goff et al. (1988). Biotite from the lava was dated by K/Ar at 356±61 ka (Gardner et al., 1986; this date was erroneously reported as 365+61 ka by Goff et al., 1986). At the time this date was obtained, an age of 356 ka was thought to be significantly older than the accepted age of the BR and EC deposits. Therefore, VC1R and the underlying VC-1 Tuffs were considered to be related units produced by an earlier eruptive event. The VC1R is here interpreted to be the result of an effusive phase following deposition of the BR ignimbrite. It remains unrecognized in surface outcrop. The petrography and

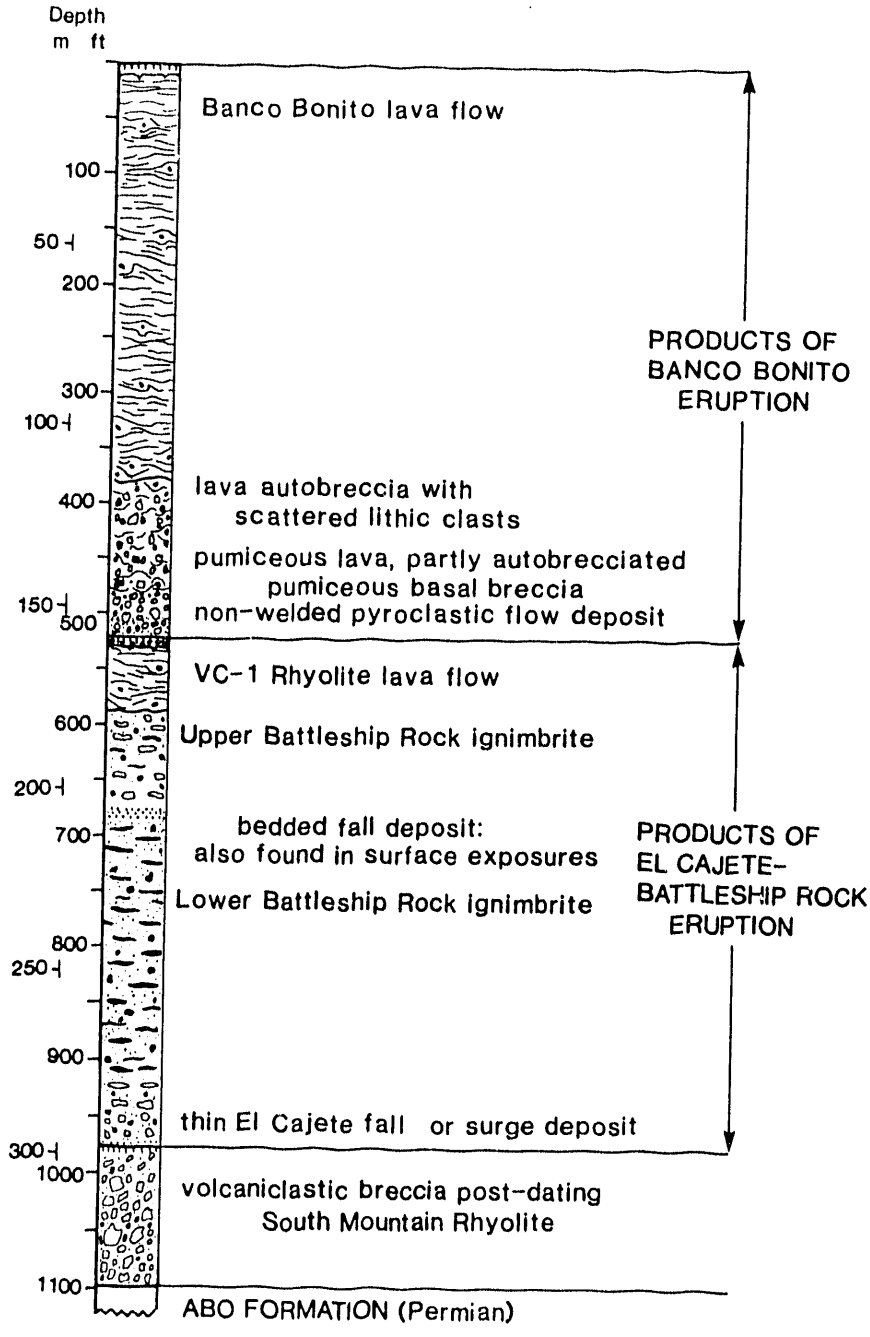

Fig. 2. Preferred interpretation of the stratigraphy of corehole VC-1.

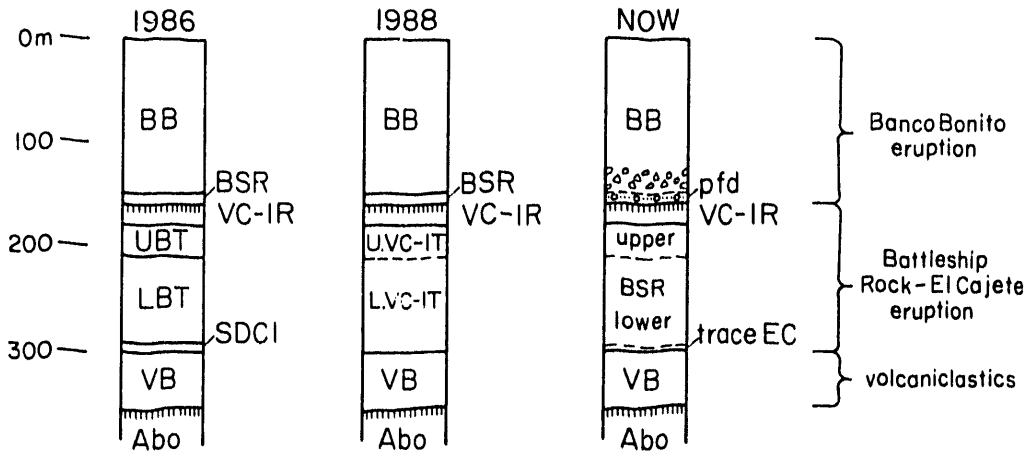

Fig. 3. Comparison of the present interpretation of VC-1 with the earlier schemes of Goff et al. (1986) and Self et al. (1988).

chemistry of this lava (Spell, 1987; Spell and Kyle, 1989) are very similar to the BR ignimbrite, EC pumice, and BB obsidian (Gardner et al., 1986).

3. VC1R rests conformably on a thick ignimbrite (179.9-298.2 m; 590.1-978.3 ft), previously called the VC-1 Tuffs (Goff and Gardner, 1987). The 118 m (387 ft) thickness of this ignimbrite in the core is similar to exposed thicknesses of BR ignimbrite near the core hole site (Self et al., 1988). The petrographic and compositional similarity of the VC-1 Tuffs to the BR ignimbrite has already been noted (Gardner et al., 1986). We reinterpret the VC-1 Tuffs as the subsurface equivalent of the Battleship Rock ignimbrite. As described below, field exposures of the BR ignimbrite correlate well with the cored sequence of VC-1 Tuffs. Correlation of VC-1 Tuffs and BR ignimbrite permits a revision of the age of the BR ignimbrite and the related EC pumice deposit.

4. At the base of the BR section in VC-1 at 298.0 m (977.7 ft) is a thin (3-4 cm), moderately well-sorted pumiceous layer containing traces of carbonized material that we interpret as an EC fall or surge deposit. It cannot be positively correlated to any one of the fall or surge units in the EC key section (Self et al., 1988).

5. Under the BR-EC units is a heterolithologic volcanic breccia composed of clasts of South Mountain Rhyolite lava (Ar/Ar age 529 ka; Spell and Harrison, in press) and other local lithologies in a fine matrix. This is the lowest unit containing volcanic rocks in the VC-1 core hole.

The reinterpreted VC-1 core stratigraphy correlates convincingly with nearby exposures (Fig. 4). In particular, the exposure of EC pumice and BR ignimbrite at La Cueva (locality 1 on Fig. 1) has not been described before (see Self et al., 1991, their fig. 4). A prominent parting in the BR section here is interpreted as a hiatus in BR deposition, and therefore a flow unit boundary. This hiatus is also recognized in the VC-1 core at 206.1 m (676.2 ft), and is also exposed near Battleship Rock (Self et al., 1988, their fig. 10), where it was previously interpreted as an erosion surface marking the contact between BR ignimbrite and VC-1 Tuffs.

Paleomagnetic data, summarized in Self et al. (1991), also supports the revised stratigraphy.

The reinterpreted sequence of events simplifies the record of deposition at the VC-1 core site and removes the need for the complex deposit geometries implied by the

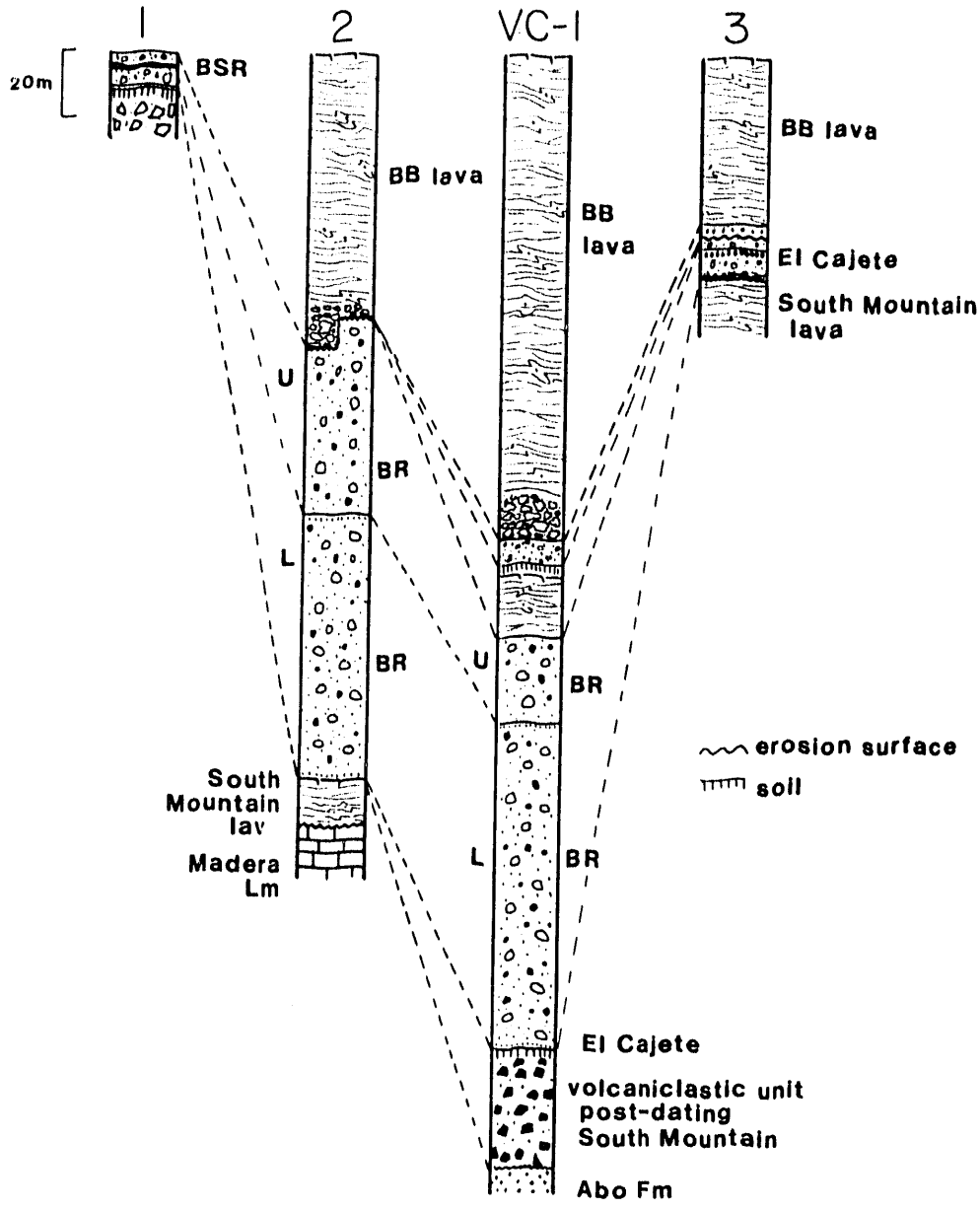

Fig. 4. Correlation of the VC-1 core with nearby exposures. Locations 1 - 3 are shown on Fig. 1.

presence of older VC-1R and VC-1 Tuffs in relationship to surrounding surface exposures. It also implies that the EC pumice fall was largely deposited before the BR ignimbrite and that the two were produced by the same eruptive event, which also yielded the VC1R.

Ages

Obtaining realistic age determinations of these units has been extremely difficult (see discussion in Self et al., 1991). New $^{40}Ar/^{39}Ar$ age determinations for the BB lava and EC pumice deposit (summarized in Self et al., 1991) obtained by laser fusion of biotite crystals suggest that the BB lava erupted after a short hiatus following the EC-BR-VC1R event. Dates for the BB lava (n=9) range from 205±34 ka to 1.300±0.062 ma. Four dates from EC pumices range from 519±101 ka to 923±81 ka. The data suggest either that biotites from these units have incorporated variable amounts of excess ^{40}Ar, or have a xenocrystic origin. The youngest dates obtained should be regarded as potential maximum ages for the Banco Bonito lava; thus the BB may be about 200,000 years old or less.

Based on previously reported U-Th and K-Ar analyses (see Self et al., 1988) and on stratigraphic relations with other dated units, the age of the EC, BR, and VC-1R event is considered to be ~300-350 ka. $^{40}Ar/^{39}Ar$ determinations on the EC and BR do not affect this interpretation. Table 1 of Self et al. (1988) included a U-Th disequilibrium age of 151 ka on pumice from the lower part of the EC which unfortunately was in error (M. Ivanovich, personal communication, 1988). The isochron obtained actually indicates that the data obtained by the U-Th method has no age significance and may be the result of some complex mixing process that produced the magma batch. Therefore at present we have no direct geochronologic constraints to suggest that the EC pumice deposit, the BR ignimbrite, and the VC-1 Rhyolite are part of the same eruptive sequence. However, it is strongly supported by the contacts of the units in the core and by field relationships. The younger limit of $^{40}Ar/^{39}Ar$ ages for the BB lava suggests that the BB lava was erupted somewhat later than the EC-BR-VC1R group. The minimum duration of this time interval, based on the present data, is about 30 ka.

Thus a poorly constrained but short interval separates the eruptive event that formed the EC, BR, and VC-1R from the Banco Bonito eruption. The erosion surface at the base of the BB lava and between El Cajete unit I and unit J (Self et al., 1988) was formed during this interval, as was the paleosol at 158.5 m (520.0 ft) in the VC-1 core. Units J and K of Self et al. (1988), lying above the erosion surface, were produced during the Banco Bonito event and are thus not part of the EC-BR-VC-1R eruption sequence.

Macroscopic descriptions of eruptive units

Products of the Banco Bonito eruption

The Banco Bonito vitrophyric rhyolite consists of about 0.9 km^3 of lava with minor pyroclastic, autoclastic, and epiclastic deposits. The lowermost unit of this group of deposits, both in exposure and in the VC-1 core, is a fines-poor pyroclastic flow deposit containing white pumice and denser gray juvenile clasts of similar appearance to the BB lava. About 1 m is exposed in the main EC road cut section, where it was designated unit J (Self et al., 1988). Some 4.5 m (15 ft) of similar material occurs in the VC-1 core, where pumice clasts are up to 4 cm in diameter and lithics, including those of welded Bandelier Tuff and Paliza Canyon andesite, are up to 8 cm. In field exposures a unit occurs above the pyroclastic flow, and this is interpreted to be an autoclastic deposit derived from the front of the lava flow, with possible fluvial reworking; it is absent from the core.

Only one flow unit of the BB lava flow is present down to 110 m (360.0 ft), in agreement with Manley and Fink (1987). This thick flow unit is underlain by a 30 m thick lava autobreccia. The lowermost 12 m of the lava is moderately pumiceous and is underlain by 5.2 m of pumiceous basal breccia. The lower 30 m of the lava breccia contains sparse small lithic clasts.

Products of the El Cajete-Battleship Rock eruption

El Cajete pumice deposit

A thin-bedded, 42 cm thick sequence of EC fall deposits underlies nonwelded BR ignimbrite at La Cueva, extending the upwind limit of EC fallout from that shown in Self et al. (1988). The sequence includes pumice fall units B, D, and F, and fine ashes that are interpreted as co-ignimbrite ash falls. New data on thickness and stratigraphy of the EC pumice deposit have been obtained in proximal areas from corings made during exploration for commercial deposits of pumice. The improved isopach map (Self et al., 1991) allows a more accurate volume to be calculated. Using the method of Pyle (1989) a bulk volume of 2.6 km^3 is obtained. This is somewhat smaller that the volume given in Self et al. (1988) and suggests that only about 0.8 km^3 of magma was erupted during the EC plinian phase.

Detailed correlations of field occurrences of the EC fall and flow units corroborate the sequence and distribution of units described by Self et al. (1988); see fig. 6 of Self et al., 1991).

Battleship Rock Ignimbrite

The BR ignimbrite is typically 100-120 m thick in exposures in San Diego Canyon. Only the lower 60 m is exposed at the type locality of Battleship Rock. An eruptive break separates this ignimbrite into two cooling units; the prominent "prow" of Battleship Rock itself lies within the lower cooling unit. At La Cueva the cooling unit break is marked by a layer of carbonaceous silty material deposited fluvially on the lower flow unit. This carbonaceous material probably represents vegetation burned by earlier pyroclastic flows and surges then washed into the caldera moat from adjacent high ground.

In the VC-1 core, this eruption hiatus is represented at 205.6 m (674.5 ft) depth by about 30 cm of bedded secondary lithic-rich pyroclastic fall or surge deposits containing rounded, moderately well-sorted pumice and dense juvenile clasts. A similar deposit occurs in a canyon north of Battleship Rock. There the deposits rest on the compactional surface of the lower BR that dips gently away from the paleocanyon walls and is occasionally gullied with a relief of 10-15 cm. Gullies run normal to the paleovalley axis.

A thin pumice-rich flow unit occurs beneath the deposits marking the hiatus in the VC-1 core (206.7-210.9 m depth; 678.4-691.9 ft). Other flow units occur beneath this level in the VC-1 core, but flow unit boundaries are more difficult to interpret than in field exposures. In the field, the lower cooling unit of the BR ignimbrite contains at least six flow units, the upper cooling unit contains five, hence the whole BR ignimbrite is a compound cooling unit of at least 11 flow units.

Prominent rosettes of columnar joints occur at the base of the BR ignimbrite at the type section. These have been previously described as due to cooling of the ignimbrite in proximity to canyon walls. Another basal exposure (Self et al., 1988, their fig. 12) rests against a paleocanyon wall about 200 m west of the main type section , implying that the rosettes did not form near a paleocanyon wall. We suggest that they formed in response to fumaroles in the ignimbrite, similar to those described from the Bishop Tuff by Sheridan (1970).

VC-1 Rhyolite Lava

The VC-1R lava is an apparently canyon-confined, single flow unit of vitrophyre about 22.8 m thick. The vent for this flow has not yet been located.

Volcaniclastic unit

At the base of the volcanic section of the VC-1 core underlying the EC-BR units in the VC-1 core and beneath a thick paleosol at 298 m (977.7 ft) is a very heterogeneous unit extending from 300.0-334.5 m (984.3-1097.4 ft). This unit has an ashy matrix, and a

prominent clay layer at 305.0 m (1000.7 ft). Clasts of South Mountain Rhyolite, Bandelier Tuff, Paliza Canyon andesite, and Permian red sandstone (Abo Formation) occur in chaotic relationship with other lithologies, including a pyroclastic flow deposit containing South Mountain rhyolite clasts. At least part of this unit may be a slump or rock slide, most likely derived from the Valles caldera wall which is presently 2.5 km to the south and 1.6 km to the west of the VC-1 core site. Slumping post-dated eruption of the South Mountain lava.

Summary of microscopic properties of eruptive units from VC-1 core samples

Details of hand sample and thin section descriptions of the VC-1 core are given in Appendix 1B.

Banco Bonito lava flow and related deposits

This vitrophyric rhyolite contains a whole range of lava types from dense glass to pumice. The latter is particularly prominent where it occurs as an agglutinated breccia at 497.5 ft. The rhyolite appears unaltered, and has both clear and tan glass components. Crystal clots of plagioclase, hornblende, biotite and pyroxene are associated with the tan glass component; these minerals also occur singly. Hornblende partly replaces biotite. Occasional quartz crystals have patchy, undulose extinction. Both alkali feldspar and plagioclase show disequilibrium textures.

Beneath the lava flow is a partly lithic-rich (30-40%), non- to moderately welded pyroclastic flow unit. Fresh glass is generally clear but some tan glass also appears. Crystals include alkali feldspar, plagioclase, biotite flakes, hornblende and rare quartz. Plagioclases are wormy and resorbed. Glass in pumices is fresh, but the matrix is incipiently devitrified. A recurrent lithic type is a dense, welded reddish ignimbrite containing spherulitically devitrified pumices.

VC-1 Rhyolite Lava Flow

A dense rhyolitic vitrophyre flow with a pumiceous carapace, the VC-1R contains sparse crystals of resorbed/wormy plagioclase and alkali feldspar, biotite flakes, and small hornblende crystals and opaques. Some flow banding occurs, prominent in places.

Battleship Rock ignimbrite

The BR ignimbrite in the VC-1 core contains ubiquitous hornblende and biotite, with pyroxene and resorbed, wormy plagioclase. Exsolved alkali feldspar is common, and there is rare quartz; both these phases are xenocrystic (McCormick, 1989; Self et al.,

1991). The unit is essentially unaltered throughout, except for incipient devitrification of the matrix in some sections, and minor vapor phase crystallization. The upper cooling unit ranges from moderately to slightly welded, whereas the lower cooling unit ranges from a crystal-rich fall unit and welded pumice-rich tuff just beneath the base of the upper cooling unit, then from nonwelded through very densely welded in the lower parts of the cooling unit.

El Cajete pumice deposit

No material from this part of the VC-1 core was examined in thin section.

Interpretation

Our interpretation of the volcanic units in the VC-1 core and of the surface-exposed, young pyroclastic and lava units in the southwestern part of the Valles caldera, and of their history, is as shown below. In stratigraphic sequence the oldest to the youngest events (Figs. 2, 3) are as follows:

1. An altered, complex volcaniclastic breccia, probably caldera moat fill, underlies the primary volcanic units in the VC-1 core. It contains clasts of the South Mountain Rhyolite lava, as well as blocks of a pyroclastic flow deposit containing South Mountain-like pumice clasts. These clasts have been dated at about 500 ka (J.N. Gardner, pers. comm.), implying that the breccia is somewhat younger than 500 ka. This deposit may represent a landslide, or a deposit related to other mass movements, perhaps caused by incision of the San Diego Canyon.

2. The EC-BR eruption produced the El Cajete pumice deposits, the BR ignimbrite, and the VC-1 Rhyolite, in that order. This was the first appearance of low-silica rhyolite magma from the Valles caldera since eruption of the Tshirege Member of the Bandelier Tuff at 1.14 Ma (Spell et al., 1990). The aggregate volume of these eruptives is about 1.5 km^3 DRE. This eruption has been difficult to date accurately, as discussed in Self et al. (1991).

3. After a repose period of unknown duration, at perhaps about 200 ka (Self et al., 1991), the latest eruption from the Valles caldera formed the low silica rhyolite BB lava and attendant minor pyroclastic, autoclastic, and reworked deposits. The volume of this material totals about 0.9 km^3.

Part II. Results of studies on VC-2A core hole

Background

The VC-2A stratigraphic borehole is on the western edge of the Valles caldera inside the inferred structural margin (ring-fracture zone) of the Valles II caldera (Fig. 5), which formed at 1.14 Ma (new age determination from Spell et al., 1990). It was expected that the core hole would intersect intra-caldera Bandelier Tuffs on the edge of the resurgent block (western edge of Redondo Border). The sites of core holes VC-2A and 2B are both in the Sulphur Springs hydrothermal field, which has shown young eruptive activity and has warm and acid sulfate springs.

Our interpretation of the rock units penetrated in VC-2A core hole is based on logging and sub-sampling of the core by S. Self in May, 1988, and on hand sample and thin section examination by M. L. Sykes and S. Self. A detailed core log is given in Appendix 2A, and the detailed hand and thin section descriptions in Appendix 2B. This core log is independent from, but largely agrees with, the log prepared by Hulen et al. (1988b). The differences between the two logs, and the significance of these differences, will be discussed after the stratigraphy has been presented. Geological and volcanological implications of the cored sequence will be treated at the end of this section. Relationships with the sequence in core hole VC-2B will be discussed using the Hulen and Gardner (1989) log of that hole.

Stratigraphy and Interpretation of VC-2A

The sequence of units in VC-2A is shown on Figure 6 and in Appendix 2A; sample descriptions are in Appendix 2B. Most units in the core are extensively hydrothermally altered, and textural characteristics are not always clear.

Surface to 21.6 m

These local deposits are associated with the Sulphur Springs hydrothermal area and are interspersed with sediments and debris flow deposits, probably derived from the steep terrain on the resurgent block immediately to the east of the core site. The coarse breccias may be landslide deposits or could alternatively be interpreted as hydrothermal explosion deposits, which are common in hot spring areas. Of most volcanological interest in this top sequence are primary and reworked phreatic or phreatomagmatic tuffs containing accretionary lapilli. There is a suggestion of depositional cross-bedding at 10 m depth that could indicate base surge deposition but is more likely to be fluvially produced. These observations suggest that a small tuff ring or cone built up in this area in recent times, but it has been buried, modified and masked by hot-spring activity and

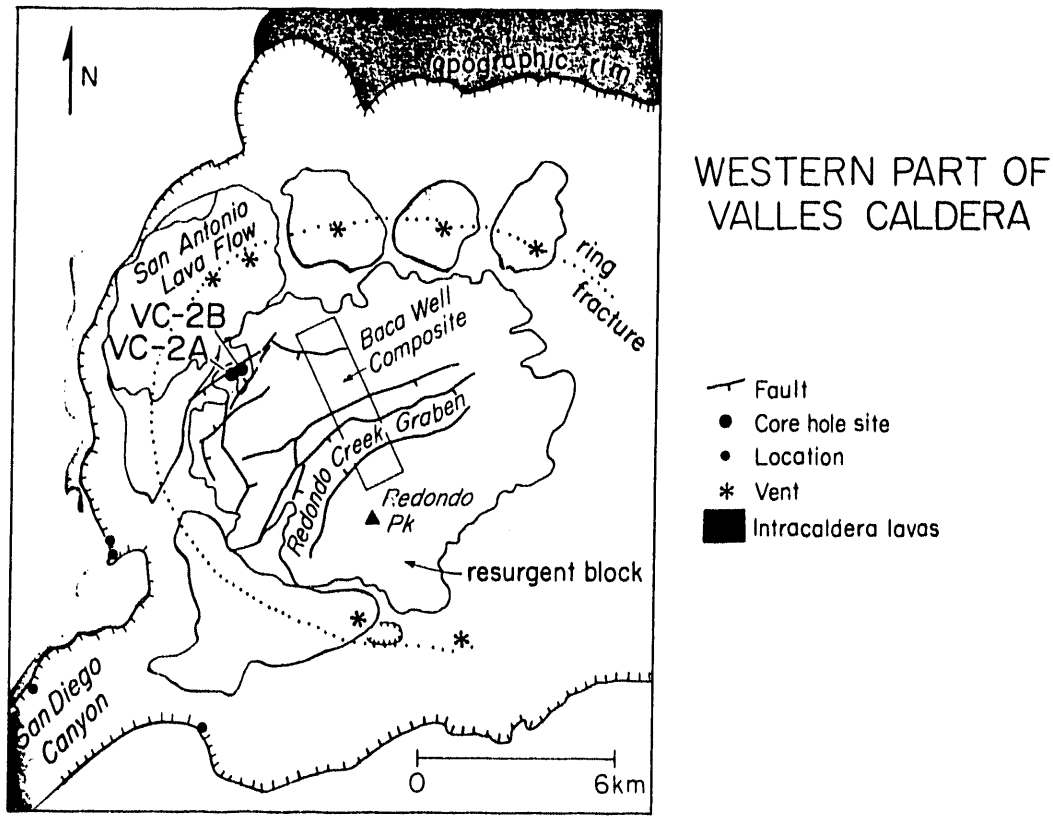

Fig. 5. Location map showing sites of core holes VC-2A and VC-2B. Rectangle labelled "Baca Well Composite" encloses locations of Union Oil Co. drill holes used by Nielson and Hulen (1984) and Hulen et al. (1991) in reconstructing subsurface geology of the Valles Caldera, summarised in Fig. 6.

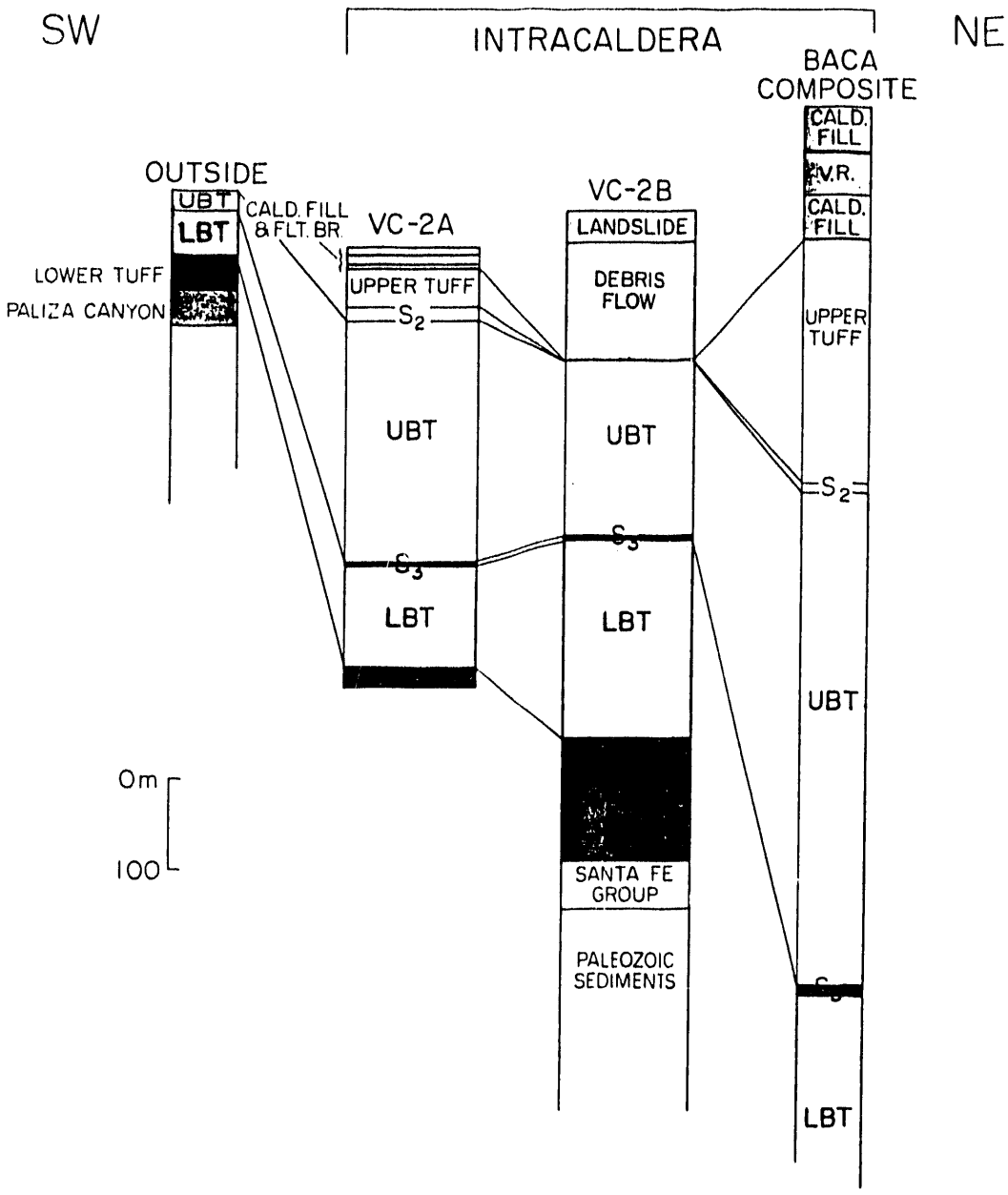

Fig. 6. Correlation of VC-2A, VC-2B, Baca Composite (Fig. 5), and nearby caldera rim exposures ("outside"). Note the increasing thickness of both Bandelier Tuffs towards the center of the caldera, most closely represented by the Baca Composite section.

perhaps by hydrothermal explosions. Extensive alteration prevents recognition of juvenile clasts in this upper sequence, so it is not known whether the explosive activity that formed the tuffs was totally driven by steam or if there was a magmatic component.

Below this upper sequence all units in VC-2A posses a dip, defined by inclined eutaxitic foliation and contacts.

Upper Tuffs (21.6 to 67.1 m)

This unit consists of a 46 m-thick ignimbrite that is less welded at the top, suggesting that the surface in the core hole is near the original, depositional upper surface. This unit has been previously termed the "upper tuffs" (Nielson and Hulen, 1984; Hulen et al., 1988a,b). A lithic concentration at 30 m depth suggests the base of a flow unit. Welding increases down hole until the texture of the ignimbrite becomes moderately compact with apparent eutaxitic texture in hand specimen. It is possible that the macroscopic eutaxitic texture is partly induced by load failure due to the intense alteration of the rock, i.e., the ignimbrite appears to be more densely welded and compacted than it actually was after it cooled. As observed in thin section (sample from 67.1 m depth) the rock has considerable pore space and little evidence of eutaxitic texture. Similar "pseudo-eutaxitic" textures in silicic tuffs have been documented from Australia and elsewhere (Allen, 1990; R.L. Allen and K. Dadd, personal communication).

This ignimbrite hosts a molybdenum hydrothermal deposit (Hulen et al., 1987) and characterization or correlation of the tuff on the basis of the petrology or geochemistry of its component clasts is impossible. The major question about the Upper Tuffs is what they represent and where they occurred in the eruptive history of the Valles caldera. Similar tuffs occur at the same stratigraphic position in Union of California (UOC) Baca drill holes in an area extending to the east of Sulphur Springs under the apical graben of the resurgent block (Nielson and Hulen, 1984). They do not occur in UOC Baca 12 hole to the SSE of Sulphur Springs, nor are they found in the VC-2B core where they would be predicted. Obviously they are of local extent and have been extensively faulted, which may explain their absence in VC-2B. The remnant mineralogy suggests a high-silica rhyolite composition, similar to the Bandelier Tuff or the Valles Rhyolites up to 0.5 Ma (Self et al., 1988; Spell and Kyle, 1989).

Dips of the eutaxitic foliation in the Upper Tuffs up to 15^{o} are most probably due to faulting along the Jemez Fault Zone (locally the Sulphur Creek and Freelove Canyon faults). Based on evidence from VC-2A alone, the Upper Tuff sequence could be interpreted as a slumped, repeated section of Upper Bandelier Tuff (UBT; Tshirege Member of Bailey et al., 1969), as it is bounded above and below by faults. However,

based on the apparent extent of the Upper Tuffs under the caldera, it is likely that they are a separate unit as proposed by Hulen et al. (1988b). In this case, they may be caldera-confined ignimbrite units related to the eruption of the San Antonio lava dome and flow complex at 0.53 Ma (new dates on San Antonio I and II lavas by Spell and Harrison, in press). Other ring-fracture rhyolite lavas in the Valles caldera have related ignimbrites that were produced before the major effusive phase. The Battleship Rock ignimbrite is related to the VC-1 Rhyolite and is welded where it is canyon-confined and the South Mountain Rhyolite has an extensive, non-welded pyroclastic flow deposit associated with it (S. Self, unpublished data).

Below the Upper Tuffs, the next interval, from 67.1 -79.3 m, consists of a heterolithologic breccia, possibly a debris flow deposit, overlying a sandstone (the S2 sandstone of Hulen et al., 1988a and b) with a thin mudstone layer at the base.

Bandelier Tuff: Upper Bandelier ignimbrite (Tshirege Member) (79.3 to 354 m)

The top of the next unit at 79 m depth consists of crystal-rich sandstone. This is the reworked top of the UBT and is very similar in appearance to the top in the outflow ignimbrite. About 275 m of upper Bandelier tuff (UBT) were cored in VC-2A, which, due to structural dips up to 40^{o}, represents 200 m true thickness. This amount is not considerably more than is usual in exposures of the ponded ignimbrite outside the caldera. A few locations on the southern-southeastern parts of the outflow sheet expose more than 200 m of UBT where it filled paleocanyons. Therefore the UBT in VC-2A is thick, as would be expected in the intracaldera environment, but not significantly thicker than in parts of the outflow sheet. In the region of the core holes it probably ponded in the pre-existing Valles I caldera. The ignimbrite, aside from pervasive alteration, resembles the UBT from outside the caldera but detailed correlation is difficult, especially as the UBT is thin or absent at locations on the caldera rim nearest the VC-2 sites. .

Very few flow unit boundaries can be recognized in the UBT, but the intense alteration may mask the contacts of depositional units (pyroclastic flows). A thin unit at 320 m depth is described in the Hulen et al. (1988b) log as a pyroclastic fall deposit, but it resembles more a thin, fine-grained flow unit. No intra-ignimbrite fall units are recognized in the outflow ignimbrite sheets.

At least two cooling units occur in VC-2A, whereas up to four are recognized in the outflow sheet. Two facts suggest, though do not prove, that the intracaldera UBT in the core is correlative with the upper part of the outflow UBT. First, the proportion of densely welded ignimbrite in the UBT sequence of VC-2A is considerably greater than in the ignimbrite outside the caldera, but this cannot simply be attributed to its intracaldera

nature. In general, in the outflow sheet the intensity of welding increases upwards, the densest ignimbrite being in the upper cooling unit, even in the thickest ponded sections. The most intense welding in the cored intracaldera UBT is not, however, significantly denser than in the most welded parts of the outflow sheet. Furthermore, the non- to incipiently welded lower cooling unit, a major characteristic of the outflow UBT, does not occur in the intra-caldera VC-2A or -2B sequences, suggesting that the lower unit was not extensively deposited in the area that the core represents. Second, the cored UBT sequence is quite fine-grained, crystal-rich, and lacks large lithic clasts and pumices except for one or two intervals. This is also a characteristic of the upper part of the outflow UBT (Self et al., 1986). It would be advantageous to be able to correlate the VC-2A UBT with outflow by pumice or fiamme chemistry, but the highly altered state does not permit this.

As noted by previous students of the VC-2A core, the UBT sequence is fine-grained with respect to pumice (fiamme) and lithic clasts. In this respect it does not differ significantly from the upper part of the ignimbrite outside the caldera. The observed lack of coarse lithics in the cored UBT is not, however, consistent with expected intra-caldera ignimbrite characteristics. It is generally held, for several reasons, e.g., proximity to the source vents, well-described examples of intra-caldera ignimbrites (Lipman, 1984), that caldera-filling ignimbrites should be more coarse-grained than their outflow equivalents and contain lithic breccias. The VC-2A UBT sequence contains no lithic breccias, although it should be noted that they are present in the same ignimbrite in VC-2B (Hulen and Gardner, 1989), where the overall thickness is a little less.

The paucity of lithic breccias in the Tshirege Member as a whole is indicative of some inherent process of the Upper Bandelier eruption; perhaps it was erupted from a well established vent system that contributed few lithics to the eruption column. Welding persists to within 1 to 2 m of the base of the UBT where it rests on the S3 sandstone. Hulen et al. (1991) have given details of this unusual contact, suggesting that the sandstone was wet when the ignimbrite was deposited. Excess water may have promoted welding to the very base by lowering the effective viscosity of the glass shards, and this would be consistent with deposition into shallow water. Even more surprising is the absence of the bedded, early flow units of the UBT and the plinian fall deposit that are so prominent at the base of the outflow sheet. Extrapolating from the dispersal and thickness of the plinian units on the western edge of the caldera only 2 to 3 km away (Self et al., 1986), there should be 4-5 m of pumice and ash fall layers at the base of the UBT in the vicinity of VC-2A. The significance of this will be discussed later.

The section below 354 m depth presents the most problematic zone of the VC-2A core, in terms of interpretation of units. They will be described first and then possible interpretations will be discussed.

S3 beds (355.7 to 361.7 m) 1166-1186 + 1186-1248'

A six meter thick ashy, crystal-rich sandstone is the unit below the base of the UBT; the contact is conformable. We follow Hulen et al. (1991) in terming these the S3 beds. In VC-2B this interval has epiclastic sandstone, breccia and a lithic-rich layer.

The uppermost sandstone bed was probably deposited immediately prior to the UBT, as evidenced by eruption timing and lack of a soil horizon. It has an ashy appearance, especially near the base, and Hulen et al. (1991) recognize accretionary lapilli in its lower part, although they were not recognized in this work. The horizon is certainly a sediment, a feldspathic litharenite, and not a pyroclastic deposit. The S3 horizon is widespread under the Valles caldera in the part known from drilling (Nielson and Hulen, 1984) and thickens eastward. A sandstone of this nature is not known outside the caldera between the two Bandelier ignimbrites, the only substantial sediments found in that position are mostly fluvial associated with Toledo deposits on the east, and occasional small gravels down paleo San Diego canyon. It was almost certainly derived from erosion of Bandelier-like materials, but its precise origin is unknown at present.

Bandelier tuff: Lower Bandelier ignimbrite (Otowi Member) (381 to 487 m) 1248'-~1597'

The sequence of Lower Bandelier ignimbrite cored by VC2A is quite similar to that of extracaldera exposures of the LBT. Two features worth mentioning are:

1. Co-ignimbrite lithic breccias (1370-1450', 420-442 m). These include a prominent lag breccia at 1440' which correlates well with a horizon in the LBT around the southwest caldera rim (Self et al., 1986).

2. A bedded, surge-like layer at 1570' (478 m) also seen in field exposures near the base of the LBT.

It is no surprise that no other LB pyroclastic deposits are found at the base of this unit because the plinian is only 4 to 6 cm thick on this side of the caldera. This throws doubt on Hulen et al.'s (1991) interpretation of the lower 5 m of LBT in the VC2A as fall and surge deposits.

Lower Tuffs (487.1 to 527.7 m) ~1597'-1730'(t.d.)

The Lower Tuffs correlate with the San Diego Canyon Ignimbrite (Turbeville and Self, 1988). Samples are altered but apparently non- to moderately welded, moderately lithic-rich ignimbrite. Core samples exhibit the apparent eutaxitic structure observed higher in the core hole.

Interpretations of the Problem Sequence

Interpretation of the sequence from the top of the S3 (399.7 m) to the top of the undisputed Lower Bandelier Tuff (381.0 m) presents several problems; there are at least three plausible explanations. To facilitate this discussion, a summary of the pertinent known data follows:

- The UBT is ~ 200 m in original thickness in VC-2A and is moderately to densely welded throughout, except for the basal meter.

- The 150-200 m thick UBT ignimbrite always has a nonwelded 10-100 m thick zone at the base and probably represents no more than 400 m original thickness.

- The S3 beds in VC-2A appears to be closely related to the UBT due to the gradational, intertonguing nature of the contact.

- All beds in this section dip at about 40°.

- The initial phases of the UBT eruption were in part phreatomagmatic (Self et al., 1986).

- The beginning of the UBT event was a large plinian eruption (Self et al., 1986) that formed the Tsankawi pumice deposit (Bailey et al., 1978). Based on the isopach map compiled from extracaldera plinian deposit thicknesses, there should be 4-5 meters of Tsankawi plinian pumice fall at the VC-2A/B core sites.

- Thick plinian deposits do NOT occur in the VC-2A or VC-2B cores at the base of the UBT, or anywhere lower in the sequence.

- The bedded interval above the undisputed LBT sequence appears to be largely sedimentary in origin, although Hulen et al. (1988b; 1991) place it as part of the LBT.

Keeping these facts in mind, the three possible interpretations of the sequence from ~1160 to 1250' are as follows (see Fig. 7).

Interpretation A. The base of the UBT occurs at or near at the base of the bedded sequence, i.e., at about 1248'(380m). This implies that the S3 beds must be a rapidly emplaced sediment occurring during a hiatus in the Tshirege eruption, after the first ignimbrite flow units were emplaced. There is limited evidence for this hiatus early in the extracaldera UBT sequence, in the form of surfaces overlain by pyroclastic surges. Generation of this sediment could have included reworking early UBT phreatomagmatic deposits to yield the accretionary lapilli noted in the base of the S3 beds by Hulen et al (1991), but not found in our S3 samples.

In this scenario, the ignimbrite under the S3 interval (1186-1225') would be an early UBT flow unit, but a welded intracaldera facies (as opposed to the nonwelded extracaldera occurrences of early UBT flow units). The pinkish, very crystal-rich ignimbrite immediately under S3 in VC2A (see Appendix - , our core log) is similar to a thin crystal-rich flow at the base of the UB ignimbrite sequence on the western side of the Jemez Mountains, but this layer is not underlain by welded ignimbrite as in VC2A; however, it was hot when emplaced. Also, at least some of the bedded material from 1225-1248' would be equivalent to the UBT plinian deposit, plus interbedded finer phreatomagmatic deposits (units A and C of Self et al., 1986, for example).

One problem with this scenario is that the bedded sequence does not have typical characteristics of plinian deposits. The black bed at ~1235' is definitely a sediment.

Another, more general, problem common to all the Valles caldera drill hole sequences is the absence of significant sedimentary deposits between the UBT and LBT that might be expected from 300,000 years of deposition in the Valles I (Toledo) caldera. There is ample evidence for volcanic activity and sediment sources within the Jemez Mountains during this time period (Toledo domes and tuffs, etc.).

Another problem with interpretation A is the correlation of the S3 beds with those in the VC-2B and Baca wells, discussed in more detail by Hulen et al. (1991).

Interpretation B. The base of the UBT occurs at the top of the S3 beds (~1166'); from the base of the S3 sandstone to the top of undisputed LBT (at 1248') are a number of different deposits emplaced in the Valles I caldera between the end of the LBT event and the beginning of the UBT event (Valles II), including:

(1) a thin, moderately to incipiently welded, crystal-rich ignimbrite under the S3 (1186-1225');

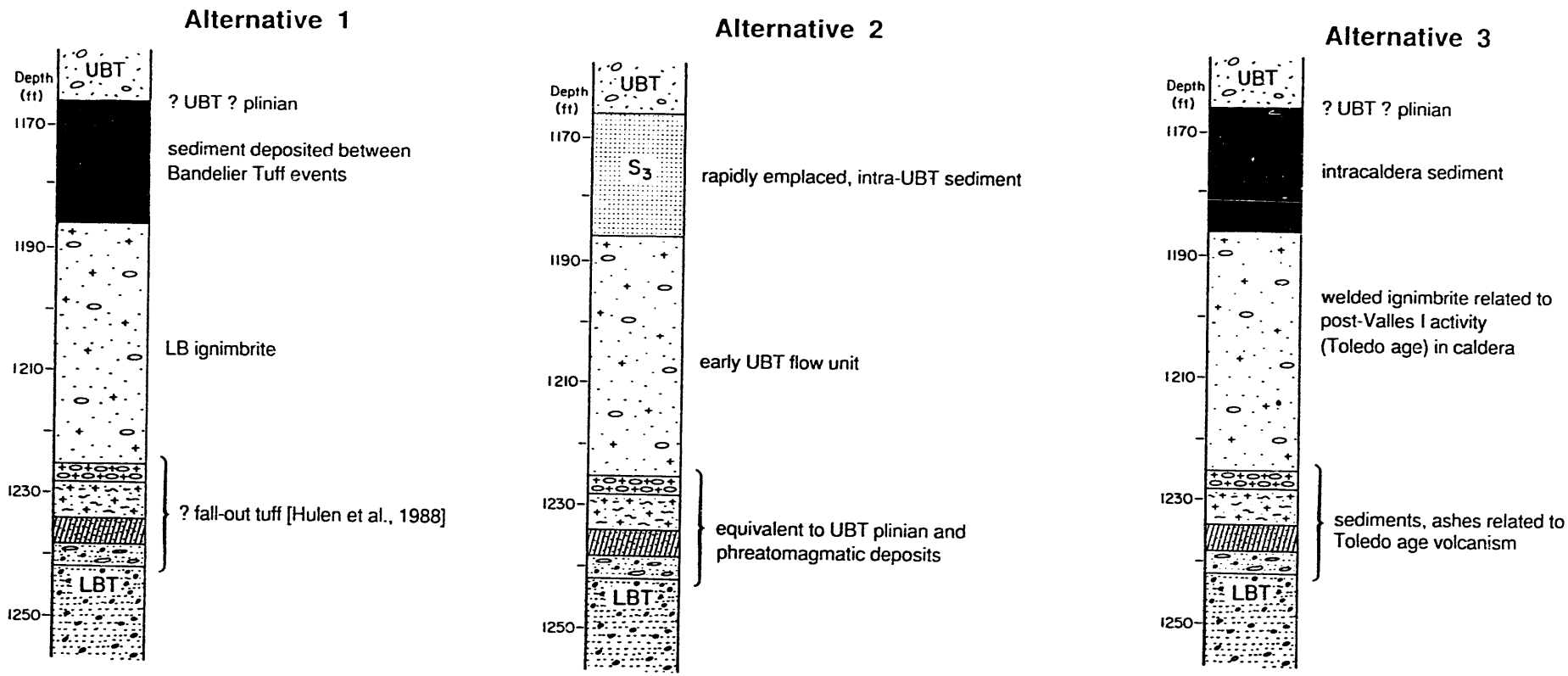

Fig. 7. Three possible alternative interpretations of the VC-2A core at around 1200' depth. See text for description and discussion.

(2) sediments (1225-1238'); and

(3) ashes and ashy sediments (1238-1248').

Sources for these beds are plentiful but largely conjectural and they had 300,000 years to form; Toledo age fall deposits and lava domes occur extensively in other parts of the Jemez Mountains. At the La Cueva locality in the caldera wall, only minor sediments occur between the UBT and LBT, but there may be a different sequence within the caldera. Post-Valles I activity in the western part of the caldera could have produced the ignimbrite below the S3 sandstone. No pyroclastic flow deposits are known in extracaldera sections between the LBT and UBT. An attractive feature of this interpretation is that it allows more latitude in explaining the differences between the VC2A and VC-2B sequences.

Again, the major problem with this scenario is the absence of any deposits, plinian or other types, at the base of the UBT, in contrast to the extracaldera sequence. There are no other major problems with scenario B, but it does require a fortuitous combination of timing and locale of deposition of post-Valles I and pre-Valles II activity.

Interpretation C. The base of the UBT occurs at the top of the S3 sandstone (~1166'); the S3 sandstone is a sedimentary unit deposited between the Valles I and II events; the LBT includes the welded ignimbrite and bedded sequence beneath the S3 sandstone (the chosen interpretation of Hulen et al., 1988b, 1991). In this scenario the beds above the top of the main flow units of LBT (at 1248') are equivalent to surge horizons between the more welded upper LBT flow units, as seen in a few locations outside the caldera in the SW Jemez Mountains (Self et al., 1986).

Again, a major problem is the absence of a thick sequence of sediments that would be expected in 300,000 years of deposition between Valles I and II; the S3 sandstone is only about 20 feet thick. This could be explained if the core site was situated on a horst that existed in post-Valles I time. Also, the bedded sequence does not have the typical characteristics of surge deposits, but they are crystal-rich. Again, the absence of the basal UBT plinian sequence at the VC-2A location requires explanation.

Microscopic description of units sampled from VC-2a

Upper Tuffs

In the VC-2a core, the Upper Tuffs consist of welded, white to grey ignimbrite that has been altered in places to a pale lemon yellow. Pumice clasts are sparse, from 1 mm to ~ 1 cm diam, and darker grey. No accretionary lapilli were observed. Welding is

variable and obscured by the alteration. Although the fine-grained matrix is usually leached, relict shards and some relict pumices are visible under plane light or under crossed nicols. The matrix has been altered to very fine-grained clays and/or micas. Anhedral silica mosaics both line cavities and, in the sample at 190 ft, infill fractures (which cross-cut phenocrysts). Vugs are also lined by fine-grained acicular phases which outline former shard/vesicle boundaries. Traces of axiolitic devitrification are apparent in some areas. Phenocrysts include anhedral to large subhedral quartz and some sanidine, with some resorbed plagioclase. Fe-Ti oxides are abundant. The breccia at 190 ft contains clasts of rounded sandstone (mostly unaltered), and highly altered fine-grained volcanics.

Debris flow deposit or lithic-rich ignimbrite

The single sample examined from this unit is part of the Hulen et al. (1988b) S2 interval, a highly altered breccia containing angular to subrounded clasts of volcanic rocks (including andesite), shale/siltstone, and unaltered microcline fragments. The matrix consists of fine-grained material, an aggregate of lithic material, phenocryst fragments plus clay/mica. Pervasive crystallization of secondary phases has occurred in pore spaces.

Upper Bandelier Tuff

Thick flow unit in upper cooling unit

In VC-2a the UBT consists of non- to densely welded ignimbrite, generally crystal-rich. Matrix and pumices are altered to very fine-grained clay/mica aggregates, or (sample from 938 ft) to coarser grained aggregates approaching granophyric. Relict shards, pumices and eutaxitic textures are usually visible. Alteration of pumices tends to be coarser-grained than the matrix. Phenocrysts include quartz and sanidine with skeletal or exsolved plagioclase. Pyroxene, when present, is completely altered to fine-grained material. Some feldspars are sericitized.

Lower cooling unit

This part of the core contains a thin flow unit over a thick one. The upper thin flow unit is volcaniclastic, consisting of very fine-grained devitrified material with no apparent shards or pumices, but with abundant small phenocrysts and occasional larger lithics. Phenocrysts are as in the rest of the UBT, some feldspar is sericitized. The underlying thick flow unit is formed of very similar material to that in the upper cooling unit.

S3 sandstone

This sandstone contains euhedral to rounded crystals of quartz, sanidine, microcline and plagioclase of about the same size. A few linear bands with more matrix and fewer crystals occur in the thin section. No primary or reworked volcanic clasts are present.

Bedded deposits

This interval contains various thinly bedded lithologies. A two foot thick pumice and crystal-rich fall, surge or sediment layer overlies a six foot thick densely welded, fiamme and crystal-rich ignimbrite unit. Phenocrysts appear to be quartz although some sericitized feldspar is present. Both these layers are completely devitrified/altered.

A nearly black, altered horizon about four feet thick underlies the ignimbrite. This horizon contains abundant crystals and lithics, and perhaps pumices. Abundant small crystal fragments include quartz and some sanidine and microcline. The dark appearance comes from a black fine-grained substance dispersed through the altered, fine-grained, low birefringence material which composes the matrix. In plane light the matrix appears to be epiclastic rather than pyroclastic; if these clasts are shards, they are blocky with no evidence of bubble-wall textures.

Underlying the black horizon is a bedded deposit of highly altered lithic-rich matrix-supported pumiceous breccia. Abundant crystals include hexagonal quartz and alkali feldspar; the latter is largely sericitized or exsolved. Lithics include ?andesite lavas, granophyrically devitrified tuff, altered pumice (or flow-banded lava) and others. This could be a pumice and lithic fall deposit.

Lower Bandelier Tuff

The LBT is non- to very densely welded in the VC-2a core, with moderate to abundant crystals of apparently unaltered quartz, sericitized or exsolved alkali feldspar. Lithics are abundant only in a lag breccia zone at ~ 1450 feet; minor concentrations occur at 1370, 1410, and 1505 feet. Lithics are probably volcanic, but alteration is so complete that identification is difficult. Alteration products are mostly very fine-grained, very low birefringence material; relict pumice and shard structure can sometimes be observed in plane light.

Lower Tuffs

These tuffs are non- to densely welded in the VC-2a core and highly altered. Abundant small phenocrysts of quartz, alkali feldspar and minor plagioclase are present;

feldspars are more often completely replaced by low to high birefringence phases. This ignimbrite is moderately lithic-rich; the dominant lithic is a felted plagioclase-rich ?lava.

Part III. Extracaldera Bandelier and related volcanics: petrography, petrology, geochemistry and geochronology.

Geochemical data collected for the Bandelier Tuff and associated volcanic rocks, funded by this grant, include major elements, trace elements, stable and radiogenic isotopes, and electron microprobe analyses performed on single whole pumices and/or on mineral separates from whole pumices, as appropriate. All analyzed Bandelier samples were collected from precisely measured points in logged sections, with the intention of defining any systematic compositional stratification within the deposits. Approximately one-third of all collected samples were analyzed; to our knowledge, the resultant 130 analyzed samples nonetheless represents the largest database on a continental silicic ignimbrite (ash-flow tuff) formation. The remaining *ca.* 250 samples form a valuable collection should further work be required.

The research of several graduate students is incorporated into this section, notably Skuba (1990) for isotopic data, and Kuentz (1986) and Balsley (1988) for most major and trace element data. The data presented by Kuentz (1986) and some of the trace-element data obtained by Balsley (1988) were funded from other sources, but are included here as an integral part of the whole project. Oxygen isotope data on associated basaltic rocks presented by Duncker (1988) and Duncker et al. (1991) were also funded from this grant. Aliquots of mineral separates were forwarded to T. Spell at SUNY- Albany for single-crystal $^{40}Ar/^{39}Ar$ dating; the results have important implications for the early evolution of the Bandelier magmatic system (Spell et al., 1990). The results of this dating, which was enabled by work carried out under this grant (but funded from another source), will therefore be discussed first. Geochemical data on the various stratigraphic units will then be discussed in turn. Isotopic data are listed in Tables 2 through 5, major and trace element data are given in Appendices 3A and 3B, and microprobe analyses of mineral separates are found in Appendix 4.

Geochronology

This section is a summary of the results presented by Spell et al. (1990).

From oldest to youngest, the previously accepted dates for the San Diego Canyon (SDC) and Bandelier ignimbrites were: SDC unit A, 3.64 ± 1.64 Ma; SDC unit B, 2.84 ± 0.07 Ma; Lower Bandelier Tuff, 1.45 ± 0.06 Ma; Upper Bandelier Tuff, 1.12 ± 0.03 Ma

(Doell et al., 1968; Izett et al., 1981; Self et al., 1986). Despite geochemical similarity to Lower Bandelier, it seemed that the SDC units were not directly related to Bandelier magmatism because of the very long time separating SDC unit B from the LBT (at least 1.26 Ma).

Ages for the UBT and LBT are not much different, but the ages for the San Diego Canyon units are significantly younger than previously reported. This discrepancy is attributed to xenocrystic contamination of the samples analyzed by conventional K-Ar, a common problem in young volcanic rocks. The new ages for the Bandelier units are within error of the older determinations, but are more precise. The SDC units are now seen to be early eruptions from the Bandelier magma system, as they predate the LBT by only 0.27 Ma, and are chemically identical to some of the least-evolved compositions in the LBT. This places important constraints on the time required for the Bandelier system to develop the range of trace element concentrations exhibited by the LBT (see below), which in turn allows evaluation of dynamic models for magma chamber evolution as they apply to the sub-Valles caldera system.

San Diego Canyon Ignimbrites

SDC unit A consists of up to three lithic-rich pyroclastic flow units with a low content of lapilli-size pumice. The pumice is nearly aphyric, with a phenocryst assemblage of sanidine + quartz + trace pyroxene + trace magnetite. Its major and trace element composition is identical to that of SDC unit B (Table 6). Units A and B are separated by reworked ash and fluvial deposits, which represent an interval of not more than 0.11 Ma; given the extent of magmatic differentiation between the eruptions of SDC B and LBT over 0.27 ± 0.07 Ma and the lack of any similar chemical variation between A and B, the actual time interval is probably much less than the maximum allowed by experimental error. Unit B consists of up to four pumice-rich flow units, and is correlated on the basis of identical age, petrography and chemistry with an airfall deposit in the upper part of the Puye Formation on the east side of the Jemez Mountains (Turbeville and Self, 1988; Spell et al., 1990). The pumice is poorly phyric high-silica rhyolite in composition with a phenocryst assemblage identical to that of the underlying unit. Trace amounts of a grey rhyodacitic pumice occur as bands and streaks mingled with the dominant high-silica rhyolite. The grey pumice contains disaggregated, broken crystals of quartz and microcline, and is enriched in compatible elements with respect to the dominant rhyolite (Table 6). It is petrographically identical to the grey pumice component of the overlying Lower Bandelier Tuff, which has isotopic characteristics indicating assimilation of a significant quantity of local Proterozoic crust, and in both units is thought to represent

melted country rock incorporated into the magma shortly before or during the ruption. Most of the small isotopic and chemical shifts which occur between major members (SDC - LBT - UBT) are in the direction of this component, and it is argued below that contamination of the Bandelier system was continuous, and can be observed on a variety of time-scales, throughout its history.

Apart from the trace amount of grey pumice, pumice clasts from SDC unit B and the correlative airfall exhibit no compositional variation. The trace element abundances are very closely similar to those of some of the least evolved pumice compositions in the LBT ignimbrite, suggesting that parts of the magmatic system remained unchanged over the 0.27 Ma between the SDC B and LBT eruptions, while others became strongly differentiated. Isotopically, SDC unit B has $^{87}Sr/^{86}Sr$ within the range of that of the LBT, while $^{143}Nd/^{144}Nd$ and $^{206}Pb/^{204}Pb$ are higher and lower, respectively.

Lower Bandelier Tuff

The Lower Bandelier Tuff (LBT) includes the Guaje airfall pumice bed (product of the plinian phase which opened the eruption) and the Otowi member, the main ignimbrite phase. The collective volume is approximately 330 km^3. The dominant composition is high-silica rhyolite (Table 6), with trace amounts of grey pumice described hereafter. The phenocryst assemblage, in decreasing order of abundance, is sanidine, quartz, clinopyroxene, magnetite, fayalite, orthopyroxene, biotite, zircon, and allanite. The total weight percentage of phenocrysts in pumice ranges from 7.5% in the Guaje plinian deposit to 19.5% in the least differentiated Otowi pumices. Only sanidine and quartz are ever present in amounts greater than 1%; both contain occasional glass inclusions.

Major element oxide concentrations show little variation through the suite of 63 analyzed samples. In fact, of the usual list of "major" elements, only SiO_2, Al_2O_3, total Fe, Na_2O and K_2O are present in quantities greater than 1%, the others only attaining trace to minor abundances.

Trace element concentrations, however, vary widely, and form the basis for recognition of evolutionary trends within the suite. Elements which partition strongly into solid phases during magmatic crystallization (e.g., Ni, Cr) were not detected in any high silica rhyolite sample. In contrast, incompatible elements such as Cs, Rb, Th, U, Nb, Ta, and Hf increase by up to a factor of five from the least differentiated to the most differentiated pumices, as do Y and the heavy rare earths Yb and Lu. Correlations between these elements are extremely tight (e.g., whole-pumice Ta *vs.* Th, r = 0.99, Fig. 8). Light rare earths La and Ce show a slight decrease from least to most differentiated, while other elements usually regarded as incompatible in most systems (Nd, Sm, Tb, and

Zr) show little variation or modest increases. This behavior is typical of high-silica rhyolites, where the presence of allanite (a rare-earth mineral of the epidote group) and zircon in the crystallizing assemblage determines the behavior of rare earths and Zr.

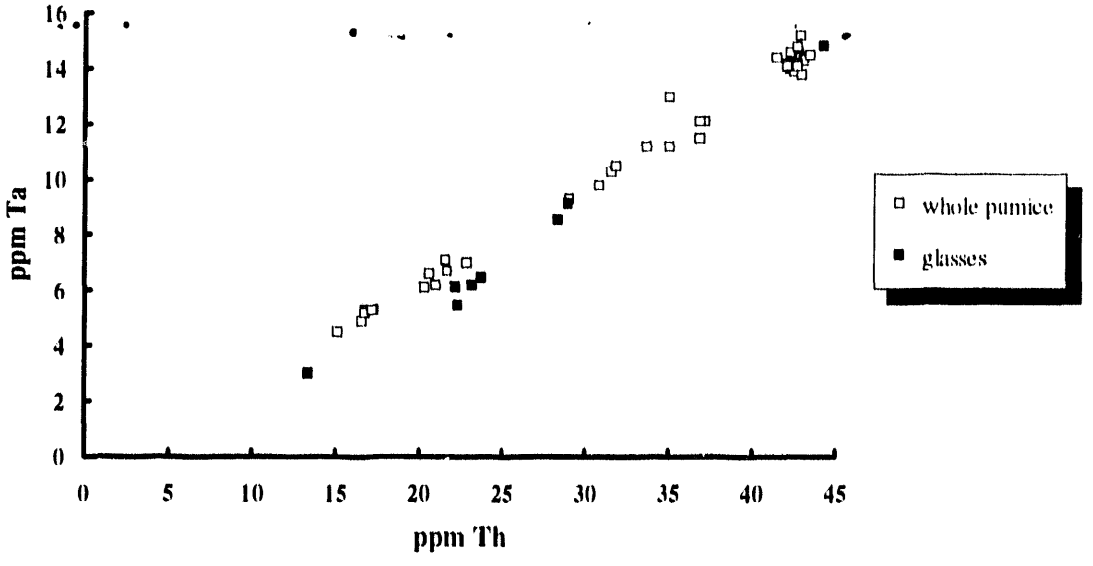

Figure 8. Ta vs. Th for whole pumices and glasses from the Otowi Member (Lower Bandelier Tuff). The samples clustering between 40 and 45 ppm Th are mostly from the Guaje plinian fallout deposit.

Strong evidence for progressive fractional crystallization as the differentiation mechanism for the Bandelier system is provided by glasses separated from pumices, which plot on the same trends as the whole pumices (Fig. 8). Also, four glasses separated from one pumice show that the pumices are heterogeneous. This is probably an eruptive drawdown effect, where magma of different compositions from different parts of the chamber were drawn into the conduit at the same time. If it is assumed that, prior to eruption, the magma was a stably-stratified system with more differentiated compositions overlying less differentiated, then drawdown calculations for silicic systems (Wolff et al., 1990) using density and viscosity values calculated from LBT analyses indicate that the length scale of detectable chemical layering in the Bandelier system was of the order of 200 m; this is further discussed below.

Effects of post-eruptive alteration

Rhyolitic ignimbrites are very susceptible to chemical modification by secondary processes. These processes include oxidation, hydration, ion exchange with groundwater (and leaching at more severe levels of alteration), devitrification, vapor-phase alteration in

the cooling tuff, and diagenetic cementation. The concentrations of mobile elements such the alkalies and alkaline earths may be significantly affected even at modest degrees of alteration, as is $\delta^{18}O$. To avoid these problems as much as possible, our sampling program focussed on white or clear, glassy, non-consolidated pumice and ash. This strategy avoids material affected by any of the above processes except hydration and exchange with groundwater. Oxygen isotope ratios of glasses have been affected by exchange (Table 2), but this can be circumvented by only using $\delta^{18}O$ values from quartz phenocrysts. Alkali ion exchange causes a decrease in the Na/K ratio of silicic volcanic glasses (Scott, 1971), and this ratio can therefore be used as a filter. There is a clear dependence of Na/K ratio on sampling location, with samples from Pueblo Canyon, Cat Mesa, Wildcat Canyon, and Pueblo Mesa (Locations 13, 18, 177, 22 respectively) failing to pass the filter (Fig. 9). Note that in Fig. 9, the inflections in the trend of highest

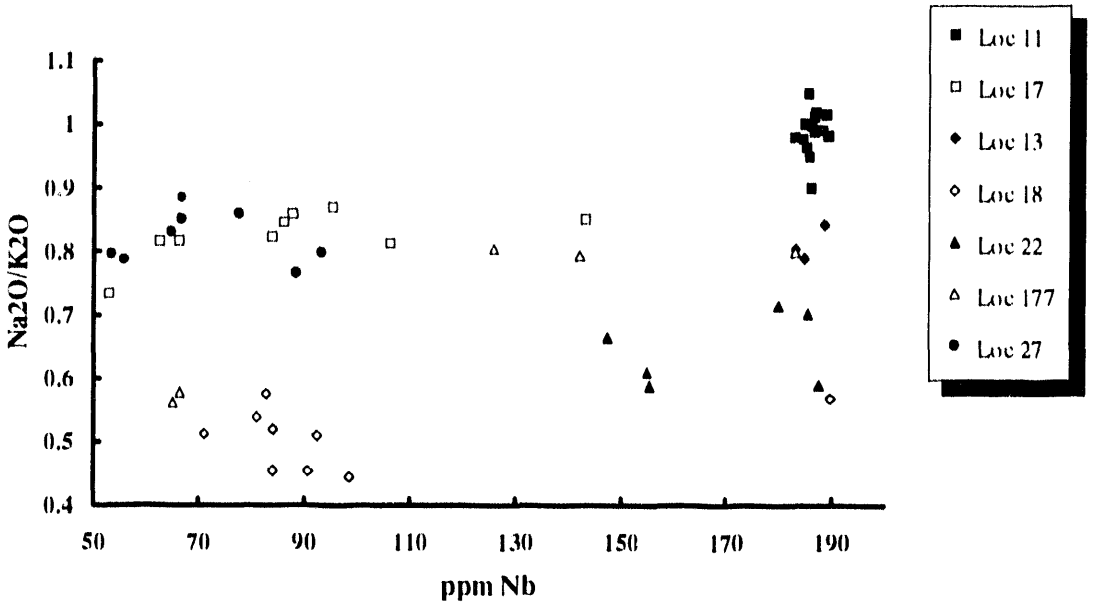

Fig. 9. Na_2O/K_2O (weight ratio) vs. Nb for whole pumice samples from the Otowi Member. Note that Na_2O/K_2O is dependent on sampling location, with samples from Location 18 having suffered the greatest loss of Na due to post eruptive hydration. Samples from Locations 11, 17 and 27 are considered to have preserved pristine Na_2O/K_2O.

Na_2O/K_2O (*ca.* 0.8) at approximately 70 and 150 ppm Nb are mirrored by plots of immobile elements *vs.* Nb, and are therefore considered magmatic. In the analyzed LBT sample suite, only Na, K, and Cs appear to have been mobilized; all other elements (including, surprisingly, Rb) are not affected. Therefore, when major elements (because

changes in the abundances of one major element necessarily affects all others) or Cs are considered, only those samples passing the filter are used; otherwise, all samples are used. For reasons of immobility, high abundance and analytical precision, element abundance variations within the suite will be referenced to either Nb or, where only an INAA determination was made, Th. Nb varies from 53 to 189 ppm, and Th from 13.4 to 44.2 ppm from least-differentiated to most-differentiated samples.

Major element variations

Although there is some scatter due to analytical precision, samples of least-differentiated Otowi have slightly higher silica contents (SiO_2 = 77.71 ± .23 wt. %) than most-differentiated plinian samples (77.10 ± 0.16 wt.%). This is accompanied by an increase in Na/K, and appears to reflect migration of the granite minimum in Petrogeny's Residua towards the albite corner with increasing magmatic PH_2O. Water behaves as an incompatible species during magmatic differentiation, thus is expected to be enriched in the most differentiated compositions, unless it is completely decoupled from non-volatile elements by degassing or some other process. The decrease in SiO_2 content with increasing abundances of incompatible trace elements suggests that this is not the case.

Phenocryst-whole pumice relations

Compositions of magnetite and clinopyroxene phenocrysts, though scattered, vary systematically with degree of differentiation of pumice clasts as monitored by incompatible trace-element content (Fig. 10). Mean Mg number decreases and Mn content of clinopyroxene increases with host pumice differentiation, while Mg number, Al content and Ti content of titanomagnetite decrease. These variations are expected during the course of normal magmatic differentiation. Unfortunately, the details of the plots in Fig. 10 are difficult to interpret. It is unclear whether the clinopyroxene compositions represent a smooth trend with increasing scatter towards more evolved compositions, or whether two populations of clinopyroxene are represented, with high-Nb pumices bearing both populations. The latter interpretation would support a model of (the erupted portion of the) Bandelier magma chamber as a two-layered system, while the former would be expected for a continuously zoned system. Taken together, the clinopyroxene and titanomagnetite variations may indicate a smoothly zoned system for the range 50 - 100 ppm Nb, overlain by a markedly more fractionated capping magma layer of 140 - 190 ppm Nb, with some mixing of phenocryst populations during eruptive drawdown. Trace element covariations, however, suggest otherwise (see below).

Trace-element covariations

As mentioned above, trace element behavior in the LBT is consistent with a differentiation mechanism dominated by fractional crystallization of the observed phenocryst assemblage. Cs concentrations show the greatest increase (among filtered samples) of any incompatible element analyzed, with a five-fold variation from least-differentiated to most-differentiated compositions. Assuming pure closed-system fractionation and a bulk distribution coefficient of zero (i.e., Cs is assumed to quantitatively remain in the liquid phase during fractional crystallization), the most-evolved Guaje pumice represents 20% liquid remaining from fractional crystallization of the least-evolved compositions. With the same assumptions, bulk distribution coefficients for the other, well-correlated incompatible trace elements (Rb, Th, Nb, Ta, Yb, Lu) are all about 0.2. Compatible elements (Sc, La, Eu) decrease more or less smoothly from least-evolved to most-evolved compositions; the compatibility of La is attributed to the presence of allanite in the fractionating assemblage, while Sc and Eu partition strongly into clinopyroxene and feldspar respectively.

Plots of moderately incompatible (Zr, MREE) versus strongly incompatible elements show inflections which can be used to place constraints on fractionation, zoning and eruptive drawdown processes. Zr behavior is controlled by zircon, a trace phase in the LBT; moderate incompatibility of Hf (bulk distribution coefficient = 0.45) and the decrease in Zr/Hf (Fig. 11) are characteristic of zircon fractionation. MREE partition into allanite, but not as strongly as LREE. This discussion focuses on Zr and Sm, which are determined to high precision by XRF and INAA respectively. Zr decreases in concentration from 53 to 90 ppm Nb, and increases thereafter. Presumably, this reflects a decrease in the proportion of zircon in the fractionating assemblage at around 90 ppm Nb. We have not been able to test this by examination of the phenocryst assemblage because the very small quantities of zircon present make quantitative modal abundance estimates extremely difficult to perform; in any case, the possibility of fractionation occurring mostly at the walls of the magma chamber implies that observed assemblages may not be representative of actual fractionating assemblages. Independent circumstantial evidence for a decreasing proportion of zircon over this fractionation interval is provided by increasing Na_2O and total alkali content from 53 - 80 ppm Nb; increasing alkali content increases zircon solubility in felsic liquids (Watson and Harrison, 1983). The majority of samples group around the baseline on the Zr-Nb plot; those that plot above baseline may be slightly accumulative in zircon or may represent mixtures of end members on either side of the Zr minimum. The latter is more likely, as these samples do not have elevated Hf or U contents (Fig. 11). The amount of mixing (i.e., the number of samples affected, rather

than separation between end members) seems rather limited. The trend from 53 to 90 ppm Nb is accordingly interpreted as a crystal fractionation trend (consistent with

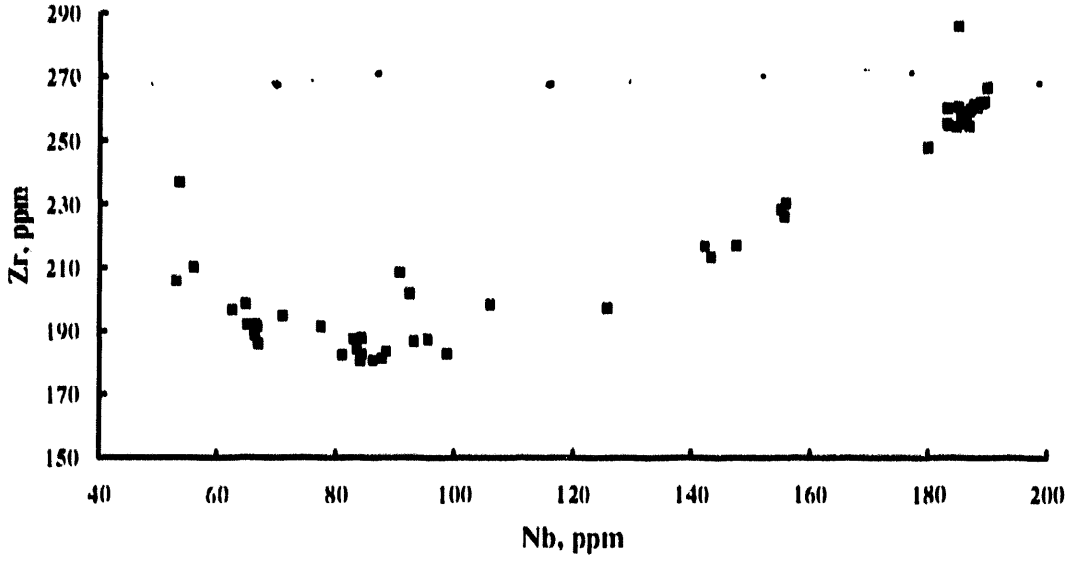

a

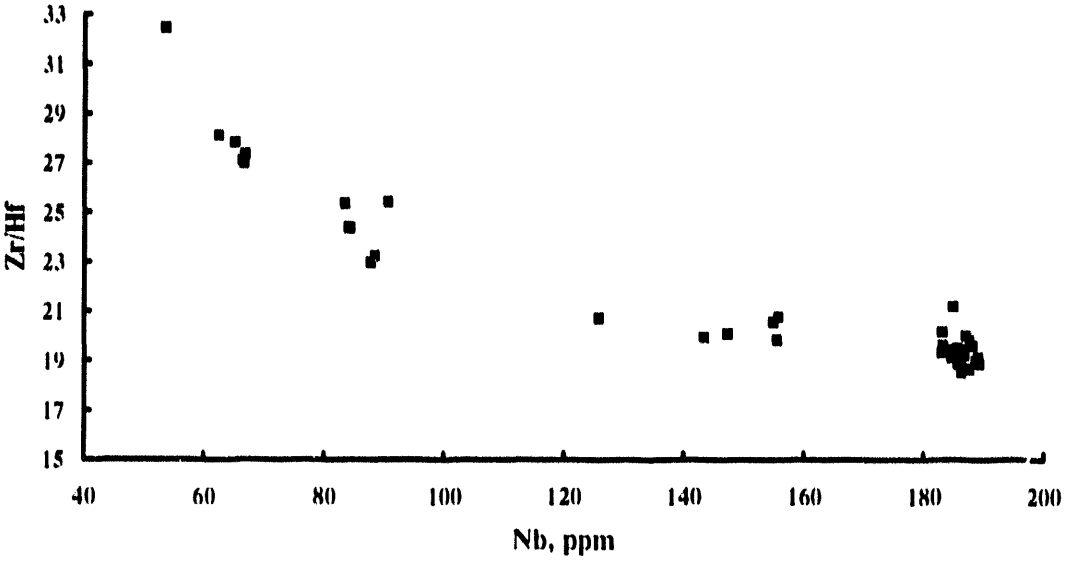

b

Fig. 11. Zr *vs.* Nb (**a**) and Zr/Hf *vs.* Nb (**b**) in whole pumices from the Otowi Member.

indications from clinopyroxene compositions), with limited mixing either prior to eruption, or due to eruptive drawdown, with an end member having >90 ppm Nb.

For the nature of the trend between 90 and 189 ppm Nb, we turn to Sm, which shows a maximum at about 155 ppm Nb (Fig. 12), which is again considered to be a fractionation trend. The high-Sm samples between 120 and 160 ppm Nb cannot be accumulative in allanite, because La would then be greatly enriched. In fact one sample does have an elevated La content and may be accumulative, but the others do not.

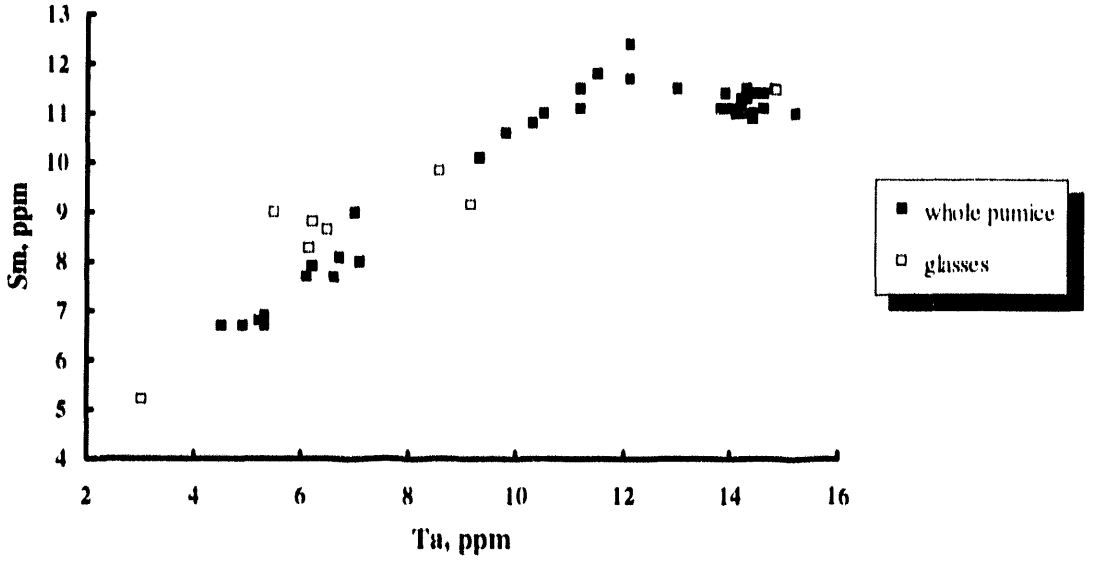

Fig. 12. Sm *vs.* Ta in whole pumices and glasses separated from pumices from the Otowi Member.

Furthermore, one glass separate from this compositional range plots among the whole-pumice points. These samples lie well off mixing lines between most-evolved (>180 ppm Nb) compositions and those with <120 ppm Nb. Although there are few samples within this compositional range, they therefore represent magma which was present in the chamber during establishment and stabilization of the zoned system, and are not any kind of mixing product. The decrease in Sm concentration between 160 and 189 ppm Nb is most likely the result of an increased proportion of allanite in the fractionating assemblage. We can conclude that essentially all of the compositional variation displayed by the LBT pumices represents a range of compositions present in the magma chamber well prior to the eruption, and are not the result of mixing of two end members. The portion of the LBT chamber represented among the erupted products was therefore continuously zoned, possibly with some minor compositional gaps (see below), from 53 ppm to 189 ppm Nb.

Pumice matrix glasses

Several 100 mg samples of glassy matrix were extracted from porphyritic pumice clasts and analyzed by INAA. The results were surprising, with general significance for phenocryst-matrix element partitioning studies on silicic igneous rocks. In many cases, analyzed glasses have lower concentrations of incompatible elements than the bulk pumice clast; the reverse of what would be expected for phenocryst-matrix equilibrium (one glass sample is actually the least differentiated composition of the whole LBT suite). Four separate glasses from one pumice clast define a compositional trend coincident with that for the whole suite of pumices and glasses. Despite the arguments of the previous section, some mixing between different compositions has clearly occurred, most likely due to eruptive drawdown.

Modelling water contents

Pre-eruptive magmatic water contents can be estimated if it is assumed that water behaves as an incompatible component during fractional crystallization, and the water content is known at one point along the fractionation path. The lack of significant quantities of any hydrous phase in the phenocrysts assemblage implies that water was quantitatively retained in the liquid phase during fractionation, and thus an approximately fivefold increase in water content from the least to most differentiated magma. This is in complete agreement with measured water contents of 1% to 5% in isolated glass inclusions within quartz phenocrysts, which are assumed to remain closed during eruptive degassing of the bulk magma (Hervig and Dunbar, 1989). Because water is the only major component exhibiting significant variation, it effectively controls density and viscosity variations in felsic magmas (Wolff et al., 1990). The density contrast between least-evolved and most-evolved LBT magmas is then 160 kg m^{-3}.

Compositional gaps and magmatic layering

There are a number of compositional gaps within the LBT suite, most apparent on plots of two incompatible elements (Fig.13). The gap at 18 - 20 ppm Th may not be analytically significant, but those at 23 - 29 ppm Th and 37 - 42 ppm Th are. These gaps could be sampling artifacts. However, pumices taken from a single flow unit at one location straddle the gaps, and the 37 - 42 ppm Th gap is found at the top of the Guaje plinian deposit, which was continuously sampled form base to top. Also, the 23 - 29 ppm Th gap is straddled by glass separates taken from a single pumice clast. Significantly, these two gaps respectively coincide with the two inflexions on plots of moderately incompatible elements versus compatible elements discussed above. They are therefore

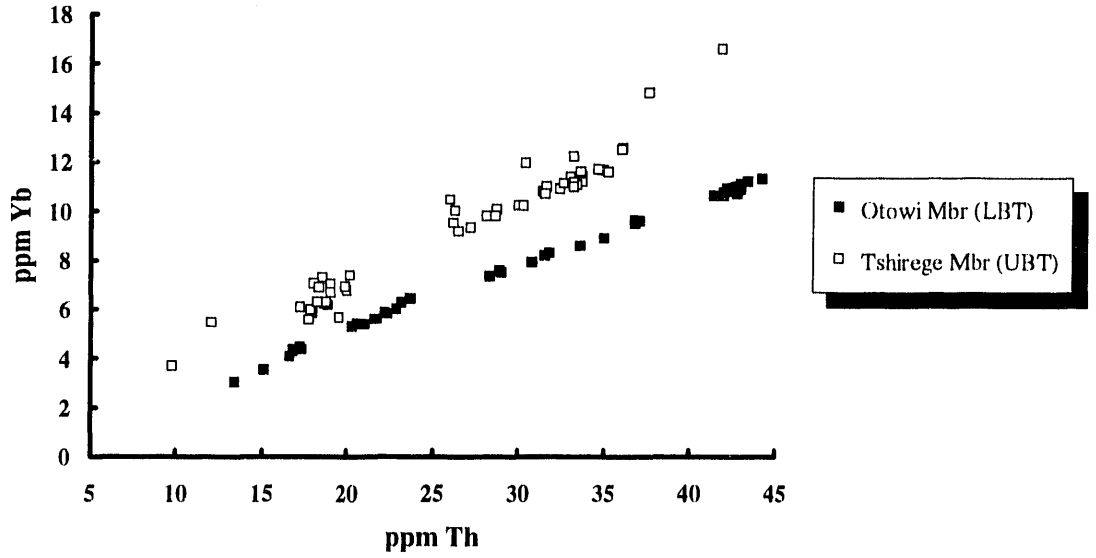

Fig. 13. Yb *vs.* Th in whole pumices from the Otowi and Tshirege Members.

considered to be petrologically significant, and divide the LBT suite into three compositional groups which each exhibit internal variation. Because of the covariation in water content and therefore density, these groups must have been arranged in three layers in the magma chamber, with the densest least evolved layer at the bottom and the most evolved, lightest layer at the top.

The thicknesses of these layers are difficult to constrain, because relations between compositions and erupted volumes are poorly known; nonetheless some progress can be made for the Guaje plinian magma. All but the uppermost layer of the Guaje (156 ppm Nb, 37 ppm Th) has 184-189 ppm Nb, 42-43 ppm Th. Although some Guaje-type pumice has been recovered from basal Otowi flow units elsewhere in the Jemez Mountains, it is not abundant. Therefore, a reasonable approximation for the volume of the uppermost magma layer is the dense rock equivalent volume of the Guaje deposit, which is 20 km^3. If the LBT magma chamber is assumed to be a cylinder with equivalent diameter to the Valles caldera, the thickness of the uppermost magma layer was 65 m. This is much less than calculated eruptive withdrawal layer thicknesses (200 - 800 m, depending on the model chosen) for this chamber geometry; in other words, the Guaje deposit should contain a range of pumice compositions. The lack of correspondence between prediction and observation suggests a different chamber geometry; possibly, the Guaje magma differentiated in a narrow cupola above the main chamber.

Grey pumice component

Rare clasts of banded black-and-white or grey-and-white pumice occur in the Guaje plinian deposit and the basal Otowi flow unit on the Pajarito Plateau. In overlying flow units, the material is exceedingly rare; although abundances are too small to be easily quantified, it is clear that the proportion of banded clasts diminishes upwards through the eruption sequence. In thin section, the dark glass bears small fragments of quartz and microcline. Although mixed with high-silica rhyolite, the dark component is clearly less differentiated, being richer in the compatible elements Sc and Eu (analyses 11-85-P5 and 11-85-10-1 in Appendix 3A contain the highest proportion of the dark component). Isotopically, the material is very distinct, with low $^{143}Nd/^{144}Nd$ and greatly elevated $^{87}Sr/^{86}Sr$ (Tables 4, 5). It can be simply modelled as a mixture of LBT high-silica rhyolite and basement Proterozoic granite. The isotopic and petrographic evidence point unequivocally to an origin by melting and assimilation of Precambrian country rock into the LBT magma, shortly before or during the eruption. Possibly, the basement material was incorporated into the magma at the walls of a dike as the magma body broke through to the surface.

Isotopic data and petrogenesis

Sr, Nd, Pb and O isotope data are given in Tables 2 - 5. Within the LBT, there is a very slight decrease in $^{143}Nd/^{144}Nd$ with differentiation, suggesting very minor assimilation of upper crust (Sr isotope ratios from high-silica rhyolite glasses are considered unreliable because the very small concentrations of Sr (<5 ppm) render them subject to syn- or post-eruptive modification by a variety of mechanisms (Halliday et al., 1984; Palacz and Wolff, 1989)), while Pb isotope ratios also vary slightly. SDC unit B has $^{143}Nd/^{144}Nd$ within error of the least-evolved LBT, however the distinct Pb isotope contrast requires some contamination of the chamber between the two eruptions. Within the LBT, $^{208}Pb/^{204}Pb$ decreases with differentiation in the whole pumice, but increases in feldspars separated from those pumices. Taken together, these observations suggest that minor contamination of the LBT magma chamber was a continuing process, but that the nature of the contaminant was subject to variation (local Proterozoic rocks exhibit a very wide range in Sr, Nd and Pb isotopic characteristics). The preservation of banded pumices, and phenocryst-matrix disequilibrium, indicate maximum time scales for contamination on the order of years and thousands of years, respectively (the time scales required for diffusive equilibration). Syn-fractionation contamination, indicated by covariation of Nd and Pb isotope ratios with incompatible element concentrations, operated on a time-scale of less than 0.27 Ma (the time between the SDC B and LBT

eruptions). It is unclear exactly when the isotopic shifts from unit to unit (Fig. 14) are generated; one possibility is that contamination events coincide with major eruptions, and the residual magma - erupted at a later date - carries this signature.

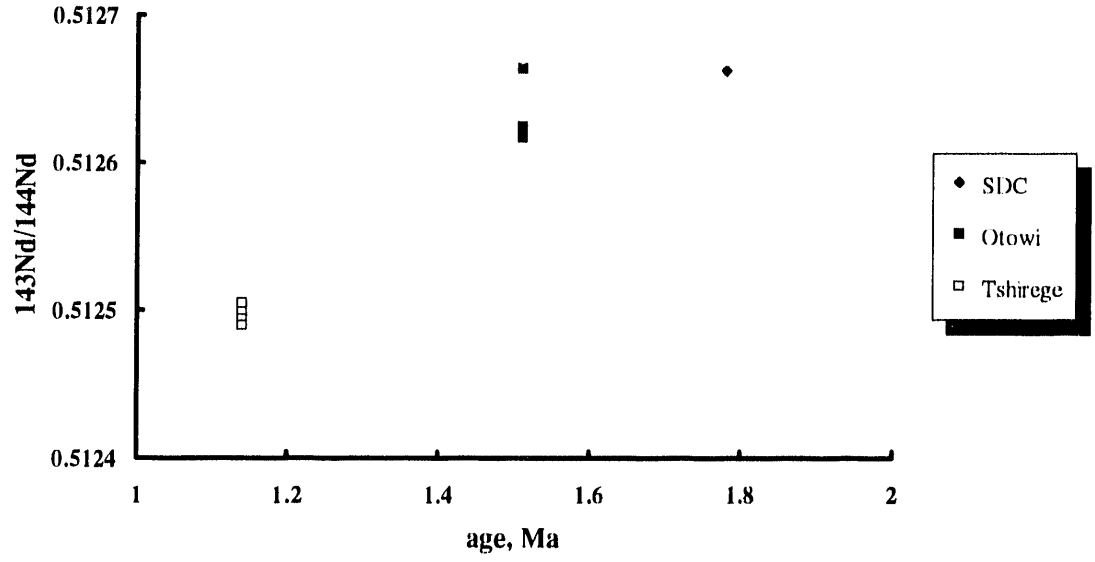

a

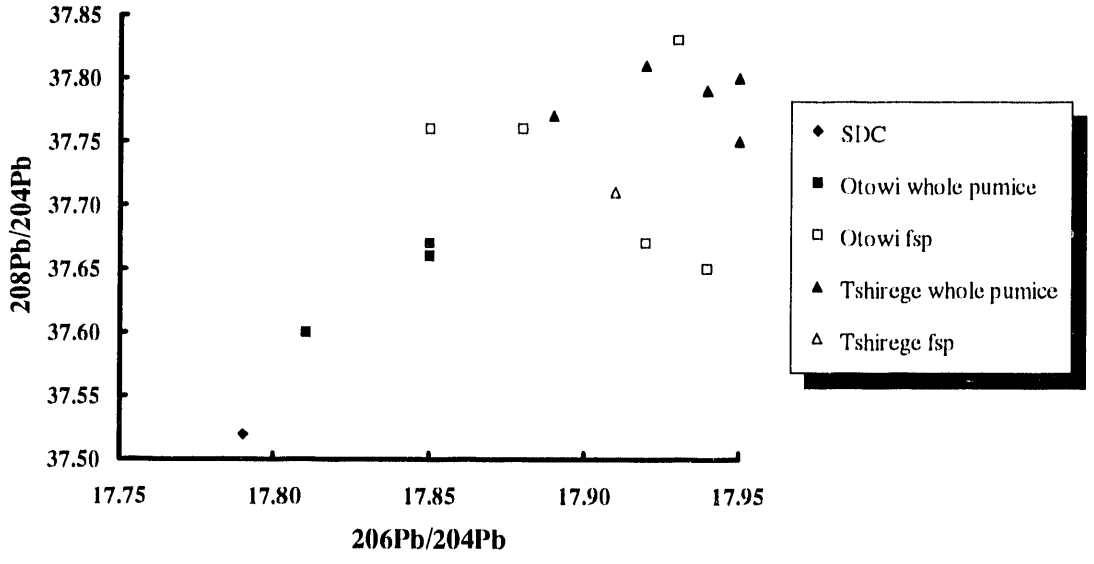

b

Fig. 14. **a.** Nd isotope ratio vs. time for Tewa Group rhyolitic ignimbrites. **b.** Lead isotope ratios in whole pumice and feldspars from Tewa Group rhyolitic ignimbrites.

Oxygen isotopes show little variation within the LBT; the total variation of $\delta^{18}O$ in quartz is at the limits of experimental error, while that in feldspar is just outside error. Both phases become slightly lighter in oxygen with fractionation. The sign and degree of variation can be reproduced by a Rayleigh fractionation model using $^{18}O/^{16}O$ fractionation

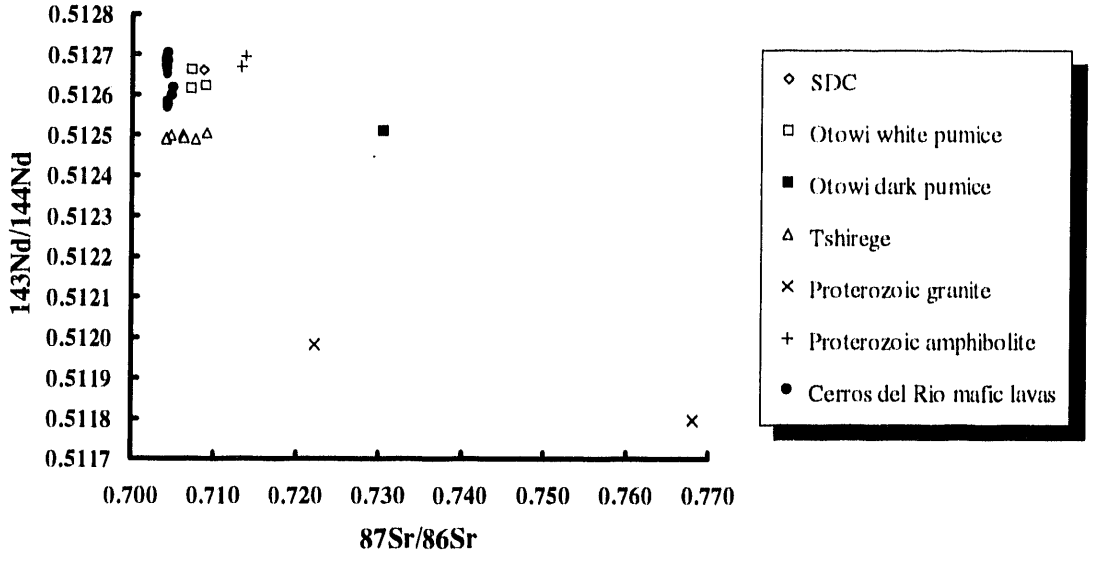

a

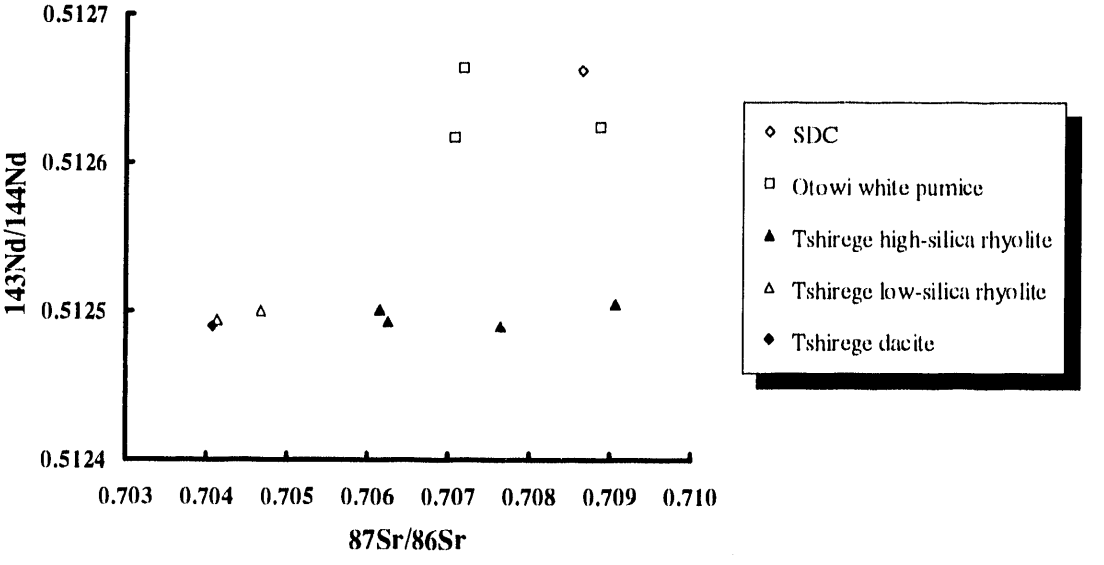

b

Fig. 15. Sr-Nd isotope plots for Tewa Group rhyolitic ignimbrites, Cerros del Rio lavas, and Proterozoic basement rocks.

factors from the literature, and liquid fractions calculated from incompatible trace element abundances. Although it is therefore likely that the small variations observed are due to isotopic fractionation, we cannot be sure without more precise data.

Due to post-eruptive exchange, $\delta^{18}O$ values in LBT glasses are typically 2 - 3 per mil heavier than quartz and feldspar. Pristine glass $\delta^{18}O$ values would be similar to those for feldspar, assuming crystal-liquid equilibrium, i.e. about +7‰ SMOW. This is rather low for upper crustal rocks, and is at the low end of the range (+6.7 ‰ to +10.6 ‰ SMOW) for crustally-derived quartz xenocrysts in basalts of the nearby Cerros del Rio volcanic field (Duncker et al., 1991; see also a later section of this report). This severely limits the proportion of upper crustal - paticularly sedimentary - material in the LBT magma, and suggests that the dominant components are derived from high-grade metamorphic rocks of the lower crust and/or the mantle.

Nd isotope ratios of both Bandelier Tuffs are bracketed by local Proterozoic crustal rocks; depleted mafic amphibolites are slightly more radiogenic in Nd, while local granites are much less radiogenic (Table 3, Fig. 15). Both types are however much more radiogenic in Sr. Equivalent rock types with lower $^{87}Sr/^{86}Sr$ may exist in the lower crust beneath the area (Duncker et al., 1991), and the Bandelier magmas could then be derived from a mixture of mafic and granitic granulites, with the granitic compositions forming a minor component as required by the Nd isotope relations. However, depleted mafic granulites are extremely refractory and difficult to fuse. More probably, the Bandelier magma was a mixture of both mantle and fusible lower crustal components. Local mantle-derived mafic magmas in the Cerros del Rio volcanic field are of two types; one type is similar to oceanic magmas (specifically, E-type MORB) and is presumably derived from the asthenosphere, while the other is an unusual type derived from arc- source-like mantle modified by lithospheric extension, which may be present in a thermal boundary layer at the base of the lithosphere (Duncker et al., 1991). The latter type has a distinctive chemical signature with low Rb/Th and K/Th ratios. On a plot of Th/Yb vs. Rb/Yb (Fig. 16), the E-MORB-like lavas lie on the extension of a regression through all Tewa Group rhyolites projected to mafic compositions, while the other magma type lies well off this trend. Therefore, the mantle component in the Bandelier rhyolites is probably MORB-like. We note that MORB-like magmas have played a fundamental role in volcanism elsewhere in the Rio Grande Rift region, for example the Taos plateau to the north- east of the Jemez Mountains (Dungan et al., 1986).

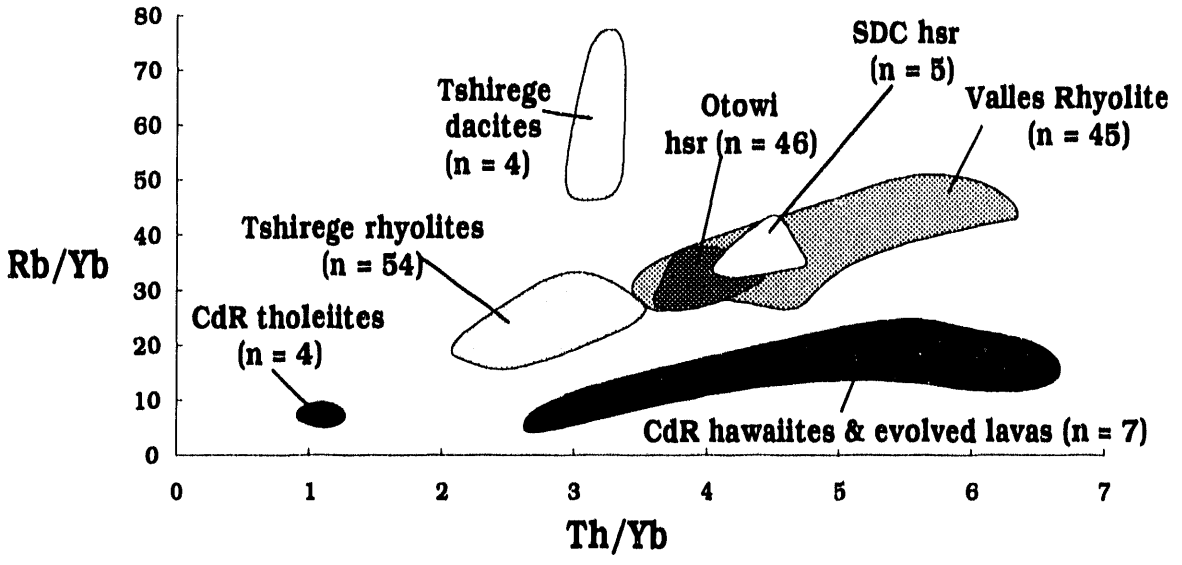

Fig. 16. Rb/Yb *vs.* Th/Yb in Tewa Group rhyolites and Cerros del Rio basalts.

The paths by which these components became blended to form the parental Bandelier magma is far from clear. Given the 12 Ma history of the JMVF prior to Tewa Group magmatism (Gardner et al., 1986), a simple first-cycle mixture of mantle-derived basalt with melted Precambrian lower crust is perhaps unlikely. More probably, remelting of intrusions related to earlier JMVF magmatism played a role in Bandelier petrogenesis. This cannot be addressed at present as there is insufficient high-quality trace element and radiogenic isotopic data on the early JMVF rocks of the Keres Group; this will form the subject of future research.

Upper Bandelier Tuff

The Upper Bandelier Tuff (UBT) consists of the initial Tsankawi plinian pumice bed and the main-phase Tshirege ignimbrite. Sampling of the Tshirege flows proved more difficult than for the Otowi, because of the much greater degree and extent of thermal induration in the former, ranging from orange-pink discoloration, through cementation, vapor-phase alteration and partial to dense welding. Typically, all but the basal few thin flow units have suffered some alteration. Our main strategy for avoiding these effects rested on sampling through sections where the pyroclastic flows were banked and chilled against steep paleocanyon walls (Fig. 17). For the most part, we were able to sample white vitric pumice from non-consolidated pyroclastic flows. In some cases, thermally oxidized orange or pink pumice was perforce sampled.

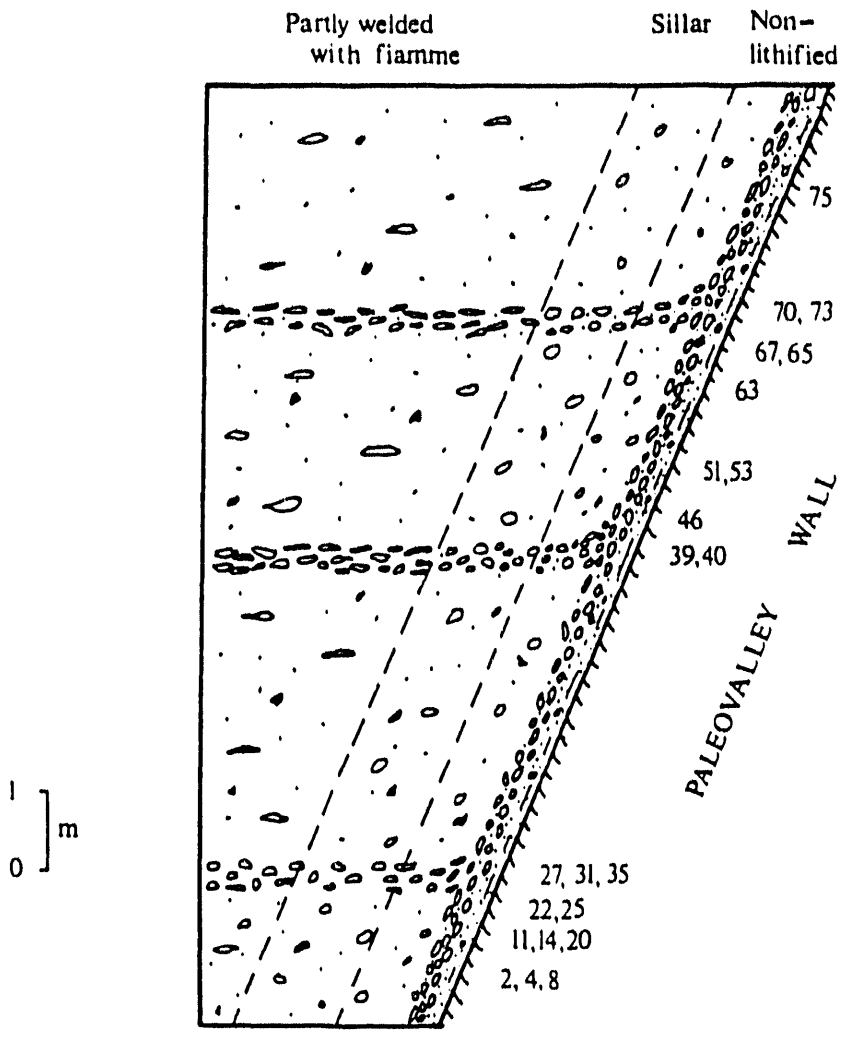

Fig. 17. Sketch of highly inclined thermal zonation in the Tshirege Member (Upper Bandelier Tuff) flow units at Location 20 in Cochiti Canyon. Whole vitric pumice clasts were taken from the non-lithified zone as indicated by the numbers. With this strategy, essentially fresh pumice was recovered from a significant vertical interval within the Tshirege. Where the unit rests on flat pre-existing topography, most of its thickness is vapor-phase altered (sillar) or welded.

In general, petrologic and geochemical variations in the UBT are more complex and chaotic than in the LBT; several pumice types are present. The most abundant is high-silica rhyolite, with sanidine, quartz, clinopyroxene, fayalite, magnetite, orthopyroxene, biotite (tr.), hornblende (tr.), chevkinite (tr.) and apatite (tr.). This pumice type varies from nearly aphyric, finely vesicular frothy white pumice to coarsely vesicular porphyritic pumice similar to Otowi pumice. Biotite and hornblende are more abundant, and are joined by plagioclase, in porphyritic 73% silica rhyolite pumice, referred to here for convenience as low-silica rhyolite. A sugary-textured, finely vesicular porphyritic dacite pumice occurs throughout the UBT in quantities of around 1%. Typically this pumice type is found as discrete clasts, often of surprisingly regular orthogonal morphology. Occasionally an orthogonal dacite clast is found with a thin skin of coarsely vesicular high-silica rhyolite, and a few banded pumice clasts have also been found containing both types. The dacite has phenocrysts of plagioclase, hornblende, biotite, hypersthene, augite, and magnetite. The groundmass is highly variable from completely vitric to 70-80% crystallized (neglecting vesicle volumes); groundmass crystals frequently show hopper and tuning- fork morphologies, sometimes split by vesicles, indicating rapid growth prior to vesiculation. The dacite magma is thought therefore to have been injected into, and chilled against, the dominant rhyolite. The common orthogonal shapes reflect the form taken by the chilled dacite blobs upon mixing with rhyolite. Geochemically, the dacite is unrelated to the rest of the Tewa Group magmas (see below). A second type of banded pumice is texturally closely similar to that in the Otowi, and is considered to have a similar origin, i.e. melted country-rock granite.

General geochemical characteristics

Many arguments for the origin and evolution of the UBT are similar to those discussed in detail for the LBT.

Na/K variations within the UBT suite suggest that, unlike the LBT, all samples have been affected to some degree by post-eruptive alteration. Cs and Rb has clearly been mobilized, as their abundances in the Tsankawi plinian are negatively correlated with immobile elements such as Nb; consequently the degree of fractionation within the UBT cannot be as accurately calculated as for the LBT. Trace element behavior is again consistent with fractionation of the observed phenocryst assemblage. The low silica rhyolite pumices lie on trends of incompatible and moderately elements back-projected through the high-silica rhyolite suite, and are therefore plausible parents for the high-silica rhyolites (Fig. 13); this is not true of the dacite pumices, particularly for REE. The degree of incompatible element enrichment from low-silica rhyolite to most evolved high-

silica rhyolite is again approximately fivefold. The UBT overall contains higher abundances of compatible elements (e.g., Sr, Eu), and slightly lower abundances of incompatible elements, than the Otowi. Incompatible-incompatible element trends are much less tightly correlated than for the LBT. This is particularly well seen for Yb and Th (Fig. 13). Among the high-silica rhyolites, Yb/Th varies randomly from 0.3 to 0.4 regardless of the degree of differentiation (Th abundance). This is interpreted as a fractionation trend from magma heterogeneous in Yb/Th. Note that the low-silica rhyolites plot at higher Yb/Th because the fractionation step from low-silica to high-silica rhyolite involves crystallization of significant quantities of pyroxene, and therefore greater compatibility of Yb than Th. Also, Yb/Th is higher in the UBT than LBT. Assuming that the two Bandelier Tuffs are petrogenetically related by being derived from the same magmatic system, then clearly there was a variable net influx of Yb into the system between 1.51 and 1.14 Ma. The higher abundances of compatible elements (Sc, Sr, Ba, Eu) in the UBT indicates that this influx was in the form of a more mafic magma. Isotopic data allow two scenarios. The $^{87}Sr/^{86}Sr$ ratios measured on two UBT low- silica rhyolites are relatively primitive, at 0.70413 and 0.70467, while their Sr contents are high compared to other Tewa group rhyolites (ca. 200 ppm); $^{143}Nd/^{144}Nd$ is constant in all measured UBT samples at 0.51250. This isotopic shift from LBT to UBT could either be the result of addition of melt derived from high- grade, lower crustal rocks with time-integrated low Rb/Sr and Sm/Nd, or combined addition of crustal and mantle-derived components. In the latter case, the crustal input could be coincident with the addition of country rock to the system during the LBT eruption, with the mantle input occurring at some later date. Conventional K-Ar and trace element data on the intra-Bandelier Cerro Toledo ashes (Heiken et al., 1986; Stix et al., 1988) suggest that the shift from LBT-like to UBT-like trace element character occurred at 1.2 - 1.3 Ma, which may coincide with the timing of the mantle-derived input. Sr and Nd isotope data, and precise age dating of the Cerro Toledo tephras by single-crystal $^{40}Ar/^{39}Ar$, are required to elucidate what happened to the Bandelier magmatic system between 1.51 and 1.14 Ma. The latter is currently underway (in an independent study by T. Spell of the Australian National University, while the Sr-Nd work will be the subject of future research by our group) .

Zonation of the UBT magma chamber

As with the LBT, the most strongly differentiated compositions are found in the initial plinian pumice deposit. Tsankawi-like compositions also occur in flow units near the base of the Tshirege on the Pajarito Plateau, and in the north Jemez Mountains. In contrast, the Tshirege section sampled in the south (Cochiti Canyon) dominantly contains the least-differentiated material. This may indicate that the Tshirege flows that moved southwards were erupted later than those to the east and north; alternatively eruption from several vents within the caldera may simultaneously tap different parts of the magma body (this may particularly be the case for a vertically zoned body if the chamber has a sloping roof).

In contrast to the Guaje deposit, compositional zonation is detectable in the Tsankawi (Fig. 18), despite the smaller estimated dense rock equivalent volume of 15 km^3. UBT pumices display prominent compositional gaps between 20 and 26 ppm Th, 80 and 110 ppm Nb. Although there are no associated identifiable inflexions in trace-element covariations (in part this could be due to scatter masking any subtle inflexion), the gap is considered real because it is well-defined by a large number of samples, and because samples on either side of the gap have been recovered from a single flow unit at one locality. The compositions on either side of the gap are therefore interpreted as two discrete layers within the magma chamber, the upper one of which was continuously zoned. Although the degree of water enrichment with differentiation (and therefore in density) can be modelled as very similar to the LBT, there are no independent estimates of pre-eruptive water content for the UBT. The very wide dispersal of fall unit B of the Tsankawi plinian pumice deposit suggests a water content at the top of the chamber in excess of 5 wt.%, neglecting the possible influence of external water.

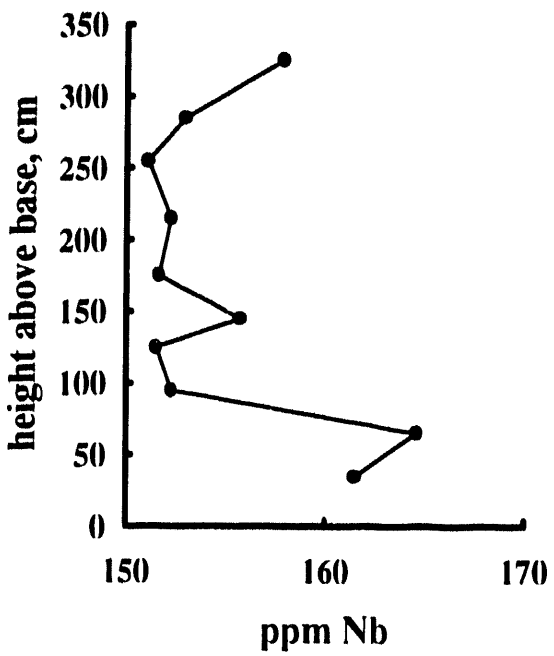

Fig. 18. Nb vs. height in the sampled section of the Tsankawi plinian pumice deposit.

A similar gap separating the low-silica rhyolites from the least-evolved high silica rhyolite cannot be evaluated at present, because we have very few samples of this composition. Several samples predicted to fall in this general compositional range are being analyzed; due to a serious delay in the laboratory where the samples were sent, the data are not available at the time of writing of this report.

Within the UBT, there is a crude correlation of $^{87}Sr/^{86}Sr$ with degree of differentiation, although phenocryst-matrix disequilibrium is found as in the LBT. Because evolved high-silica rhyolite has very low Sr contents, this is most likely the result of a small amount of wall-rock contamination during zonation. Variations in Nd, Pb and O isotope ratios are not detectable.

Quartz in Cerros del Rio mafic magmas

This section summarizes the findings of Duncker et. al. (1991), a copy of which is attached to this report.

The Cerros del Rio is a small (ca. 60 km^3) mafic volcanic field in the Espanola Basin, east of the Jemez Mountains; its westernmost part is buried beneath the Bandelier Tuffs on the Pajarito Plateau, but is well exposed in canyons. The field was active between roughly 2 and 4 Ma, and the younger end of this range is approaching the time at which the Tewa Group rhyolitic magma system became established at some time before 1.78 Ma. The field could potentially contain mantle-derived magmas representative of those which were involved in producing the Bandelier ur-magma. Several of the Cerros del Rio lavas contain quartz in reaction with the mafic host liquid; three hypotheses were entertained for the origin of this quartz. First, that it could be a relict high-pressure phase; second, that it is a crustal contaminant; third, that it records magma mixing with rhyolitic compositions, possibly during establishment of the Tewa Group system. For these reasons, it was decided to extend an initially independent unfunded study of these mafic lavas to include oxygen isotope analyses of quartz separates, to determine the origin of the quartz and thus assess the implications for petrogenesis of the Bandelier Tuffs. The oxygen isotope analyses were funded from this grant; results are in Table 2 of Duncker et al. (1991).

Relevant conclusions of this study are:

1. Quartz phenocrysts are out of oxygen isotopic equilibrium with host lavas. Some also have petrographic features that indicate derivation from metamorphic rocks (wavy extinction, internal recrystallized bands, included oriented needles of rutile). The total range in quartz oxygen isotopic composition is 4‰, indicating derivation from a variety of

crustal lithologies. There is no evidence for a mixed rhyolitic component in the Cerros lavas.

2. Two mantle magma sources are present among the Cerros lavas. One appears to be a local product of extension, while the other corresponds to ocean-basin sources of the E-MORB to tholeiitic OIB type. Both have been contaminated with continental crust; the MORB/OIB-like magmas appear to have interacted with both lower and upper crust.

3. The MORB/OIB-like magmas preferentially erupted late in the history of the field (i.e., *ca.* 2 Ma) from vents located beneath the Pajarito Plateau, i.e. close to the central Jemez Mountains (this conclusion is largely based on work by Dransfield and Gardner (1985) and D. Dethier (pers. comm.).

The MORB/OIB-like magmas are therefore temporally and spatially closest to the establishment of the Tewa Group magma system. As discussed above, they are also geochemically more appropriate as a Tewa component than the extension-produced lavas, and are therefore believed to represent the transport medium for the mantle thermal input which melted a substantial volume of crust (minimum 1,000 km^3) to ultimately yield the Bandelier Tuff and associated rhyolites. As outlined in our earlier report on grant DE-y5-85-ER13413, and in Self et al. (1988, 1991), we believe the products of this input to have largely been exhausted, probably by the time of the UBT eruption and certainly by 0.5 Ma. The current thermal regime of the Valles Caldera is probably dominated by the column of hot rock extending to the base of the crust (and probably the lithosphere) beneath the Jemez Mountains. Melt may still be present within this column, and may be capable of reaching the surface in small quantities, but - unless very recently established - there is probably no large magma body beneath the Valles Caldera at the present time.

References

Allen RL (1990) Subaqueous welding or alteration-diagenetic compaction and tectonic dissolution. IAVCEI International Volc. Congress, Mainz, Abstracts p.

Bailey RA, RL Smith and CS Ross (1969) Stratigraphic nomenclature of volcanic rocks in the Jemez Mountains, New Mexico. U.S. Geol. Surv. Bull. 1274P, 1-19.

Bailey RA and RL Smith (1978) Guide to Jemez Mountains and Espanola Basin. Circ. N.M. Bur. Mines Miner. Resour. 163, 184-196.

Balsley SD (1988) The petrology and geochemistry of the Tshirege Member of the Bandelier Tuff, Jemez Mountains volcanic field, New Mexico, USA. MS thesis, Univ. of Texas at Arlington, 188 pp.

Doell RR, GB Dalrymple, RL Smith and RA Bailey (1968) Paleomagnetism, potassium-argon ages, and geology of rhyolites and associated rocks of the Valles Caldera, New Mexico. Geol. Soc. Amer. Mem. 116, 211-248.

Duncker KE (1988) Trace element geochemistry and stable isotope constraints on petrogenesis of Cerros del Rio lavas, Jemez mountains, New Mexico. MS thesis, University of Texas at Arlington.

Duncker KE, JA Wolff, Harmon RS, Leat PT, Dickin AP and Thompson RN (1991) Diverse mantle and crustal components in lavas of the NW Cerros del Rio volcanic field, Rio Grande Rift, New Mexico. Contrib Mineral. Petrol 108, 331-345.

Dungan MA, MM Lindstrom, NJ McMillan, S Moorbath, J Hoefs and LA Haskin (1986) Open system magmatic evolution of the Taos Plateau volcanic field, northern New Mexico. 1. The petrology and geochemistry of the Servilleta basalt. J. Geophys. Res. 91, 5999-6028.

Gardner JN, G Goff, S Garcia, and RC Hagan (1986) Stratigraphic relations and lithologic variations in the Jemez volcanic field, New Mexico. J. Geophys. Res. 91, 1763-1778.

Gardner JN, F Goff, S Goff, L Maassen, K Mathews, D Wachs, D Wilson (1987) Core lithology, Valles Caldera #1, New Mexico. LA-10957-OBES, April, 1987, Los Alamos National Laboratory Report, 273 pp.

Goff F and JN Gardner (1987) Jemez volcanics cored in second D.O.E. hole. Geotimes 32, 11-12.

Goff F, J Rowley, JN Gardner, W Hawkins, S Goff, R Charles, D Wachs, L Maassen, and G Heiken (1986) Initial results from VC-1, first Continental Scientific Drilling

Program core hole in Valles Caldera, New Mexico. J. Geophys. Res. 91, 1742-1752.

Goff F, L Shevenell, JN Gardner, F-D Vuataz, and CO Grigsby (1988) The hydrothermal outflow plume of Valles Caldera, New Mexico, and a comparison with other outflow plumes. J. Geophys. Res. 93, 6041-6058.

Halliday AN, AE Fallick, J Hutchinson and W Hildreth (1984) A Nd, Sr, and O isotopic investigation of the Bishop Tuf, California. Earth Planet. Sci. lett. 94, 274-290.

Heiken GH, F Goff, J Stix, S Tamanyu, M Shafiqullah, S Garcia, R Hagan (1986) Intracaldera volcanic activity, Toledo caldera and embayment, Jemez Mountains, New Mexico. J. Geophys. Res. 91, 1799-1815.

Hervig RL and NW Dunbar (1989) Direct determinations of volatile gradients in the Bandelier Tuff through analysis of melt inclusions. NM Bur. Mines Miner. Resour. Bull. 131, 129.

Hulen JB and JN Gardner (1989) Field geologic log for Continental Scientific Drilling Program core hole VC-2B, Valles caldera, New Mexico. Earth Sci Lab MS ESL-89025-TR, 92 p.

Hulen JB, DL Nielson, TM Little (1991) Evolution of the western Valles Caldera complex, New Mexico: evidence from intracaldera sandstones, breccias, and surge deposits. J. Geophys. Res. 96, 8127-8142.

Hulen JB, JN Gardner, F Goff and others (1988a) Site-specific science plan for Continental Scientific Drilling Program core hole VC-2B, Sulphur Springs area, Valles caldera, New Mexico. Earth Sci Lab Publ ESL-88004-TR, 98 p.

Hulen JB, JN Gardner, DL Nielson and F Goff (1988b) Stratigraphy, structure, hydrothermal alteration and ore mineralisation encountered in CSDP corehole VC-2A, Sulphur Springs area, Valles Caldera, New Mexico: a detailed overview. Earth Sci Lab Publ ESL-88001-TR, 55pp.

Hulen JB, DL Nielson, F Goff, JN Gardner, RW Charles (1987) Molybdenum mineralization in an active geothermal system, Valles caldera, New Mexico. Geology 15, 748-752.

Hulen JB, JN Gardner, DL Nielson, F Goff (1988b) Stratigraphy, structure, hydrothermal alteration and ore mineralization encountered in CSDP Core hole VC-2A, Sulphur Springs area, Valles caldera, New Mexico: A detailed overview. Earth Sci. Lab. Publ. ESL-88001-TR, 44 p.

Izett GA, JD Obradovich, CW Naeser and GT Cebula (1981) Potassium-argon and fission-track zircon ages of Cerro Toledo rhyolite tephra in the Jemez Mountains, New Mexico. US Geol. Surv. Prof. Pap. 1199-D, 37-43.

Kuentz DC (1986) The Otowi Member of the Bandelier Tuff: a study of the petrology, petrography, and geochemistry of an explosive silicic eruption, Jemez Mountains, New Mexico. MS thesis, Univ. of Texas at Arlington, 168 pp.

Lipman PW (1984) The roots of ash flow calderas in western North America: Windows into the tops of granitic batholiths. Jour Geophys Res 89, 8801-8841.

Manley CR and JH Fink (1987) Internal textures of rhyolite flows as revealed by research drilling. Geology 15, 549-552.

McCormick TC (1989) Partial homogenization of cryptoperthites in an ignimbrite cooling unit. Contrib. Mineral. Petrol. 101, 104-111.

Musgrave JA, F Goff, L Shevenell, PE Trujillo Jr, D Counce, G Luedemann, S Garcia, B Dennis, JB Hulen, C Janik, FA Tomei (1989) Selected data from Continental Scientific Drilling Core Holes VC-1 and VC-2a, Valles Caldera, New Mexico. LA-11496-)BES, UC-403, Los Alamos National Laboratory, Los Alamos, New Mexico, 77 pp.

Nielson DL and JB Hulen (1984) Internal geology and evolution of the Redondo dome, Valles caldera, New Mexico. Jour Geophys Res 89, 8695-8711.

Palacz ZA and JA Wolff (1989) Strontium, neodynium and lead isotopic characteristics of the Grandilla pumice, Tenerife: a study of the causes of strontium isotope disequilibrium in felsic pyroclastic. In Saunders AD and MJ Norry (eds) Magmatism in Ocean Basins, Geol. Soc. ondon Spec. Pub. 42, 147-160.

Pyle DM (1989) The thickness, volume and grainsize of tephra deposits. Bull. Volcanol. 51, 1-15.

Scott RB (1971) Alkali exchange during devitrification and hydration of glasses in ignimbrite cooling units. J. Geol. 79, 100-110.

Self S, DE Kircher and JA Wolff (1988) The El Cajete Series, Valles Caldera, New Mexico. J. Geophys. Res. 93, 6113-6127.

Self S, F Goff, JN Gardner, JV Wright, WM Kite (1986) Explosive rhyolitic volcanism in the Jemez Mountains: vent location, caldera development and relation to regional structure. Jour. Geophys. Res. 91, 1779-1798.

Self, S, JA Wolff and D Kircher (1987) Volcanological investigation of the Banco Bonito eruption and subsurface geology of the ring fracture zone, Valles Caldera, New Mexico. Final technical report, US DOE Grant #DE-FG05-85ER13413.

Self S, JA Wolff, CE Skuba, MM Morrissey and TL Spell (1991) Revisions to the stratigraphy and volcanology of the post-0.5 Ma units and the volcanic section of VC-1 core hole, Valles caldera, New Mexico. J. Geophys. Res. 96, 4107-4116.

Sheridan MF (1970) Fumarolic mounds and ridges of the Bishop Tuff, California. Geol. Soc. Amer. Bull. 81, 851-868.

Skuba CE (1990) Sr, Nd, Pb and O isotopic constraints on the genesis and evolution of the Bandelier Tuff. MS thesis, Univ. of Texas at Arlington, 98 pp.

Spell TL (1987) Geochemistry of Valle Grande Member ring fracture rhyolites, Valles Caldera, New Mexico. Unpublished MS thesis, New Mexico Inst. of Mining and Technology, 212pp.

Spell TL and PR Kyle (1989) Petrogenesis of Valle Grande Member rhyolites, Valles Caldera, New Mexico: Implications for evolution of the Jemez Mountains magmatic systems. J. Geophys. Res. 94, 10379-10396.

Spell TL, TM Harrison and JA Wolff (1990) $^{40}Ar/^{39}Ar$ dating of the Bandelier Tuff and San Diego Canyon ignimbrites, Jemez Mountains, New Mexico: Temporal constraints on magmatic evolution. J. Volcanol. Geotherm. Res. 43, 175-193.

Spell TL and TM Harrison (in press) $^{40}Ar/^{39}Ar$ geochronology of post-Valles Caldera rhyolites, Jemez Mountains volcanic field, New Mexico. J. Geophys. Res.

Starquist, VL (1988) Core log Valles Caldera #2A, New Mexico. LA-11176-OBES, UC-66b, Los Alamos National Laboratory, 87 pp.

Stix J, F Goff, MP Gorton, H Heiken and SR Garcis (1988) Restoration of compositional zonation in the Bandelier silicic magma chamber between two caldera-forming eruption. J. Gephys. Res. 93, 6129-6147.

Turbeville BN and S Self (1988) San Diego Canyon Ignimbrites: Pre-Bandelier Tuff explosive rhyolitic volcanism in the Jemez Mountains, New Mexico. J. Geophys. Res. 93, 6148-6156.

Watson EB and TM Harrison (1983) Zircon saturation revisited: temperature and composition effects in a variety of crustal magma types. Earth Planet Sci Lett. 64, 295-304.

Wolff JA (1985) The effect of explosive eruption processes on geochemical patterns within pyroclastic deposits. Jour. Volcanol. Geotherm. Res. 26, 189-201.

Wolff JA, G Wörner and S Blake (1990) Gradients in physical parameters in zoned felsic magma bodies: implications for evolution and eruptive withdrawal. J. Volcanol. Geotherm. Res. 43, 37-55.

Table 1: Oxygen isotope analyses (after Skuba 1990 Table 3)

Sample No.	Phase	$\delta^{18}O$ (‰)	qz-fsp (‰)	qz-gl (‰)	f - g (‰)
Lower Bandelier Tuff (Otowi Member)					
11-14	quartz	7.68			
	feldspar	7.33	+0.35	-2.02	-2.37
	glass	9.70			
13-2	quartz	7.77			
	feldspar	7.16	+0.61	-1.61	-2.22
	glass	9.38			
17-3	quartz	7.79			
	feldspar	7.42	+0.37	-2.30	-2.67
	glass	10.09			
17-29	quartz	7.77			
	feldspar	7.17	+0.60	-1.93	-2.53
	glass	9.70			
17-31	quartz	7.91			
	feldspar	7.78	+0.13	-1.77	-1.90
	glass	9.68			
Upper Bandelier Tuff (Tshirege Member)					
8-12	quartz	7.54			
	feldspar	7.72	-0.18	-2.05	-1.87
	glass	9.59			
8-38	quartz	7.95			
	feldspar	7.31	+0.64	+0.20	-0.44
	glass	7.75			
20-55	quartz	8.07			
	feldspar	6.84	+1.23	-0.66	+1.89
	glass	8.73			
22-50	quartz	7.76			
	feldspar	7.48	+0.28	-1.79	-2.07
	glass	9.55			
22-70	quartz	7.78			
	feldspar	6.37	+1.41	-0.29	-1.12
	glass	7.49			

All glass separates pre-fluorinated

Table 2: Sr isotopic analyses (from Skuba, 1990, her p. 78)

Sample No.	Rb (ppm)	Sr (ppm)	Rb/Sr	$^{87}Rb/^{86}Sr$	$(^{87}Sr/^{86}Sr)_m$	$(^{87}Sr/^{86}Sr)_i$
San Diego Canyon Ignimbrite						
861-6	148.00	5.07[a]	29.19	84.45	0.710782±16	0.70865
Lower Bandelier Tuff (Otowi Member)						
11-85-2	73.00	1000.[c]	0.07	0.21	0.704450±5	0.70445
11-85-P5	187.00	47.75[a]	3.91	11.35	0.730673±7	0.73043
13-2	348.75	5.79[a]	60.13	174.32	0.712604±20	0.70887
17-29	281.98	4.67[a]	60.00	174.72	0.710820±17	0.70707
17-31	119.05	5.43[a]	21.95	63.43	0.708528±9	0.70717
17-31 fsp	47.61[a]	18.04[a]	2.65	7.63	0.706612±21	0.70645
Upper Bandelier Tuff (Tshirege Member)						
8-20	353.90	18.71[a]	18.93	54.71	0.707033±14	0.70615
8-20 fsp	97.18[a]	19.94[a]	4.88	14.10	0.707110±18	0.70688
8-38	336.11	7.80[a]	43.09	124.66	0.708270±18	0.70625
8-38 fsp	107.22[a]	19.11[a]	5.61	16.23	0.707281±25	0.70702
20-35	88.65	225.34	2.54	1.14	0.704693±8	0.70467
20-51 fsp	109.[b]	210.[b]	0.52	1.50	0.704150±3	0.70413
20-53	158.35	16.77[a]	9.44	27.32	0.708080±19	0.70764
22-70	178.51	432.78	0.41	1.19	0.704090±4	0.70407
27-9	295.64	45.66[a]	6.47	18.73	0.709364±16	0.70906
Local crust						
B4	112.00[a]	394.29[a]	0.29	0.82	0.722180±4	0.72216
B8	181.74.	164.84[a]	1.10	3.21	0.768150±4	0.76806
SdCl-a	40.	176.	0.23	0.66	0.713640±5	0.71362
SdCl-b	35.63[a]	180.50[a]	0.22	0.57	0.713110±5	0.71309

All isotopic ratios were determined on whole rock powders except where noted.
fsp = feldspar separate
[a] : by isotope dilution; all others by XRF
[b] : whole rock values
[c] : estimate based on concetration of Ba

Table 3: Nd isotopic analyses (after Skuba, 1990, p. 80)

Sample No.	Sm (ppm)	Nd (ppm)	$^{147}Sm/^{144}Nd$	$^{143}Nd/^{144}Nd$
San Diego Ignimbrite				
861-6	7.39	34.30	0.1208	0.512662±20
Lower Bandelier Tuff (Otowi Member)				
11-85-2	10.80	59.30	0.1096	0.512640±2
11-85-P5	14.28	57.90	0.1484	0.512511±9
13-2	11.10	39.90	0.1674	0.512624±6
17-29	11.50	44.50	0.1555	0.512617±6
17-31	5.80[1]	30.76[1]	0.0978	0.512664±12
Upper Bandelier Tuff (Tshirege Member)				
8-20	10.90	39.50	0.1661	0.512501±8
8-38	10.80	44.80	0.1451	0.512493±10
20-35	8.20	44.90	0.1099	0.512500±7
20-51	12.00	60.40	0.1196	0.512494±9
20-53	14.20	69.10	0.1234	0.512490±7
22-70	5.10	25.80	0.1109	0.512490±25
27-9	11.10	40.30	0.1658	0.512505±12
Local crust				
B4	8.82[a]	42.94[a]	0.1236	0.511983±11
B8	10.49[a]	60.56[a]	0.1043	0.511797±15
SdCl-a	n.d.	n.d.	n.d.	0.512696±28
SdCl-b	3.18[a]	10.80[a]	0.1328	0.512671±35

n.d. = not determined
All isotopic ratios determined on whole rock powders
[a] : by isotope dilution; all others by INAA

Table 4. Pb isotopic analyses (after Skuba 1990 p. 80)

Sample No.	U,ppm	Th,ppm	Pb,ppm	$^{206/204}Pb$	$^{207/204}Pb$	$^{208/204}Pb$
San Diego Canyon Ignimbrite						
861-06	6.90	19.24	n.d.	17.79	15.49	37.52
Otowi Member						
11-14			n.d.	17.94	15.51	37.65
13-2	16.40	42.30	46.30	17.81	15.51	37.60
13-2 fsp			n.d.	17.93	15.54	37.83
17-3			n.d.	17.88	15.54	37.76
17-29	12.80	35.0	10.56	17.85	15.52	37.66
17-29 fsp			n.d.	17.85	15.55	37.76
17-31	n.d.	n.d..	8.29	17.85	15.52	37.67
27-31 fsp			n.d.	17.92	15.51	37.67
Tshirege Member						
8-12	12.90	37.60	55.90	17.92	15.54	37.81
20-53	5.30	18.30	53.00	17.95	15.53	37.80
20-55	5.50	20.20	36.36	17.94	15.53	37.79
20-55 fsp			n.d.	17.91	15.51	37.71
22-70	2.20	7.70	36.90	17.89	15.53	37.77
SU IV	5.80	19.50	16.60	17.95	15.52	37.75
Local crust						
B4	n.d.	n.d.	21	17.76	15.52	36.94
B8	n.d.	n.d.	25	18.77	15.62	38.11
SdCl-a	n.d.	n.d.	7	18.27	15.55	37.55
SdCl-b	n.d.	n.d.	13	19.41	15.70	38.79

n.d. : not determined
All isotopic ratios determined on whole rock powders except where noted
fsp = feldspar separate

APPENDIX 1: VC-1 Core Hole Data

Appendix 1A: Detailed Log

Key to textures:

Pumice: C = coarse, M = medium, F = fine

Lithics: C = coarse, M - medium, F = fine

Groundmass: P = pyroclastic, E = epiclastic, B =

Welding: D = dense welding, M = moderate welding, I = incipient welding

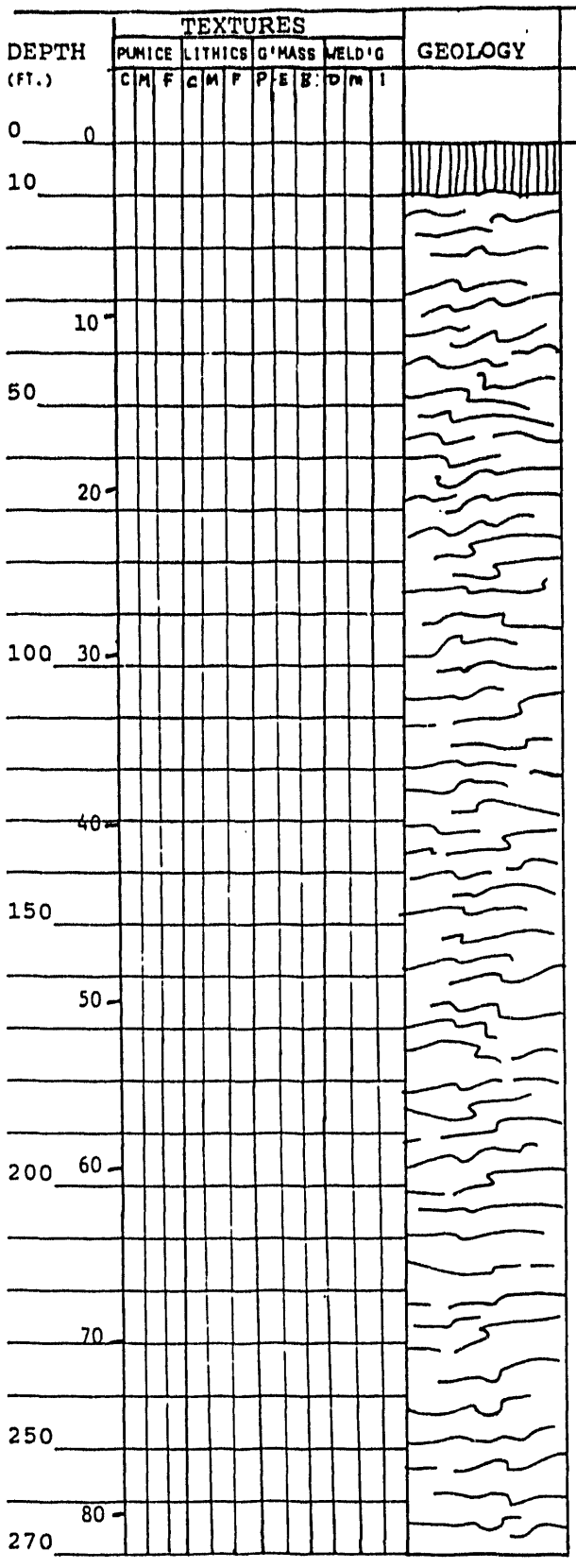
TEXTURES
DEPTH
(FT.)
PUMICE
LITHICS
G'MASS
WELD'G
C M F C M F P E G D M I
GEOLOGY
DESCRIPTION
0
0
10
10
50
20
100
30
40
150
50
200
60
70
250
80
270
Soil
BANCO BONITO LAVA - not logged in any detail; see notes at 240 ft and near base of unit
No evidence for flow unit boundary here

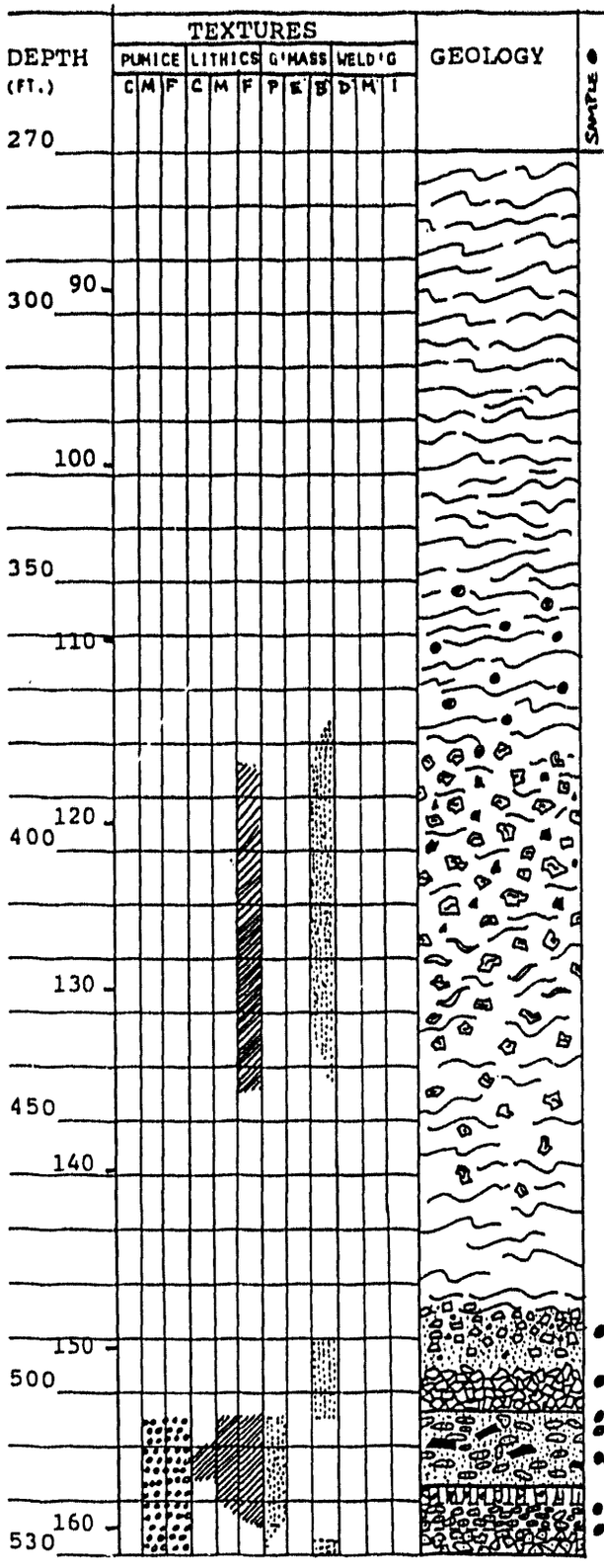

DESCRIPTION

BANCO BONITO LAVA · continued·

Zone of lithophysae.

Base of more·or·less massive lava.

Top of extensive brecciated lava section; ? separate flow unit

Breccia contains lithic clasts (vent debris); could be breccia pile at base of paleo·valley wall?

Clayey stringers mixed in with lava; not lacustrine sediment; possibly ground·up and devitrified pumiceous material.

Lava less brecciated.

Unbrecciated lava, some pumiceous lava.

Finer breccia; clasts of pumiceous lava, devitrified in places

Ground·up pumiceous lava gives ashy appearance.

Sparse small lithics.

Matrix·free pumiceous lava breccia with fractures through clas

?Base of Banco Bonito at 503±1 ft.

Pumice·rich deposit with matrix; non·welded; ignimbrite and andesite lithics < 8 cm: pyroclastics at base of BB lava.

Rubbly zone with soil: time break.

Pumice (?) deposit; may be reworked, related to VC·1 Rhyolite.

Pumiceous breccia at top of VC·1 Rhyolite lava.

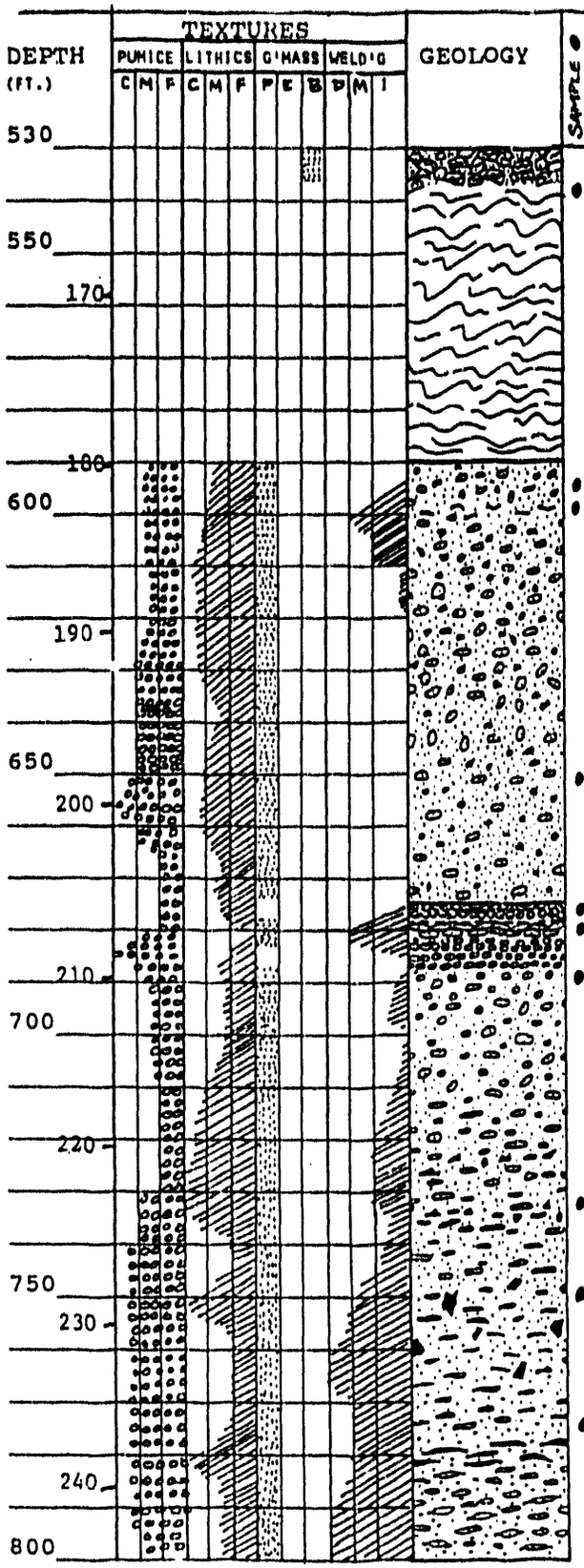

DESCRIPTION

Indurated pumice flow-top breccia w/ obsidian clasts and banded pumice, includes ashy gouge zone in top of lava.

VC-1 RHYOLITE LAVA FLOW - flow banded obsidian.

Porous flow-banded obsidian

Non-welded lithic-rich, buff colored ignimbrite; crystal-poor; slightly indurated - small brownish fiamme at 600 ft.

BATTLESHIP ROCK IGNIMBRITE - UPPER COOLING UNIT

Lithic-rich, incipiently welded ignimbrite: lithics may be welde Upper Bandelier ignimbrite.

?Base of flow unit.

Recovery rubbly: incipiently welded, lithic-rich unit, probably fines-poor pyroclastic flow deposit.
Non-welded, lithic-rich, fines-poor becoming fines-rich below; welded crystal-rich ignimbrite lithics are common

Homogenous, incipiently welded, crystal-poor, buff ignimbrite.

Base of upper cooling unit (upper set of flow units) of Battles Rock ignimbrite.
Medium-grained, matrix-free, bedded pumice layer (? fall unit) over 6" thick; overlies welded deposit of deformed pumices; la clasts - flow unit top?

Pumice fall with obsidian grading down to incipiently welded gr matrix-poor ignimbrite. By color, fall layers above related to these flows. Relatively crystal-poor juvenile material.

Same incipiently welded ignimbrite.

Welding gradually increasing down hole; some lithic-rich horiz pumices deformed and become brownish; matrix grey.

BATTLESHIP ROCK IGNIMBRITE - LOWER COOLING UNIT

Welded grey ignimbrite with well-developed fiamme and scattere coarse lithics, some of Upper Bandelier ignimbrite.

Ignimbrite densely welded, grey; very similar appearance to Battleship Rock in surface exposures.

Zone of large fiamme (> 10 cm); ? top of flow unit.

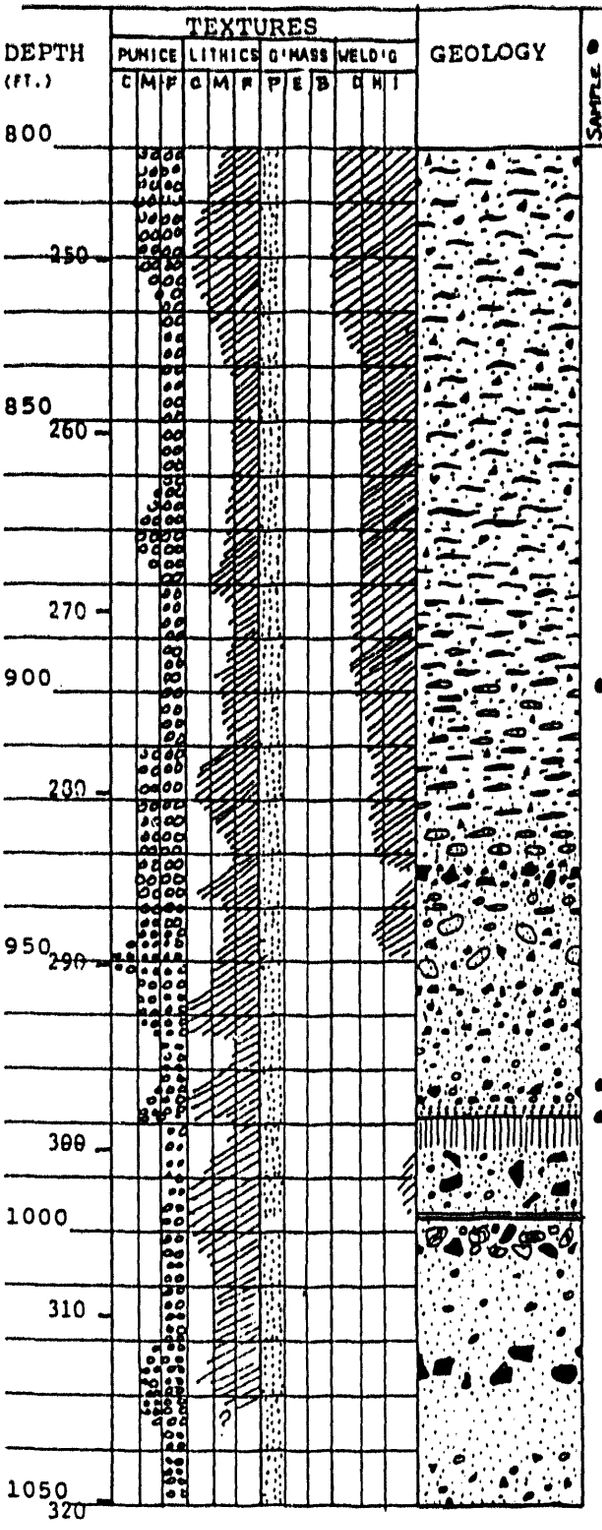

DESCRIPTION

BATTLESHIP ROCK IGNIMBRITE (cont'd)
Grey, densely welded, lithic-rich, crystal poor. Flamme - 3-5 cm; lithics - 4-5 cm.

Color change grey - brownish.

BATTLESHIP ROCK IGNIMBRITE - LOWER COOLING UNIT

Some larger flamme.

Densely welded but grade decreasing slightly.

Lithic concentration (?pod); ignimbrite less welded around it.

Grey, moderately welded ignimbrite.
Scattered large pumices, lithic swarm.
Buff, non-welded, lithic-rich ignimbrite.
>2 lithic-rich stringers; typical of lower parts of flow unit

Non-welded, lithic-rich base of ignimbrite.

Fine to medium-grained ash with carbon (2-3 cm thick); fall or surge at base of BR ignimbrite.
Soil w/carbonized vegetation and andesite fragments; brown, very altered, soilified ignimbrite with dark brown rhyolite clasts.
Some large clasts of ?welded upper Bandelier tuff in altered matrix buff, non-welded ign. where not altered; lithic rich.
Tan clay-alteration zone in ignimbrite.
Coarse clast rich zone; poorly vesicular South Mountain-type material (perhaps juvenile to this deposit) intermixed with coarse Bandelier Tuff clasts - a very altered, coarse zone.

Very altered ?ignimbrite - alteration zones becoming patchy.
Large lithics of Bandelier Tuff.

Very altered and "punky"; same unit.

Altered lithic-rich, non-welded ignimbrite: probably South Mountain Rhyolite pyroclastic flow deposit.

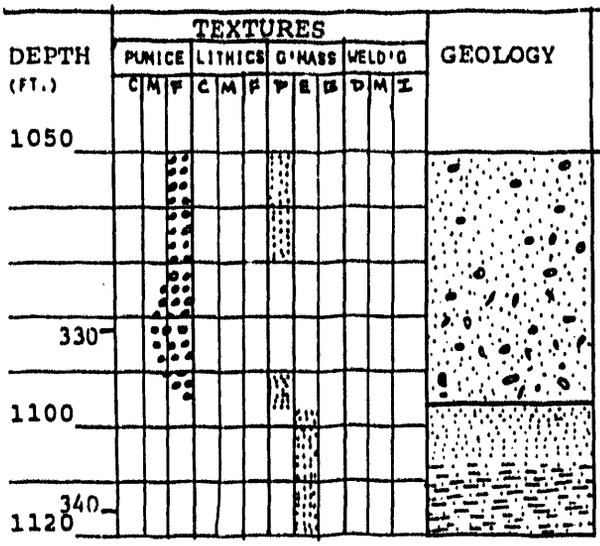

DESCRIPTION

Altered, non-welded South Mountain Rhyolite-age pyroclastic flow deposit.

(Rhyolite clast from this zone dated by JNG at ~ 0.6 Ma)

Very mixed-up zone: ignimbrite material appears to be somehow mixed into red sandstone material from below (?artifact of drilling?).

-Base of pyroclastic unit at 1097 ft (334.5m)
White sandstone - top of ABO FORMATION
Red siltstones

Appendix 1B: Detailed descriptions from hand samples and thin sections

APPENDIX 1B

VC-1 Core: Summary hand sample and petrographic descriptions

Unit
Depth (ft) Description

Banco Bonito Lava Flow 11'-503'

489.25-.65'Core: glassy rhyolitic lava flow. This sample occurs in an unbrecciated interval within a brecciated zone.

LA: Battleship Rock Ignimbrite: tan crystal-lithic welded tuff.

GG: Banco Bonito Obsidian

497.5' Core: agglutinated breccia of flow-banded and non-flow banded lava and pumiceous clasts. Flow banded clasts have random orientation. The breccia is clast supported with some pore space.

TS: Glassy pumiceous breccia, unaltered. In plane light, there are both a clear and a tan glass component. Crystals include dispersed acicular to lath-shaped crystals of hornblende and clots of hornblende, biotite, plagioclase and pyroxene. Hornblende grows at the expense of biotite. In the tan glass there is a phase with high relief and low birefringence. Plagioclases are wormy and resorbed. Alkali feldspar is exsolved, all show disequilibrium. Occasional quartz present with patchy undulose extinction. Crystal clots are sometimes surrounded by patches of non-vesicular tan glass.

Interp: pumiceous breccia at base of Banco Bonito lava flow. Clasts come from the pumiceous part of the Banco Bonito lava flow.

Chem: mafics, feldspar and glass suitable for chemistry.

LA: Battleship Rock Ignimbrite: white weathered crystal-lithic welded tuff.

GG:

Banco Bonito related pyroclastic flow deposit 503'-521'

503' Core: Volcanic matrix-supported breccia; about 20% clasts. Pale, buff-gray, sugary matrix. Clasts of (1) dense, dark gray pumices(?) or lava fragments; (2) yellowish buff gray, more vesicular pumices; (3) red-brown dense lithic clasts about 1-3 mm diam. No large lithics. Two clast size groups: (a) large clasts avg 1-2 cm diam, (b) smaller clasts avg 1-3 mm diam, a few intermediate as well. Crystals include biotite flakes, small hornblende crystals, and feldspar crystals.

Interp: Grain size distribution suggest this is a pyroclastic flow deposit beneath the Banco Bonito lava flow.

LA: Battleship Rock Tuff: white weathered crystal-lithic welded tuff.

GG: Battleship Rock Tuff

508' Core: Exactly like sample from 503'.

Interp: pyroclastic flow deposit beneath the Banco Bonito lava flow.

LA: Battleship Rock Tuff: White weathered crystal-lithic welded tuff.

GG: Battleship Rock Tuff

513.3' Core: Volcanic matrix-supported breccia. Very similar to sample at 503' but with 30-40% lithics, some large (see sample at 514.1-.4 ft). Clasts include the dark red-brown dense volcanic lithics. Crystals include biotite flakes, small hornblende(?) crystals, and larger (2-3 mm) vitreous, clear crystals.

TS: Pumice-rich volcanic tuff (pyroclastic flow), in part matrix-supported. Very similar to 497.5' in pumice appearance and mineralogy. Absence of the tan glass phase around mafic crystal clots. Crystals include plagioclase and alk feldspar with rare quartz. Shards are clearly visible in the matrix, indicating pyroclastic origin. Incipient alteration of matrix; pumices are fresh. Biotite is oxidized and the plagioclase wormy and resorbed. Lithic of reddish tuff is welded ignimbrite with spherulitically devitrified pumices.

Interp: Banco Bonito-related pyroclastic flow deposit with lithics, the same deposit as at 503' and 508'.

Chem: Mafics good and feldspars possible for analysis.

LA: Battleship Rock Tuff: white weathered crystal-lithic welded tuff.

GG: Battleship Rock Tuff

514.1-.4' Core: Reddish-brown densely welded, altered tuff. Fiamme are purplish. Opaque white circular blebs $\leq$ 5 mm diam are scattered throughout the matrix; probably a feldspar. Fiamme are oriented at -45° to core.

TS: Iron-stained welded very crystal-rich tuff. Shards and welding structures clearly visible. Pervasive but uneven staining of matrix to orange-red and black. Matrix has fibrous devitrification products and patches of granophyric devitrification (mosaics). Crystals are so abundant that they support the matrix. Crystals consist of medium to large feldspar, quartz, and plagioclase. Most plagioclases are resorbed or wormy. No hornblende, biotite or pyroxene. Some pumices show spherulitic devitrification.

Interp: Lithic fragment, possibly of Bandelier Ignimbrite, in a Banco Bonito-related pyroclastic flow. Stratigraphically this is still the Banco Bonito-related pyroclastic flow.

Chem: Feldspars suitable for analysis.

LA: Battleship Rock Tuff: white weathered crystal-lithic welded tuff.

GG: Battleship Rock Tuff

520.8' Core: Same as sample at 513.3'.

Interp: base of Banco Bonito-related pyroclastic flow deposit ?or rubbly zone with soil at base of BB-related pf?

LA: weathered soil at base of Battleship Rock Tuff.

GG: Battleship Rock Tuff

VC-1 Rhyolite Lava Flow 527'-590'

524.6' Core: Glassy, gray welded pumiceous breccia. Pumices are only partially collapsed if at all. Uniform color, no lithics, pumices distinguished by vesicular texture. Crystals include biotite flakes, small hornblende/opaques, and feldspar (clear vitreous 2-3 mm diam).

TS: A single large pumice clast with only very minor devitrification. Abundant dispersed small green hornblende crystals, large biotite flakes. Plagioclase and alkali feldspar crystals are mottled and wormy and partly resorbed.

Interp: Pumiceous carapace of VC-1 Rhyolite.

Chem: Mafics suitable and feldspars okay for analysis.

LA: reworked zone of rhyolite and lithic fragments at base of Battleship Rock Tuff

? GG: VC-1 Rhyolite

538.3-.6' Core: Very dense glass: lava flow. Some crystals, clear to white.

Interp: VC-1 Rhyolite.

LA: VC-1 Rhyolite black sparsely porphyritic obsidian with alternating zones of flow banded, perlitic, splintered obsidian.

GG: VC-1 Rhyolite

Battleship Rock Ignimbrite (590'-978')

Upper Cooling Unit (590'-674.4')

593.6-4.1'Core: Densely welded tuff. Tan-flesh pumices are collapsed, about 1 cm long and 1-2 mm thick. One dark clast 2-3 cm long, 1 cm thick, possibly fiamme. Irregular, amoeboid clasts. Small, dark lithics, avg 2-3 mm diam. Small crystals in matrix.

TS: Very densely welded tuff, very crystal rich. Very similar to sample at 514.1-.4', but with less staining. No mafic crystals observed. Spherulitic to fibrous devitrified pumice, altered feldspar, etc.

Interp: Lithic fragment, possibly of Bandelier Tuff, within the Battleship Rock Ignimbrite.

Chem: Feldspars suitable for analysis.

LA: Upper Bandelier Tuff: baked dull orange lithic-rich welded tuff.

GG: VC-1 Tuff

598.9-9.1'Core: Slightly welded buff-colored tuff. Matrix powdery but not sugary. Matrix-supported. Clasts vary from 1 mm to 1 cm diam, including ?dense, black, brown and red fragments; some light colored pumices. Small mafic crystals (hornblende)?

Interp: Battleship Rock Ignimbrite, top of section

LA: Upper Bandelier Tuff: dull orange lithic-rich welded tuff.

GG: VC-1 Tuff

651.7-2.3'Core: Moderately welded tuff, very similar to sample at 598.9' but more welded. Lithics are larger and more discernible; contain the reddish salami-like dense volcanic rock.

TS: Nonwelded pumice-rich tuff with abundant small crystals **[note in log describe as crystal-poor]**. Incipiently devitrified matrix and pumices. Hornblende, biotite, magnetite plus wormy, resorbed feldspars. Rare quartz. Lithics of lavas or shallow intrusive intermediate composition rocks.

Interp: Battleship Rock Ignimbrite.

Chem: Mafics, feldspar, and glass probably okay for analysis.

LA: Upper Bandelier Tuff: white to pink lithic-rich welded tuff.

GG: VC-1 Tuff

Battleship Rock Ignimbrite

Lower Cooling Unit (674.4'-978')

674.4-.6' Core: Crystal-rich "agglutinated" clast-supported breccia. Clasts are 1-3 mm to 1 cm diam, and are white, gray, buff or black. Abundant euhedral, black, vitreous crystals. Some lithics of dense reddish volcanics.

Interp: Fall unit just below base of upper flow unit of VC-1 (= Battleship Rock) pyroclastic flow.

LA: Tsankawi? gray lithic-rich ash and lapilli tuff.

GG: VC-1 Tuff

681.1' Core: Cohesive pumice-rich tuff. Matrix-supported, some areas are clast supported. Pumices up to 5 cm diam or more are dark gray; some smaller ones (1-3 cm) are white. Matrix gray-buff. Some gray pumices have white edges. No preferred alignment or foliation.

TS: Welded, incipiently devitrified tuff with moderately abundant very small crystals of hornblende, pyroxene and ?biotite. Small feldspars are mostly wormy or resorbed, occasional large feldspar crystals. Occasional glassy lithics.

Interp: Welded pumice deposit beneath base of upper cooling unit (upper set of flow units) of Battleship Rock Ignimbrite.

Chem: Mafics suitable for analysis, feldspar okay.

LA: Gray lithic-rich ash-flow tuff between the ?Tsankawi and Lower Bandelier Tuff.

GG: VC-1 Tuff

690.4-.8' Core: Nonwelded tuff, matrix-supported. Dirty gray matrix is sugary; clasts are 2-5 cm diam and buff-gray and

black. Biotite flakes and small ?hornblende crystals; large (2-3 cm diam) lithics.

Interp: Upper part of second cooling unit of Battleship Rock Ignimbrite.

LA: Lower Bandelier Tuff: white to pink lithic-rich welded tuff; a prominent parting occurs here.

GG: VC-1 Tuff.

732.5-.8' Core: Densely welded pumice-rich pyroclastic flow. Pumices are slightly flattened, dense, and dark gray, upt o 5 cm diam. Small pumice clasts are white-gray or black. Crystals include hornblende and clear vitreous phase (alkali feldspar). Small clasts are also abundant (2-5 mm diam). Nearly clast-supported.

TS: Moderately welded pumice-rich pyroclastic flow. Abundant small hornblende, pyroxene and occasional biotite crystals. Rare large plagioclast/alkali feldspar crystals, mostly wormy and resorbed. Occasional glassy lithic. Incipient devitrification of matrix and pumices. Often mafics and plagioclase occur in clots. Alkali feldspar is exsolved.

Interp: Middle of lower cooling unit of Battleship Rock Ignimbrite.

Chem: Mafics suitable for analysis, feldspars okay.

LA: Lower Bandelier Tuff: gray densely welded lithic-rich tuff.

GG: VC-1 Tuff

750.0-.1' Core: same as 732.5'.

Interp: Lower cooling unit of Battleship Rock Ignimbrite.

LA: Lower Bandelier Tuff: gray densely welded lithic-rich tuff.

GG: VC-1 Tuff

776.3' Core: Very densely welded tuff with large (10 cm diam) pumices; smaller pumices have collapsed or flowed. Large (3-5 cm diam) undeformed lithics of reddish-black volcanic rock. Gray matrix. Same crystals as in 732.5'.

Interp: Welded zone near fiamme horizon (possible flow unit boundary) in lower cooling unit of Battleship Rock Ignimbrite.

LA: Lower Bandelier Tuff: gray densely welded lithic-rich tuff, with large dense glassy fiamme.

GG: VC-1 Tuff.

898.8-9.0 Core: Welded, matrix-supported tuff. Matrix is a pinkish-beige/gray; clasts are dark gray or white/cream, < 1 mm - 2 cm diam. Black vitreous hornblende crystals and altered biotite crystrals apparent.

Interp: Densely welded zone of lower cooling unit of Battleship Rock Ignimbrite.

LA: Lower Bandelier Tuff: gray welded tuff with lithic fragments and fiamme.

GG: VC-1 Tuff.

973.3 Core: Matrix supported welded tuff with a clast-supported lithic pod. Matrix pale yellow/cream; pumice clasts are white-gray and appear silky. Lithics are black, brown, gray and red. Biotite crystals.

TS: Black-stained tuff, no welding apparent, with abundant small pumice clasts. Pumice clasts vary in vesicularity. Contains a large lithic clast of spherulitically devitrified rhyolite ?lava. No devitrification of pumices or matrix apparent. Rare biotite, some pyroxene and hornblende. Small feldspar crystals, occasionally large wormy and resorbed feldspar crystals. Lithics of spherulitic devitrified tuff or lava.

Interp: Base of lower cooling unit of Battleship Rock Ignimbrite. Nonwelded, lithic-rich.

Chem: Mafics and glass suitable for analysis; feldspars okay.

LA: Pre-Bandelier Tuff: gray-white lithic-rich welded tuff.

GG: VC-1 Tuff.

Appendix 2: VC-2A Core Hole Data

Appendix 2A: Detailed log

Note: dips of units not shown on columnar diagram of core.

● = sampled interval; thin sectioned

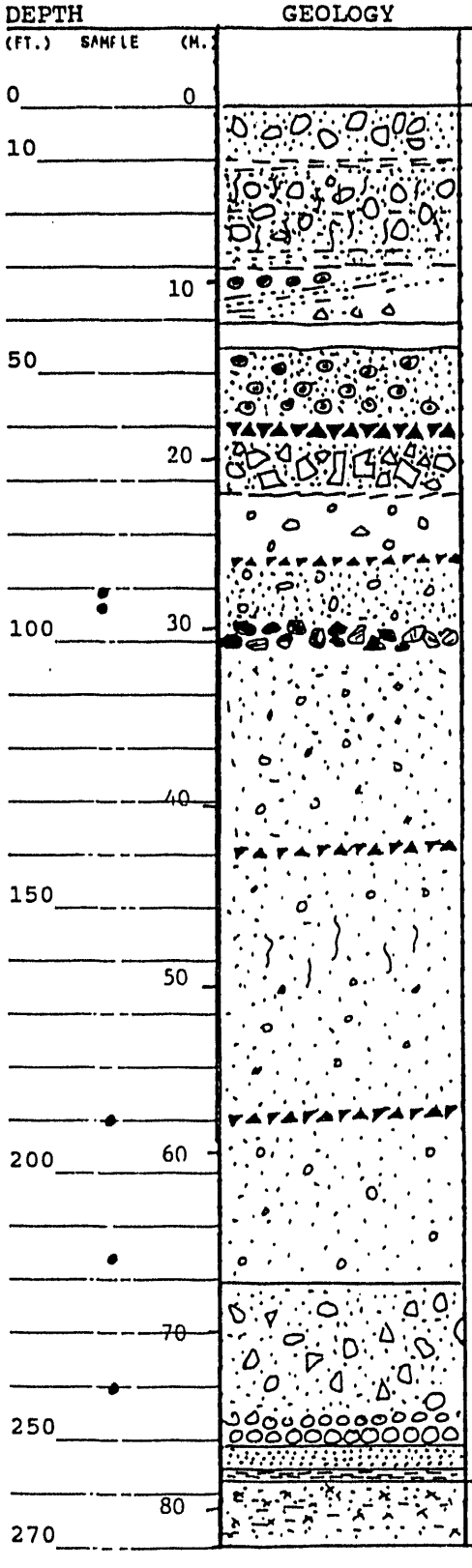

DEPTH (FT.)	SAMPLE	(M.)	GEOLOGY	DESCRIPTION
0		0		Coarse dense clasts in ashy matrix; local explosion or landslide breccia, probably latter.
10				Bedded ash & crystal-rich layers; ?primary or reworked. Local deposits associated with Sulphur Springs hydrothermal field.
				As above; explosion breccia or tuff ring sequence?
				Beds ~horizontal; relationships obscure due to clayey alteration.
		10		?Contact; slight angular disconformity.
				Ashy sediments; possibly reworked tuff ring material. Contains accretionary lapilli (0.3 cm); bedded with dips up to 15°. Might be surge deposit.
50				Lost core.
				Accretionary lapilli, fines-poor ashy sediment, looks reworked.
				Primary ash bed with accretionary lapilli; quite massive; phreatomagmatic tuff.
		20		Very brecciated and altered along fracture zone.
				Landslide breccia or explosion breccia: coarse angular clasts; ?nature of contact problematic-fault? at 71 ft.
				White, fine-grained, non-welded ignimbrite; flattening of some pumice clasts due to alteration. Pyritized; some grey, fine-grained pumice. Fault gouge at ~86 ft. All one flow unit: source?? [other possibility is a pumiceceous mudflow].
100		30		Lithic clasts of sandstone and welded ign; ML 5-10 cm. Could be lithic concentration at base of flow unit. Quite matrix-poor at 100'.
				>Matrix & small fiamme: moderately welded ignimbrite; smaller-lithics.
				Intense purple alteration.
				Possibly some flow unit boundaries in this ignimbrite marked by pumice and lithic concentrations: textures masked by alteration; welding decreases; dip ~15°; mineralization extensive.
		40		Zone of brecciation in greyish, moderately-incipiently welded ignimbrite with low crystal content.
150				>Lithics; ML 3-4 cm; ?flow unit boundary
				Same grey, moderately welded ignimbrite with blotchy alteration and mineral-filled fractures.
		50		Ignimbrite, poor in coarser pumice clasts; occasional lithics; dip ~15°.
				"UPPER TUFFS"
				Fault: altered, brecciated zone.
200		60		Same ignimbrite as above, bleached and altered.
				White, nonwelded ignimbrite with >larger pumices; nonwelded. No accretionary lapilli present.
				Breccia of angular lithics (some andesite) and pumice up to 5 cm. Some rounded cobbles. Matrix present but of ? origin; either a debris flow deposit or a lithic-rich ignimbrite. Very altered.
		70		Larger clasts and better sorted at base of ignimbrite.
250				S_2 sandstone; bleached, fine-grained, fluviatile sand overlying mudstone.
				Crystal-rich sandstone - reworked top of Upper Bandelier ignimbrite.
		80		
270				

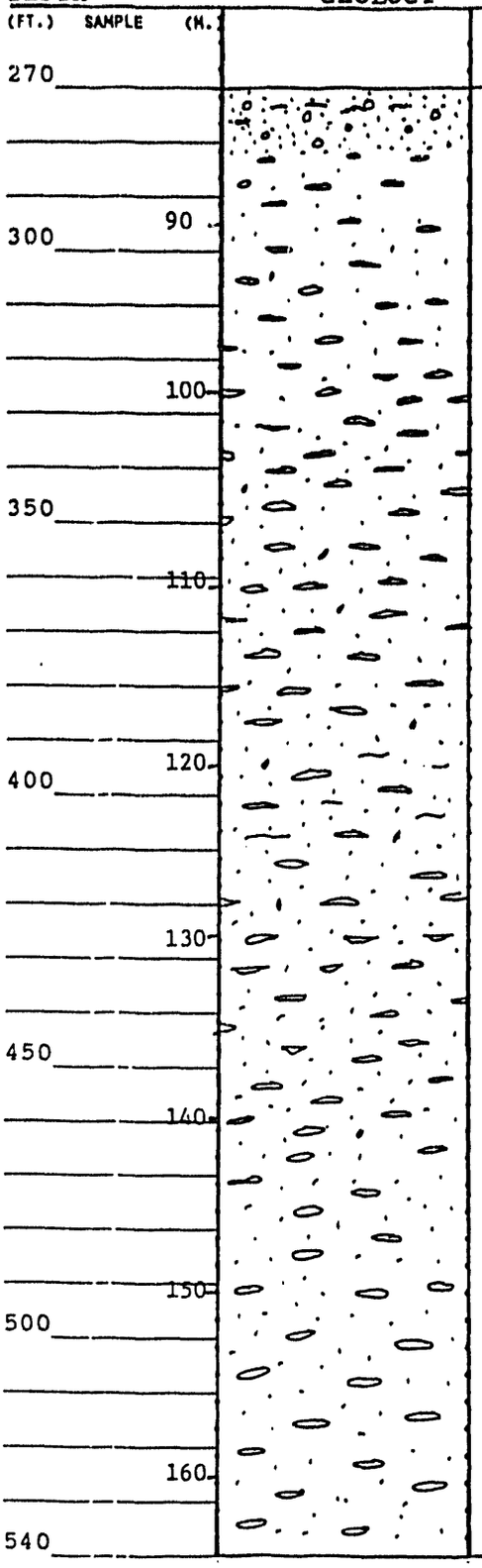

DESCRIPTION

UPPER BANDELIER TUFF (cont'd)

Crystal-rich, non-welded ignimbrite, becoming > indurated; very small lithics (< 1 cm); small fiamme at ~ 275', dips of foliation 20-25°.

Densely welded, grey, crystal-rich Upper Bandelier Tuff.

UPPER BANDELIER TUFF: very monotonous; no flow unit boundaries. Sparse, small lithics; locally no dip to fiamme, possibly due to local faulting.

Alteration extensive; fault breccias as noted in Hulen et al. (1988) core log.

Slight decrease in welding.

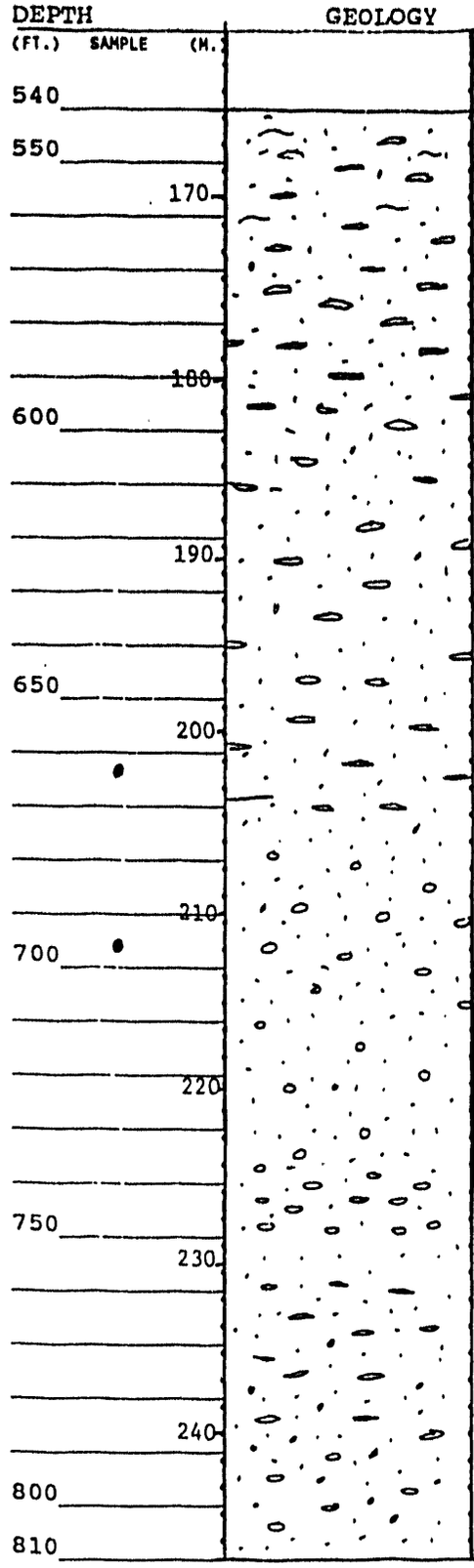

DESCRIPTION

UPPER BANDELIER TUFF (cont'd)

Blotchy alteration in welded Upper Bandelier Tuff (UBT).

More bleached, slightly less welded ignimbrite; a few fiamme; dip of foliation variable ~ 15-40°; sparse lithics.

Grey UBT becomes < welded: altered pumices; color change at 694 ft; pumices are white; lithics < 1 cm. Bottom of upper cooling unit of UBT, but no obvious flow unit boundaries.
White, incipiently welded ignimbrite; dip of foliation ~25-40°.

Ignimbrite slightly compacted; incipient welding.

Color darkens, fiamme present. Buff-brownish; high crystal content; patchy welding.

Densely welded, buff UBT; no large fiamme; dip of foliation ~30° ML=1.2 cm (sparse).

>Lithics with poorly vesicular, non-porphyritic pumices.

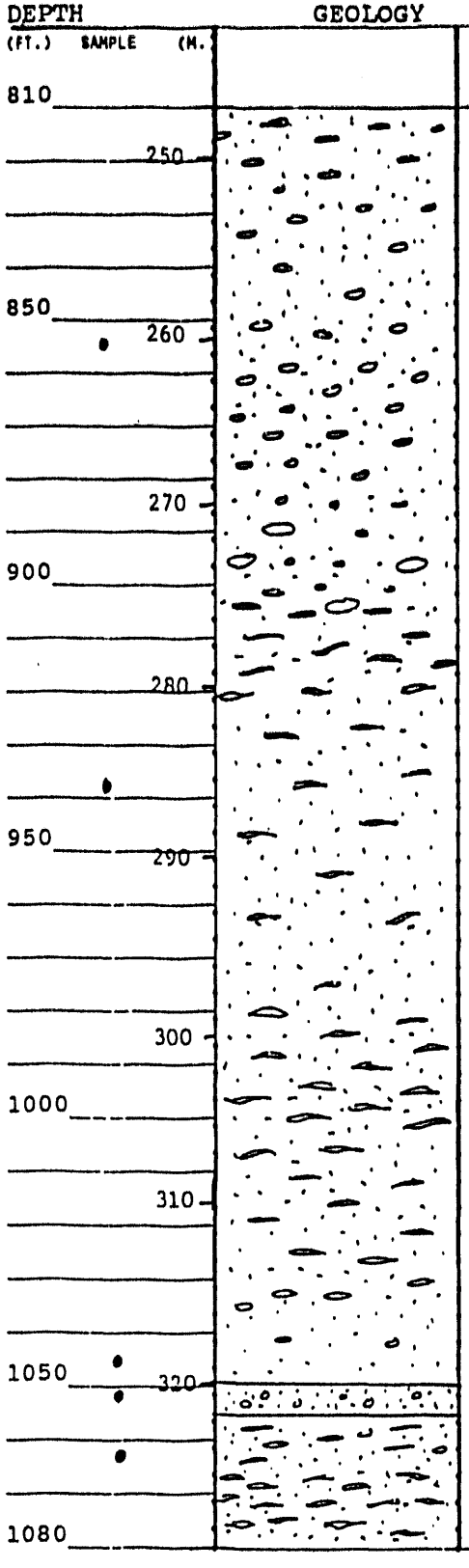

DESCRIPTION

UPPER BANDELIER TUFF (cont'd)

Buff, welded UBT; becomes less welded and > pumice-rich down core. No sign of depositional boundary, but material here is less welded. Not enough to call a cooling unit boundary.

Moderately welded, white-bleached ignimbrite.

Scattered small lithics.

Scattered large pumices (up to 3-4 cm).

Densely welded crystal-rich ignimbrite, with sparse fiamme up to 5-6 cm diam. Darker in color (?less altered).

>Fiamme; all are replaced; some black & white banded.
?Relict glass: occasional lithics up to 3 cm (andesite).

Slight decrease in welding.
Flow unit boundary: dip of contact ~45°; thin, non-incipiently welded flow unit; fine-grained. Too crystal- and lithic-rich to be a co-ignimbrite fall deposit.

Slight pumice/fiamme concentration at top of flow unit becomes more welded over ~3-4 ft; deformation of clasts increases; dip of foliation is ~45°.

Fiamme increase in abundance.

Grey, welded UBT.

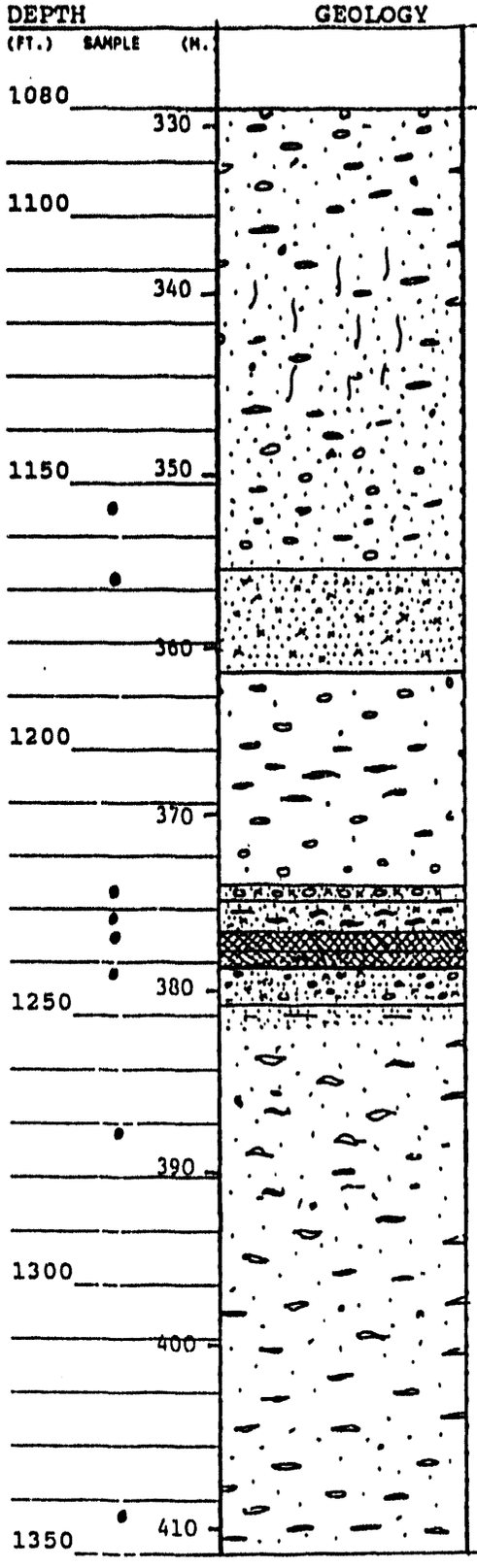

GEOLOGY

DESCRIPTION

UPPER BANDELIER TUFF (cont'd)

ML = 1.5 cm.

Grey, moderate-densely welded UBT with some glassy material.

Sparse lithic content: resembles parts of welded UBT outflow sheet.

Veined ignimbrite.

Greyish color turns to beige; equivalent to their flow units at base of UBT; still lithic-poor. Foliation dips ~45°.
Welding < to moderate: rapid changes in degree of welding; undeformed pumices with ?vapor phase alteration (overprinted by later alteration). Non-welded base of UBT ignimbrite. Note: no UBT plinian deposit, yet Unit A should be ~3-4 m thick here.
"B3" sandstone: crystal-rich. Looks like reworked deposit, but very ashy at base.
Contacts appear conformable with ignimbrite above and below.

Slightly welded ignimbrite; fine grained, white-pinkish; very crystal-rich: problem as to what this is.

Welding increases to moderate; flamme present; ML=3cm; becomes quite crystal rich but very mineralized; fine grained. Foliation dips ~45°.
Low density ignimbrite at base; still compacted; welding moderate-incipient.
Pumice and crystal-rich layer - fall or surge.
* Altered flamme & crystal-rich ignimbrite; densely welded or compacted via alteration; grey-pink; small lithics. Foliation at ~45°.
Very altered, black horizon - origin unknown; not a primary feature. ~~Possibly~~ UB plinian deposit or equivalent ?
Bedded deposit of angular pumice. Lithics + crystals = ?UB plinian fall unit interbedded with thin pyroclastic flows.
Bedded ashy unit-?reworked top of Lower Bandelier Tuff (LBT).

Top of LBT: fine-grained, white ignimbrite with wispy flamme. Bleached and altered; pore space created by dissolution of crystals. Welding moderate. Lithic-poor; some pumices up to 4 cm. Looks like LBT, except very lithic-poor. Foliation of eutaxitic texture = ~30° dip.

*This zone between 1225' and 1252' is possibly a more proximal equivalent to the UBT plinian deposit with inter-bedded thin pyroclastic flows. However the whole zone shows deformed pumices but these may (?) be due to post alteration compaction and therefore be "pseudo-flamme", giving the impression that these are a series of welded tuffs. They could be welded air-fall tuffs, but the clasts are rather small and thicknesses are modest. Alternatively they could be sedimentary layers.

A few lithics.

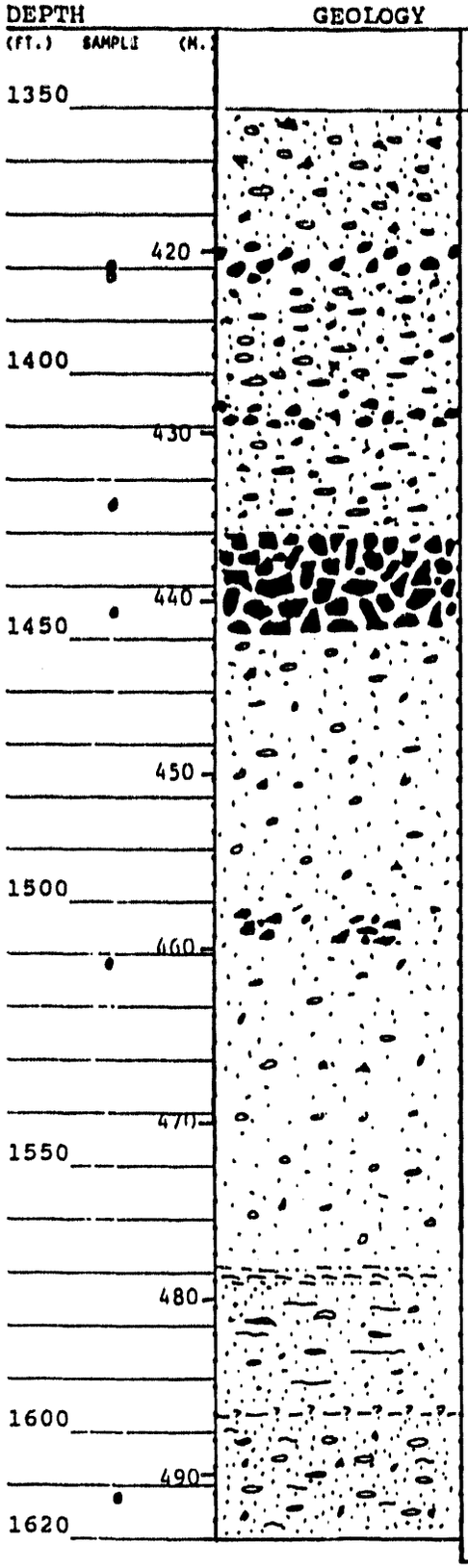

GEOLOGY

DESCRIPTION

LOWER BANDELIER TUFF (cont'd)

LBT white; pitted by alteration; moderately welded.
MP & MP - 3 cm: lithics > common, as in outflow sheet.

ML - 5 cm; pumice- and lithic-rich zone.
Slight > in welding.

Lithic rich zone- ?base of flow unit.
Slightly > dense welding.

Lithics increase in abundance, welding slight.

Zone of lithic lag breccia - probably correlative to those in LBT outside caldera.

Lithic-rich LBT with variable welding (?due to lithic content); rock is greenish.

Small lithic "pods"; moderately welded ignimbrite.

Base of LBT in Kuiken et al.
Fine-grained, interbedded layers with compacted mini-flamme; coul be a surge horizon. May be equivalent to one near base of LBT in outflow sheet.
Welded ignimbrite with shear zones cutting through.

?Fault zone.
Base of LBT is - here but cannot be pinpointed in core; possibly marked by grey altered zone at 1596.7 ft.
Grey, welded ignimbrite with lithics: less altered than ignimbri above.
Possibly LOWER TUFFS: small flamme & ?shards visible: welding moderate (= San Diego Canyon ignimbrites of Turbeville & Self, 1988).

DEPTH (FT.)	SAMPLE	(M.	GEOLOGY	DESCRIPTION
1620			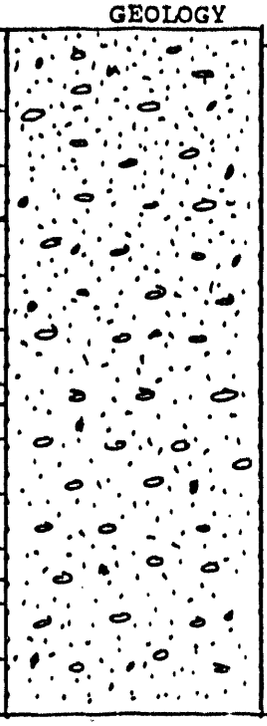	? LOWER TUFFS ? (cont'd) Moderately welded ignimbrite - Lower Tuffs? Homogenous, moderately lithic-rich ignimbrite. Might still be in LBT but tend to think this is an older ignimbrite unit.
		500		
1650				
		510		
1700				
		520		
1730				END OF CORE in ? Lower Tuffs.

Appendix 2B: Detailed descriptions from hand samples and thin sections

VC-2A Core: Summary hand sample and petrographic descriptions

Unit Depth (ft)	Description

Upper Tuffs 71-220.2'

90'8"-91 *Core*: Welded ignimbrite. Dense, white-gray matrix supports about 10% small (1-10 mm diam) gray ?lithic or ?pumice clasts. No apparent foliation; no obvious pumices. Sparse clear/gray crystals, oxidized biotite flakes and oxidized mafic clots. Pale lemon yellow alteration around oxidized mafics.

TS: Devitrified ignimbrite. Relict shard structure and some pumices visible, the former in plane light, latter under crossed nicols. Pumice foliation is perpendicular to core axis; pumices are irregularly spaced. Flattening of some pumice clasts due to alteration. Pyritized. Occasional lithics are brownish and rounded. Abundant small anhedral to large subhedral crystals include quartz and some sanidine. Occasional large clots of intergrown crystals, mostly quartz. Some wormy, resorbed plagioclase. Large, crystalline masses of iron oxides; powdery iron-manganese? opaques. Occasional needles/plates of higher birefringent, non-pleochroic, non-colored crystals, particularly in more coarsely devitrified pumices. Very low birefringent (gray-white) authigenic crystals, elongate, prismatic, hexagonal cross-section (especially in vugs at top of slide). No glass, no apparent vesicles but abundant pore space.

Interp: Lower part of white, fine-grained altered poorly to moderately welded ignimbrite. All one flow unit; source unknown. Alternatively this could be a pumiceous mudflow.

Chem: No unaltered glass; phenocrysts resistant to alteration might be suitable for analysis; feldspars would be suspect.

LA: Gray to bleached, densely welded, fragmental, crystal rich."

HN: Upper Tuffs

93' *Core*: Very similar to sample at 90'8" but contains more yellow alteration product; it is pervasive through the matrix, giving a marbled appearance to the rock. Gray, dense pumice clasts are max 1.5-2.0 cm diam.

TS: Devitrified ignimbrite. No shards visible but some relict ghosts are visible. No glass, abundant small holes, some could be from plucked crystals. Some vugs contain low birefringent tabular/prismatic crystals growing normal to vug wall. Fine-grained matrix is altered, some to a light yellow/gold birefringence product = clay, mica? Phenocrysts include quartz with undulose extinction, small to large, an- to euhedral, some spindle shaped. Sparse small rounded lithics.

Interp: As for sample at 91'.

Chem: No glass; phenocrysts very suspect.

LA: Coarse-grained breccia zone within gray to bleached, densely welded, fragmental, crystal-rich ash-flow tuff.

HN: Upper Tuffs

190' *Core*: Very dense clast-supported breccia (some areas may be matrix-supported). Medium to dark gray matrix and slightly lighter colored clasts. Very small (< 1 mm diam) white opaque crystals/blobs scattered throughout: altered feldspar? Sparse ?unaltered biotite flakes; other mafics have altered to earthy, orange-brown color on one surface. Other crystals difficult to distinguish. Very different from both samples at 93' and 216'. Pyroclastic nature not obvious.

TS: Altered breccia. Alteration products mostly very fine-grained low to yellow birefringent clay-mica plus silica. Anhedral silica mosaics both line cavities and infill some fractures (which cross-cut phenocrysts). Clasts include rounded sandstone (quartz mosaics); others unidentifiable due to extensive alteration, apparently to fine-grained

silica and ?feldspar and ?clays/micas. In plane light matrix distinguishable by lighter colors; in cross-nicols by greater abundance of fine-grained birefringent (light yellow) material. Phenocrysts include quartz, mostly as angular fragments. Abundant opaques are scattered throughout.

Interp: Altered, brecciated zone within "Upper Tuffs"

Chem: Completely altered.

LA: Splotchy, devitrified to vuggy material.

216'6" *Core*: Altered, moderately welded ignimbrite. Matrix is pale white-gray; clasts somewhat lighter. Matrix-supported. Pumice clasts from < 1 mm to 1 cm diam. No apparent lithics. Oxidized large clots of mafic minerals are centers for swarms of dispersed, very small (0.1 mm diam) crystals. No accretionary lapilli.

TS: Very altered, nonwelded pyroclastic rock. Leached; all pale yellow-white in plane light. Faint shard structure still visible but all glass has recrystallized to very fine-grained alteration products. Alteration products have low birefringence (gray/white), some areas of higher birefringence (pale yellow). These higher birefringent alteration products are very small but acicular, and tend to form aggregates outlining former shard/vesicle boundaries. Highly altered pumices are visible; alignment of alteration products parallels former stretched vesicles. Some traces of axiolitic devitrification are still visible in the upper right corner of slide. In some vugs are linings of low birefringent (gray/black) lath-shaped crystals with parallel extinction; these infill much of the pore space in this tuff.

One large ?volcanic lithic observed; smaller lithics may be present but are indistinguishable due to alteration. Phenocrysts very sparse, small and rounded, mostly quartz. Others may have been plucked during thin section preparation. Abundant Fe-Ti oxides, with square, rectangular or hexagonal outlines, both single crystals and aggregates.

Interp: Nonwelded pumiceous ignimbrite near base of Upper Tuffs.

Chem: All phases altered.

LA: Fault gouge/breccia within vuggy ash-flow tuff.

Debris-flow deposit or lithic-rich ignimbrite 220.2'-252'

240.3-.6' *Core*: Clast-supported breccia. Two size-groups of clastsz: (1) 0.5-2 cm diam (some up to 6 cm diam), and 92) 1-2 mm diam clasts. Size groups (1) and (2) are about equal in amount. Clasts are rounded to angular, pale white-gray, medium gray, dark gray and speckled beige. Medium matrix gray. White clasts are pumice.

TS: Breccia of highly altered angular to subrounded clasts of various rock types, including andesite, up to 5 cm diam. Abundant pore space perhaps due to plucking during thin sectioning. Some rounded cobbles. Matrix but of ? origin. Very altered. Larger, better sorted clasts at base. Matrix consists of a fine-grained aggregate of lithic material, phenocryst fragments, plus very fine-grained low birefringence, low relief material - clay/mica? Opaques of all sizes disseminated throughout matrix. There may be some relict shards visible in matrix, but the matrix is so altered this is problematic. Pervasive crystallization of secondary phases in pore spaces, of medium-low relief, low birefringence (white-gray lath-shaped crystals.

Clasts:

1. Very altered crystal-rich volcanic rocks, all so altered that phenocrysts have recrystallized.

2. Light-colored homogeneous fine-grained: shale/siltstone. Grains very small, interlocking very low birefringence (gray); some coarser crystallization areas look like quartz.

3. In plane light, medium brown fine-grained material. Ghosts of elongate laths/acicular crystals. Abundant fine-to medium-grained euhedral opaques.

4. Plane light: medium-brown fine-grained igneous rock (volcanic); ghosts of relict phenocrysts visible but completely recrystallized.

5. Microcline fragments (unaltered).

Interp: Basal unit of Upper Tuff ignimbrite; either a debris flow deposit or a lithic-rich ignimbrite.

Chem: All material completely altered.
LA: Tuff breccia in ash-flow tuff.

S2 Sandstone 251'-258' (Not sampled)

Upper Bandelier Tuff 258- ? 1166' (model B or C, see discussion)
? 1248' (model A, see discussion)

Thick flow unit in upper UBT cooling unit 258-1049.6'

663' *Core*: Medium to dark gray very densely ?welded volcanic rock. Pyroclastic texture of flattened pumices of variable orientation, but generally at 40° to horizontal. Pumices are 1-2 mm thick, about 1 cm long and undulose, darker gray than matrix. Unflattened dark gray clasts are also present. Areas of white alteration products rim some dark clasts and are scattered throughout sample. One edge of core is a mineralized fracture surface, covered dark, greenish gray black very fine-grained material. Some mafic crystals are present but altered.

This sample is very similar to the breccia at 190', but matrix-supported.

TS: Very crystal-rich welded ignimbrite. Pumices are collapsed but shards are distinct. Alteration to very fine-grained high birefringence (pale pink/green/yellow) mineral. Matrix consists of fine-grained ?silica and ?feldspar, not axiolitic or granophyric. Relict shards are apparent only in plane light. Pumices have somewhat coarser devitrification than matrix, and contain spherical grains of quartz/feldspar. Pyroxene (pleochroic green) altered to fine-grained low birefringence phase. Opaques are sparse, but sometimes associated with green pleochroic phase. One clot of mafics contains two high relief colorless crystals of medium birefringence (intense blue-green purple/yellow). Quartz and sanidine present, plagioclase is skeletal or exsolved.

Interp: Upper Bandelier Tuff with sparse small lithics. This sample is from a bleached, slightly less welded zone of the ignimbrite.

Chem: All phases are completely altered.

LA: Altered ash-flow tuff close to zone of abundant fiamme, distinct flow orientation in tuff.

695.7' *Core*: Altered nonwelded tuff. Matrix-supported. Matrix pale gray, clasts medium gray. Pumices are collapsed by alteration into stringers < 1 mm thick, about 1 cm long, with occasional more equant clasts. Foliation is 30-40° to horizontal. Pumices are white, lithics < 1 cm diam. Altered interior of relict pumices appears greenish to yellow and fine-grained. Small (1-2 mm diam) white blebs in matrix could be altered feldspar crystals. Occasional biotite. Crystal-rich. Very similar to sample at 663' but lighter in color.

TS: Nonwelded ignimbrite, similar to sample at 663' in crystal content and appearance in plane light, except that pumices are not collapsed. Matrix and pumices are devitrified, fine-grained to somewhat coarser, approaching granophyric in places. Some pumices are outlined by spherical/equant grained of quartz or feldspar. Pumice interiors contain a pale green to green-yellow birefringent material. Phenocrysts contain none of the exsolution textures of sample at 663' but otherwise very similar. Occasional lithics.

Interp: White, incipiently welded ignimbtrite. Sample occurs at cooling unit boundary within the Upper Bandelier Tuff; a color change occurs in the core here.

Chem: All material altered.

LA: Gray-white tuff with green clay on fractures and green sericitic alteration of fragments, fiamme, and phenocrysts.

854.1' *Core*: Altered welded crystal-rich tuff. Matrix-supported. Matrix pale gray-white with pale green blebs and stringers. Contains large clear gray crystals and small gray/beige clasts. No obvious foliation. Similar to samples at 667' and 695.7'. Occasional biotite flakes.

TS: Highly altered ?nonwelded ?tuff. No relict shards visible, occasional pumice

visible. Some volcanic (mafic lava) lithics, small to medium and rounded. Phenocrysts less abundant than samples at 663' and 695.7'. Partial to complete sericitization of feldspars (large, equant grains). Remaining more tabular forms sometimes appear skeletal but may have been plucked during thin sectioning. Some exsolution. Scattered opaques present.

Chem: All material completely altered.

Interp: Moderately welded, white-bleached, Upper Bandelier Tuff ignimbrite with scattered small lithics.

LA: Ivory ash flow tuff, with green fiamme.

938' *Core*: Very crystal-rich densely welded tuff. Matrix is pale gray with greenish clasts. Equant crystals prevent foliation from being well developed but it is present at 30-40^{o} to horizontal. Gray appearance due in part to large number of gray translucent crystals, 10-20 mm diam. Occasional large pumices 3-4 cm diam. Biotite (or another mafic phase) is present.

TS: Moderately to densely welded tuff. Shards not apparent but relict collapsed pumices are visible, and eutaxitic texture deforms around some phenocrysts. Completely altered; approaches granophyric recrystallization; sericitization present. Phenocrysts are quartz and sanidine. Some feldspar is exsolved. Fine-grained disseminated opaques. All phenocrysts are altered.

Interp: Densely welded Upper Bandelier Tuff ignimbrite with sparse fiamme up to 5-6 cm diam.

Chem: All material altered.

LA: Gray-brown poorly welded ash flow tuff with fewer fragments; crystal rich, very little green alteration.

1045.7 *Core*: Fractured welded tuff. Swirly gray and pale yellow-white matrix with medium gray clasts. Clasts 0.5-2 cm diam with random orientation. Pervasive fractures are coated with silvery gray/green material. Crystal content undetermined.

TS: Welded tuff, with buff matrix and white phenocrysts. Fiamme are clearly visible. Abundant small phenocrysts: quartz, sanidine and some with exsolution patches and sericitic alteration. Devitrification fine to medium-grained, approaching granophyric in places, other places axiolitic but patchy.

Interp: Base of an upper Upper Bandelier Tuff flow unit. Slight decrease in welding from fiamme-rich zone above.

Chem: All material altered.

LA: Dark gray densely welded fragmental tuff, swirly fabric very little green alteration.

Thin flow unit in lower UBT cooling unit 1049.6-1055'

1052' *Core*: Pale white-gray, very fine-grained welded ?tuff. No pumice clasts visible. Very pale green stringers cut tuff horizontally. Dispersed flecks of darker material present.

TS: Very fine-grained tuff. No apparent shards or pumices. Abundant small crystal fragments and occasional larger lithics. Matrix is devitrified to a uniform very fine-grained low birefringence aggregate. Some phenocrysts sericitized.

Interp: Thin, non- to incipiently welded flow unit, fine-grained.

Chem: All material altered.

LA: Air-fall tuff.

Thick flow unit in lower UBT cooling unit 1055-1166'

1063' *Core*: Very similar to sample at 1045.7': Densely welded moderately crystal-rich ignimbrite. Welding foliation is 45^{o} to horizontal. Matrix medium gray, dark gray flattened pumices up to 2 cm long. White speckles may be altered feldspar crystals. Pervasive fractures coated with green-black finely crystalline phase.

TS: Crystal-rich partly welded ignimbrite, medium to coarse-grained. Abundant

crystals are eu- to anhedral. Some relict shards and pumices are apparent but are completely devitrified, axiolitic to granophyric. Quartz phenocrysts appear unaltered but feldspars are exsolved or sericitized. Fine-grained disseminated opaques are present.

Interp: SS: Fiamme-rich top of flow unit.

Chem: All material altered.

LA: Gray, crystal-rich fragmental tuff with fiamme.

1154.5' *Core*: Altered densely welded tuff. Greenish to gray pumices up to 1.5 cm long are completely collapsed; welding foliation at 45° to horizontal. Abundant translucent crystals about 1-2 mm diam; some biotite. Fractured. Very similar to 1063' but matrix is lighter in color and clasts are greener.

TS: Welded tuff with abundant small to medium crystal fragments, sub to anhedral. Sanidines appear exsolved, some sericitic alteration. Pumices are coarsely granophyrically devitrified, matrix is also devitrified. Scattered opaques.

Interp: Moderately welded pumice-rich ignimbrite at base of UBT; equivalent to thin flow units at base of outflow UBT.

Chem: All material altered.

LA: Fragmental tuff below zones of green fiamme.

S3 Sandstone 1166'-1186'

1168.5' *Core*: Very fine-grained sandstone, very similar to sample at 1052'. Pale green/buff. Greenish stringers suggest alteration. Dark flecks may be ferromagnesians. No obvious pumices.

TS: "Sandstone" with abundant fine-grained matrix. Grains are crystals of quartz, ?sanidine, microcline and plagioclase. All about the same size, euhedral to rounded. Linear bands with more matrix/fewer crystals cross cut thin section. Some alteration of matrix: ?calcite in one area. No visible volcanic clasts.

Interp: Very immature arkosic sandstone.

Chem: May be possible on crystals.

LA: Sandy tuff/tuffaceous sandstone with bedding.

Ignimbrite 1186-1225' (for stratigraphy see discussion)

Bedded deposits 1225-1248' (for stratigraphy see discussion)

1226' *Core*: Very crystal-rich altered clastic rock. Crystals 2-3 mm diam, gray translucent. Moderately to densely ?welded/compacted but crystals interfere with fabric. Foliation at 45° to horizontal. Matrix is mottled white and gray with some stringers of dark to medium gray. White matrix appears associated with high crystal content. Other parts of the core sample with gray matrix have lower crystal content.

TS: A very badly plucked thin section. partly welded crystal-rich rock. Matrix is completely devitrified to medium-coarse granophyric crystals. Phenocrysts are large, equant and rounded, both whole and fragments. Sparse large opaques. Some sericite in matrix. No exsolved crystals.

Interp: Pumice and crystal-rich fall, surge or sediment layer.

Chem: Matrix altered.

LA: Fall-out tuffs.

1230.5' *Core*: Very altered grey-pink crystal-rich welded tuff. Densely compacted/welded via alteration; small lithics. Density is low due to ?alteration. Matrix is pale greenish gray with darker gray swirly stringers; foliation at 45° to horizontal. Marbled appearance.

TS: Completely altered ?ignimbrite. ?Fiamme relicts barely visible. Matrix is altered to uniformly fine-grained gray/yellow birefringence aggregate. Some phenocrysts are completely sericitized. Abundant lithics include medium ?sandstone clasts (or coarsely devitrified tuffs).

Interp: Altered, fiamme and crystal-rich ignimbrite; an intraplinian ignimbrite or a

reworked deposit.
Chem: All material altered.
LA: Fall out tuffs.

1234' *Core*: Altered dark volcaniclastic rock. Dark gray matrix. Dense but no foliation. Clasts angular, white/gray, pale green. Matrix-supported. Larger clasts are 0.5 cm diam, small clasts in matrix are < 1 mm diam. Abundant mafics are altered.
TS: Crysta-l, lithic- and ?pumice-rich clastic rock. Abundant small crystal fragments include quartz and some sanidine/microcline. Some larger phenocrysts are sericitized. Matrix is altered to fine-grained low birefringence aggregate. Black fine-grained substance dispersed through matrix. The matrix, though altered, in plane light shows as a clastic mixture of small, non-equant to equant fragments. If these are relict shards, they are blocky with no evidence of bubble-wall texture.
Interp: Very altered black horizon of possibly sedimentary origin.
Chem: All material altered.
LA: Fall-out tuffs.

1241' *Core*: Volcanic clast-supported breccia. Large clasts average .75-1 cm diam, small clasts 1-2 mm diam; little matrix apparent. All mottled white and greenish gray. Distinctive black lithics from 1 mm to 1 cm diam. Larger ones show banding. Some light clasts appear pumiceous. Fractured.
TS: Lithic-rich matrix-supported pumiceous breccia, highly altered. Matrix is very fine-grained low birefringence material with curvilinear areas of sericitic? alteration (pale yellow birefringence). Crystal-rich; includes large hexagonal quartz crystals and alkali feldspar; feldspar is mostly altered to sericite and wormeaten. Lithics include lavas (andesite? basalt?), granophyrically devitrified tuff, highly altered ?pumice (or flow-banded lava), and miscellaneous altered ?volcanic rocks.
Interp: Bedded deposit of angular pumice, possibly a pumice and lithic fall deposit.
Chem: All material altered.
LA: Fall-out tuffs.

Lower Bandelier Tuff 1248 - ~1597'

1272' *Core*: Altered fine-grained, white ignimbrite with wispy fiamme. Welding foliation at 30° to horizontal. Pumices are partially flattened, maximum 2 cm long by 0.5 cm thick. Bleached and altered, porespace created by dissolution of crystals. Welding moderate, lithic poor; some pumices up to 4 cm. Moderately abundant translucent gray crystals up to 2 mm diam. Matrix pale white/gray with greenish and cream cast; pumices slightly grayer.
TS: Crystal-rich granophyrically devitrified tuff. Little original texture visible in thin section other than a faint lineation possibly related to welding. Possibly some fiamme present. Some axiolitic devitrification present. Quartz crystals appear unaltered: large, equant, whole or fragments. Alkali feldspar is altered to high birefringence phase, some plucked. Lithics include highly altered vesicular clast (?scoria) with quartz mosaics in ?vesicles, and andesite-basalt lava.
Interp: Top of the Lower Bandelier Tuff: Poorer in lithics than outflow LBT.
Chem: Quartz alone may be unaltered.
LA: Moderately welded tuffs to nonwelded tuffs in grey pitted zone.

1343.5' *Core*: Moderately welded crystal-rich tuff. Pale gray/white with green and cream casts. Small (< 1 cm diam) pumice clasts. Occasional reddish lithics. Gray translucent crystals 2-3 mm diam. Biotite present.
TS: :Highly altered tuff. Matrix completely altered to granular low to medium birefringence material. Some clusters suggest shard/bubble wall structures. Not very welded. Some patches of granophyric crystallization. Crystal-rich. Quartz phenocrysts not altered but all feldspar is nearly completely sericitized. Crystals are small to medium, equant/angular.
Interp: LBT with a few more lithics than sample above.
Chem: Quartz alone may be unaltered.
LA: Moderately welded tuffs to nonwelded tuffs close to poorly welded, crystal-rich

zone.

1380' *Core*: Similar to sample at 1343.5' but more densely welded and with more pumices. White, pitted by alteration; ML ~ 5 cm. Pumices equant but irregularly shaped. Matrix-supported. Pumices darker gray than pale white-gray matrix. Areas of greenish and cream alteration. Crystal rich. Biotite may be present.

TS: Altered, ?nonwelded tuff. Matrix dark to medium beige; white-cream shards still clearly visible in plane light. Under cross nicols appears very fine-grained, very low birefringence, with some more coarse-grained patches. Relict pumices difficult to identify if present. Occasional lithic of altered ?tuff. Abundant crystals: quartz nearly unaltered; all others worm eaten and/or sericitized.

Interp: Lithic-rich zone within LBT which here is

Chem: Quartz may be unaltered.

LA: Moderately welded tuffs to nonwelded tuffs near base, close to zone of large noncompressed pumice fragments.

1381' *Core*: Same as sample at 1380'.

TS: In plane light very similar to sample at 1380': altered nonwelded tuff. Some pumice fragments are visible; occasional lithics of lava (contain magnetite and plagioclase). Under cross nicols the matrix is altered to very fine-grained low birefringence (gray/black) phase, shot with lines of higher birefringence (pale yellow) - clays, sericite? No granophyric crystallization. Crystals abundant but highly altered as in sample at 1380'.

Interp: ditto 1380'

Chem: Quartz may be unaltered.

LA: ditto 1380'.

1424' *Core*: Altered crystal-rich tuff, very similar to samples at 1380' and 1381', but distinctly greenish. Less welded than samples at 1380' and 1381'.

TS: Altered nonwelded tuff. Fewer crystals than in samples of 1380' and 1381', and obliteration of textures more complete, otherwise very similar to samples at 1380' and 1381'. Quartz crystals are resorbed.

Interp: Lithic-rich zone within LBT, ?base of a flow unit.

Chem: Quartz may be unaltered.

LA: Densely welded crystal-rich, fragmental tuff.

1445' *Core*: Clast-supported volcanic breccia. Clasts from 2-20 cm diam of pale greenish ?tuff, fine-grained tuff or sandstone, and other lithologies. Matrix medium gray/green. Dense.

TS: Breccia, with a probably volcanic matrix: in plane light relict shard structures barely visible. Clast supported, but no large clasts; clasts probably volcanic. Abundant colliform opaques. Matrix is highly altered to sericite/clay/calcite. Phenocrysts highly altered.

Interp: Lag breccia within LBT, correlative to those in extracaldera LBT

Chem:

LA: Tuff breccia ; ?lag breccia.

1512' *Core*: Altered welded tuff. Pale medium green matrix and clasts. Very similar to some of the clasts in sample at 1445'. Occasional large (3-4 cm diam) ?unaltered (gray) pumice clasts. Not especially crystal-rich but crystals present, including biotite.

TS: ?Moderately welded altered tuff. Little structure visible even in plane light. Altered to very fine-grained very low birefringence material.. Other than quartz, the small phenocrysts are completely sericitized. Occasional small lithics.

Interp: Moderately welded LBT with small lithic pods.

Chem: Quartz may be unaltered.

LA: Tuff with green-altered matrix.

Lower Tuffs ~1597'-td = San Diego Canyon Ignimbrite

1613' *Core*: Pale medium green to grey, moderately welded ignimbrite with lithics, similar

Appendix 3: Geochemistry of Selected Samples

Sample numbers for trace element, major element, radiogenic and stable isotope, and microprobe analyses refer to the sample location and position; for example, sample 17-03 is from location 17, near the top of the section. Sample locations are as listed below and in Figure 1.

Location 8: western side of caldera

Location 11: NE1/4, SW1/4, Section 32, T20N, R7E, Copar Pumice Co., Guaje plinian deposit.

Location 13: NW1/4,NE1/4, Section 21, T19N, R7E, road cut of Route 4 at base of Otowi Mesa

Location 17: Copar Pumice Mine, top of plinian and LBT

Location 18: SE1/4, NE1/4, Section 9, T18N, R3E, Cat Mesa near Vallecitos de los Indios

Location 20: Cochiti Canyon

Location 22: NW1/4, NE1/4, Section 6, T22N, R5E, Pueblo Mesa near Canones, New Mexico

Location 27: ditto Location 13

Location 177: NW1/4, NW1/4, Section 29, T19N, R3E, Wildcat Canyon SSW of La Cueva

Appendix 3A: Trace element chemistry

Smp	13-02	13-06	13-11	11-01	11-04	11-07	11-10	11-14	11-16	11-20	11-23	11-25
Unit	LBT	LBT	LBT	LBT	LBT	LBT	LBT	LBT	LBT	LBT	LBT	LBT
Pb	46.3	47.59	47.94	45.89	47.21	45.16	45.55	47.38	47.06	45.59	47.51	48.32
Rb	348.75	345.88	353.48	350.93	351.27	349.29	344.39	358.49	352.27	346.78	357.57	355.66
Sr	4.87	6.79	5.2	3.71	4.04	3.06	3.91	4.58	3.23	3.43	3.3	3.52
Y	113.3	114.57	116.94	115.44	115.1	116.83	115.35	116.4	117.13	113.62	116.79	116.44
Zr	285.87	254.68	261.89	257.2	260.52	256.35	255.37	262.23	259.21	254.65	261.82	259.92
Nb	184.79	183.11	188.54	185.19	184.83	185.76	182.93	189.27	186.68	186.68	188.92	186.93
Ga	28	28	27	28	26	27	27	28	28	27	27	28
Zn	123	127	127	123	125	124	124	125	124	125	125	128
Ba	<10	16.85	<10	0	<10	13.45	<10	<10	<10	<10	12.4	16.95
Sc	0	0	0	0	0	0	0	0	0	0	0	0
Cr	0	0	0	0	0	0	0	0	0	0	0	0
As	2	3	4.4	0	4.6	3.2	3	3.1	4.4	6	4	4
Sb	0.59	0.52	0.58	0	0.58	0.56	0.48	0.5	0.53	0.5	0.5	0.5
Cs	10.3	10.2	10.5	0	10.34	10.16	10.25	10.38	10.48	10.2	10.4	10.1
La	38.7	39.1	39	0	39.9	39.8	38.6	38.7	38.7	40.7	39.4	38.5
Ce	94	94.7	96.1	0	95.6	96.6	93.3	93.3	94.5	98	95.3	94.2
Nd	39.9	41.6	38.3	0	35.6	37.5	41.3	38.1	41.1	42.7	41.5	38
Sm	11.1	11.1	11.4	0	11.5	11.2	11	11.1	11	11.5	11.3	11.4
Eu	0.014	0.039	0.01	0	0.02	0.02	0.031	0.02	0.015	0.031	0.016	0.024
Tb	2.57	2.65	2.7	0	2.76	2.67	2.66	2.7	2.65	2.67	2.7	2.7
Yb	10.9	10.6	11.2	0	11.03	10.9	10.77	10.8	10.7	10.86	11	10.86
Lu	1.62	1.6	1.64	0	1.67	1.62	1.63	1.6	1.61	1.64	1.64	1.65
Hf	13.5	13	13.8	0	13.4	13.6	13.2	13.9	13.5	13.1	13.7	13
Ta	14.1	14.1	14.5	0	14.3	14.2	14.2	14	14.4	14.3	14.3	13.9
Th	42.3	42	43.4	0	43	42.6	42	42.2	42.8	42.6	42.8	42.4
U	16.4	17.4	17	0	17.4	17.3	16.6	17.8	17.4	16.7	17.6	17.6

Smp	11-28	11-31	11-33	11-36	11-C	11-G	11-H	17-03	17-04	17-15	17-18	17-21
Unit	LBT	LBT	LBT	LBT	LBT	LBT	LBT	LBT	LBT	LBT	LBT	LBT
Pb	46.39	47.52	46.16	48.79	47.53	47.32	39.25	23.17	23.05	23.54	25.43	15.98
Rb	349.11	350.96	347.23	355.09	354.82	352.09	301.69	183.05	183.08	188.52	199.84	137.03
Sr	2.7	6.25	3.77	4.08	6.19	4.22	8.47	6.79	18.59	3.93	6.33	5.74
Y	115.3	117.88	114.81	117.1	117.62	116.26	105.26	58.11	58.79	60.54	64.64	43.63
Zr	257.24	261.13	254.41	258.14	260.52	255.5	230.37	180.63	180.8	181.57	187.37	196.79
Nb	185.47	187.46	184.52	186.13	188.12	186.14	155.8	83.96	86.13	87.7	95.37	62.45
Ga	29	27	29	29	27	28	27	22	23	22	24	20
Zn	124	125	125	125	123	123	111	70	71	70	76	58
Ba	<10	11.21	<10	<10	<10	<10	14.63	<10	17.84	<10	<10	11.6
Sc	0	0	0	0	0	0	0	0	0	0	0	1
Cr	0	0	0	0	0	0	0	0	0	0	0	0
As	3.5	0	0	4.7	5	4.6	3.4	2.2	0	0	0	0
Sb	0.6	0.53	0.54	0.59	0.48	0.56	0.42	0.16	0	0.25	0	0.2
Cs	10.2	10.4	10.3	10.4	10.4	10.3	8.3	4.1	0	4.5	0	3.02
La	39.6	41	40.4	38.6	38.3	38.4	39.7	41.9	0	42.4	0	47.7
Ce	95.4	97	97.2	94.9	94.7	92.7	97.4	88.3	0	92.2	0	96
Nd	37.9	39.9	39.7	32.5	34.2	37.6	39.6	29.6	0	36.9	0	34.6
Sm	11.1	11.4	11.4	11.1	11.3	11.3	11.8	7.7	0	8	0	6.7
Eu	0.029	0.025	0.021	0.018	0.032	0.019	0.034	0.044	0	0.046	0	0.078
Tb	2.63	2.73	2.64	2.69	2.66	2.71	2.56	1.48	0	1.54	0	1.11
Yb	10.92	10.98	10.94	10.86	10.88	10.94	9.64	5.3	0	5.6	0	4.1
Lu	1.62	1.65	1.62	1.61	1.64	1.62	1.39	0.78	0	0.87	0	0.67
Hf	13.2	14	13.3	13.5	13.3	13.8	11.1	7.4	0	7.9	0	7
Ta	14.6	14.6	14.4	13.8	14.3	14.2	11.5	6.1	0	7.1	0	4.9
Th	42.2	42.7	42.8	42.9	43	42.6	36.8	20.3	0	21.6	0	16.6
U	16.5	17.1	16.8	17.6	17.3	17	14	7.8	0	8	0	5.9

Smp	17-24	17-29	17-30	17-31	17-37	27-39	27-53	27-56	27-59	27-63	27-70	27-75
Unit	LBT	LBT	LBT	LBT	LBT	LBT	LBT	LBT	LBT	LBT	LBT	LBT
Pb	11.69	10.56	9.82	8.29	0	16.6	17.07	16.84	18.12	17.54	17.52	12.76
Rb	146.93	281.98	215.67	119.05	0	141.2	144.14	163.08	144.3	110.98	121.02	195.66
Sr	3.46	5.17	3.62	5.25	0	8.42	7.5	3.06	4.23	5.3	5.38	7.37
Y	46.75	97.2	72.15	37.13	0	44.25	45.77	53.11	45.96	37.64	39.59	64.85
Zr	188.53	213.45	198.44	205.86	0	198.7	186.03	191.45	191.54	236.95	210:11	186.71
Nb	66.25	143.29	106.15	53	0	64.7	66.79	77.39	66.66	53.5	55.86	92.97
Ga	21	27	24	20	0	22	21	22	22	18	21	23
Zn	59	91	75	44	0	56	55	62	55	52	47	63
Ba	<10	<10	10.74	19.15	0	27.18	<10	<10	<10	18.34	10.62	15.41
Sc	0	0	0	0	0	0	1	0	1	1	0	0
Cr	0	0	0	0	0	0	0	0	0	0	0	1.19
As	0	3	0	0	2.6	0	0	0	0	0	0	0
Sb	0	0.43	0	0	0.36	0	0.2	0	0.13	0.13	0	0
Cs	0	7.8	0	0	6.3	0	3.2	0	3.2	2.3	0	0
La	0	44.4	0	0	39.7	0	45.8	0	45.4	54.1	0	0
Ce	0	102.6	0	0	992.4	0	92.3	0	90.9	106.2	0	0
Nd	0	44.5	0	0	38.6	0	33.8	0	33.6	38.6	0	0
Sm	0	11.5	0	0	10.1	0	6.8	0	6.7	6.7	0	0
Eu	0	0.021	0	0	0.029	0	0.077	0	0.07	0.142	0	0
Tb	0	2.42	0	0	2.08	0	1.2	0	1.19	0.99	0	0
Yb	0	8.9	0	0	7.5	0	4.38	0	4.3	3.56	0	0
Lu	0	1.32	0	0	1.11	0	0.69	0	0.65	0.55	0	0
Hf	0	10.7	0	0	8.7	0	6.8	0	7.1	7.3	0	0
Ta	0	11.2	0	0	9.3	0	5.3	0	5.3	4.5	0	0
Th	0	35	0	0	29	0	17.3	0	16.8	15.1	0	0
U	0	12.8	0	0	10.8	0	5.8	0	6.1	4.9	0	0

Smp	27-77	18-05	18-08	18-10	18-13	18-18	18-21	18-22	18-25	18-28	18-38	18-42
Unit	LBT	LBT	LBT	LBT	LBT	LBT	LBT	LBT	LBT	LBT	LBT	LBT
Pb	11.72	48.17	0	10.78	8.27	10.99	20.55	6.32	7.95	7.56	11.76	15.32
Rb	187.18	359.33	0	184.04	223.79	179.05	63.26	192.11	193.85	186.13	162.67	181.78
Sr	4.48	6.12	0	6.03	5.11	5.21	502.69	4.24	7.17	3.67	4.25	5.46
Y	61.27	114.86	0	56.93	67.23	62.81	19.85	58.07	58.1	57.13	52.11	65.86
Zr	183.57	266.72	0	182.55	182.95	201.84	204.25	182.66	187.85	187.53	194.95	208.44
Nb	88.4	189.69	0	81.04	98.69	92.28	20.18	84.2	84.22	82.93	71.06	900.65
Ga	25	30	0	22	24	25	17	22	22	24	22	24
Zn	63	129	0	59	59	15	55	58	48	56	31	26
Ba	<10	39.73	0	23.06	21.68	32.9	199.03	19	28.62	17.33	27.51	36.2
Sc	0	0	0	0	0	0	7	1	0	0	0	1
Cr	0	0	0	0	0	0	22	0	0	0	0	1.87
As	0	0	4.5	0	0	0	0	1.8	0	0	0	1.7
Sb	0.24	0	0.56	0	0	0	0.1	0.15	0	0	0	0.26
Cs	4.5	0	10.3	0	0	0	1.26	4.3	0	0	0	5.9
La	43	0	39	0	0	0	38	43.8	0	0	0	49.9
Ce	91.3	0	94.6	0	0	0	71	91.6	0	0	0	94.8
Nd	37.6	0	40.8	0	0	0	23	32.4	0	0	0	34.7
Sm	8.1	0	11	0	0	0	5.2	7.9	0	0	0	9
Eu	0.045	0	0.017	0	0	0	1.23	0.056	0	0	0	0.121
Tb	1.58	0	2.62	0	0	0	0.59	1.56	0	0	0	1.69
Yb	5.6	0	10.8	0	0	0	1.64	5.4	0	0	0	6
Lu	0.86	0	1.62	0	0	0	0.28	0.83	0	0	0	0.93
Hf	7.9	0	13.76	0	0	0	5.2	7.5	0	0	0	8.2
Ta	6.7	0	15.2	0	0	0	1.6	6.2	0	0	0	7
Th	21.7	0	42.8	0	0	0	6	21	0	0	0	22.9
U	8.2	0	17.6	0	0	0	1.5	8.1	0	0	0	7.6

Smp	177-01	177-02	177-03	177-05	177-06	177-07	22-32	22-33	22-35	22-43	22-48	22-03
Unit	LBT	LBT	LBT	LBT	LBT	LBT	LBT	LBT	LBT	LBT	LBT	LBT
Pb	39.2	22.1	20.21	17.1	12.59	14.48	0	31.32	26.71	0	0	46.76
Rb	353.92	283.48	256.35	155.11	191.53	152.15	0	289.46	356.9	0	0	343.1
Sr	23.09	4.58	20.89	4.21	2.28	4.68	0	7.85	7.32	0	0	8.37
Y	113.2	98.15	87.88	45.68	57.98	47.48	0	100.92	115.86	0	0	113.93
Zr	426.05	216.87	197.33	192.02	184.4	192.04	0	216.97	261.39	0	0	247.88
Nb	183.01	142.17	125.87	65.03	83.4	66.42	0	147.37	187.53	0	0	179.8
Ga	0	0	0	0	0	0	0	0	0	0	0	0
Zn	0	0	0	0	0	0	0	0	0	0	0	0
Ba	32	<10	14.47	14.28	<10	12.03	0	5.84	7.63	0	0	2.37
Sc	0	0	0	1	0	1	0	0	0	0	0	0
Cr	0	0	0	0	0	0	0	0	0	0	0	0
As	5.3	0	3.2	0.9	1.6	0	0	4.8	4.5	2.6	3.3	0
Sb	0.6	0	0.41	0.14	0.18	0.1	0	0.36	0.52	0.4	0.27	0
Cs	10.1	0	6.61	3.18	4.08	3.16	0	9.7	12.5	9	8.9	0
La	38.2	42.2	41.8	49	42.9	46.8	0	59.1	38.8	40.6	41.5	0
Ce	90.1	100.9	96.7	90.3	89.8	91.1	0	94.6	95	98	96.8	0
Nd	40.7	43.8	46.6	32.3	32	35.1	0	43.2	42.8	42.2	46	0
Sm	10.9	0	10.6	6.8	7.7	6.9	0	11.5	11	11.1	10.8	0
Eu	0.05	0	0.02	0.09	0.05	0.07	0	0.02	0.023	0.039	0.035	0
Tb	2.57	0	2.26	1.19	1.5	1.25	0	2.4	2.6	2.39	2.32	0
Yb	10.62	0	7.92	4.35	5.42	4.48	0	8.9	10.9	8.6	8.2	0
Lu	1.57	0	1.17	0.67	0.82	0.68	0	1.35	1.65	1.29	1.22	0
Hf	12.9	0	9.52	6.9	7.27	7.08	0	10.8	13.2	10.2	9.9	0
Ta	14.4	0	9.8	5.2	6.6	5.3	0	13	14.1	11.2	10.3	0
Th	41.4	0	30.8	16.8	20.6	17.2	0	35	42.6	33.6	31.5	0
U	16.8	12.9	12	6.2	8.3	6.5	0	12.9	17.4	13.2	11.6	0

Smp	22-08	22-09	22-19	22-23	22-28	17-03gl	17-29gl	17-31gl	11-85-06	13-02gl	17-30-01	11-85-10-2
Unit	LBT	LBT	LBT	LBT	LBT	LBT	LBT	LBT	LBT	LBT	LBT	LBT
Pb	43.92	38.54	30.32	0	0	0	0	0	0	0	0	0
Rb	35.72	302.05	306.91	0	0	0	0	0	0	0	0	0
Sr	4.63	9.06	11.81	0	0	0	0	0	0	0	0	0
Y	116.79	107.72	105.23	0	0	0	0	0	0	0	0	0
Zr	257.26	228.28	226.08	0	0	0	0	0	0	0	0	0
Nb	185.54	155	155.53	0	0	0	0	0	0	0	0	0
Ga	0	0	0	0	0	0	0	0	0	0	0	0
Zn	0	0	0	0	0	0	0	29.1	161	112	53	88
Ba	11.82	17.15	14.87	0.74	0	0	0	0	0	0	0	0
Sc	0	0	0	0	0	1	0	1	2.31	0.558	1.035	0.749
Cr	0	0	0	0	0	2.8	5.3	0.9	5.5	3.2	6.6	4.8
As	5.2	3.2	3.8	3.3	0	0	0	0	0.95	9	2.2	2.8
Sb	0.52	0.48	0.44	0.35	0	0.31	0.37	0.57	0.172	0	0.237	0.211
Cs	12	10.8	11.2	9	0	4.46	6.77	2.18	5.33	100.95	4.73	8.32
La	40.9	47.6	39.7	40.6	0	46.4	33.16	4.1	41.2	39.2	47.3	41.7
Ce	96.5	113	97	94.9	0	99.2	82.4	85.3	90	96.9	95.9	100.5
Nd	42.2	45.3	42.6	41.2	0	41.3	35.9	41.1	32.4	41.5	36	42.6
Sm	11.5	12.4	11.7	11	0	8.28	9.16	5.22	8.88	11.48	8.65	11.33
Eu	0.015	0.036	0.014	0.027	0	0.042	0.037	0.065	0.243	0.025	0.057	0.026
Tb	2.72	2.68	2.6	2.35	0	1.6	2.09	0.86	1.68	2.84	1.68	2.53
Yb	10.8	9.6	9.5	8.3	0	5.86	7.58	3.05	6.47	11.3	6.43	9.24
Lu	1.62	1.45	1.42	1.23	0	0.869	1.085	0.485	0.962	1.63	0.95	1.341
Hf	13.63	11.1	11.4	10.1	0	7.42	9.3	5.4	8.36	14.61	8.08	11.65
Ta	14.8	12.1	12.1	10.5	0	6.14	9.14	3.02	6.79	14.83	6.46	11.27
Th	42.6	37.1	36.8	31.8	0	22.19	28.9	13.4	24.5	44.2	23.72	35.65
U	16.1	14.9	13.8	11.6	0	8.2	11	3.2	8.9	16.8	9.2	14.1

Smp	11-85-P5	17-30-02	17-30-04	11-85-10	17-30-03	11-85-02
Unit	LBT	LBT	LBT	LBT	LBT	LBT
Pb	0	0	0	0	0	0
Rb	0	0	0	0	0	0
Sr	0	0	0	0	0	0
Y	0	0	0	0	0	0
Zr	0	0	0	0	0	0
Nb	0	0	0	0	0	0
Ga	0	0	0	0	0	0
Zn	192	84	46	175	56	108
Ba	0	0	0	0	0	0
Sc	2.863	0.98	1.4	3.625	1.057	10.24
Cr	8.3	5.4	6.7	9.1	7.6	3.7
As	1.7	2.7	1.6	1.2	2.1	0
Sb	0.29	0.87	0.2	0.136	0.219	0.052
Cs	5.14	6.23	3.98	4.74	4.42	2.02
La	59.4	45.9	60.1	41.5	50.6	64.3
Ce	97.4	103.6	116.8	88.3	102.6	122.7
Nd	57.9	35.6	40.5	34.3	35.4	59.3
Sm	14.28	9.84	9.01	8.13	8.82	10.8
Eu	0.58	0.035	0.086	0.534	0.048	2.5
Tb	2.54	1.97	1.49	1.44	1.62	1.58
Yb	7.91	7.36	5.82	5.18	6.27	6.14
Lu	1.129	1.07	0.879	0.771	0.911	0.936
Hf	7.49	9.8	8.32	7.15	8.26	18.9
Ta	5.7	8.55	5.48	4.21	6.2	2.14
Th	22.1	28.3	22.34	17.83	23.2	7.81
U	8.6	11	7.9	6.8	8.8	2.7

Sample	08-09	08-15	08-18	08-20	08-12	08-23	08-27	08-31	08-34	08-38
Unit	UBT	UBT	UBT	UBT	UBT	UBT	UBT	UBT	UBT	UBT
Pb	56.25	52.08	51.42	53.48	55.9	52.61	52.94	54.06	51.46	51.23
Rb	307.26	346.23	341.59	353.9	292.72	346.15	350.84	344.82	341.32	336.12
Sr	13.58	20.97	17.75	18.43	17.7	21.62	22.95	15.44	20.75	5.94
Y	130.67	129.03	125.2	129.21	162.02	134.37	134.81	131.2	142.56	134.84
Zr	303.31	285.59	282.45	290.31	312.13	283.12	283.2	279.98	281.6	284.86
Nb	161.47	152.25	151.46	155.72	164.56	151.6	152.23	151.05	152.92	157.85
Ga	28	27	26	28	28	26	27	0	27	28
Zn	147	141	140	144	152	141	145	0	141	140
Ba	25.12	52.02	44.3	45.04	35.82	58.2	48.49	35.58	49.75	17.09
Sc	0	0	0	0	0	0	0	0	0	0
Cr	2.5	-0.1	-0.7	-0.12	-0.1	-0.2	-0.9	-0.3	2.6	-0.5
As	4.1	4	3.8	2.8	3.6	3.4	3.3	3.8	3.9	3.5
Sb	0.48	0.44	0.48	0.39	0.5	0.48	0.5	0.47	0.5	0.48
Cs	11.94	14.6	14.3	14.9	11.17	16.05	15.6	14.6	14.3	12.7
La	68.1	58.4	57.4	57.1	85	52	54.8	52.7	52.9	54.2
Ce	111.7	109.5	111.3	110	119.8	106.7	112.1	107.7	111.3	113.8
Nd	45.4	39.2	43.1	39.5	53.7	37.2	42	39.5	44.4	44.8
Sm	11.9	10.8	10.6	10.9	14.7	10.7	11.4	10.5	11	10.8
Eu	0.083	0.076	0.072	0.074	0.1	0.082	0.073	0.076	0.082	0.049
Tb	2.94	2.71	2.54	2.71	3.84	2.62	2.65	2.57	2.71	2.64
Yb	12.57	11.42	11.1	11.66	14.8	11.03	11.18	11.07	11.23	11.58
Lu	1.89	1.69	1.65	1.75	2.15	1.64	1.69	1.63	1.66	1.72
Hf	15	14	14.2	14.7	15.8	13.9	14	14.3	13.7	14.9
Ta	11.2	10.8	11.1	10.7	11.5	10.9	10.7	10.9	10.7	11.2
Th	36.1	33.7	33.4	34.9	37.6	33.2	33.7	33.4	33.1	35.2
U	12.8	12	11.8	11.8	12.9	12.3	12.4	11.9	12.5	12.6

Sample	08-40A	22-50	22-53	22-55	22-60	22-65	22-69A	22-70UBT	SU 1V20-02
Unit	UBT	UBT	UBT	UBT	UBT	UBT	UBT	UBT	UBT	UBT
Pb	0	51.37	34.64	41.09	43.4	45.83	28.24	36.9	16.6	98.86
Rb	0	302.2	341.23	301.34	302.89	297.92	151.02	177.51	152.98	250.29
Sr	0	12.96	9.05	2.62	3.2	3.37	344.41	432.78	8.4	10.13
Y	0	120.41	124.36	122.59	120.84	120	34.93	26.04	62.54	146.42
Zr	0	276.83	281.91	260.73	262.25	258.68	201.89	210.83	223.81	260.67
Nb	0	151.52	155.27	141.24	141.18	140.74	38.36	27.36	81.23	132.95
Ga	0	0	0	0	0	0	0	0	0	28.1
Zn	0	0	0	0	0	0	0	0	0	118.24
Ba	0	29.84	32.38	23.55	11.94	17.84	966.59	902.17	53	112
Sc	1	0	0	0	0	0	5	5	1	1
Cr	3	-0.2	0	0	-0.6	0	2	1.3	2	0
As	4.5	3.1	0	1.9	4.4	0	0	0	0	15.3
Sb	0.42	0.49	0	0.48	0.43	0	0.13	0.12	0.23	0.47
Cs	16.2	9.6	0	11	10.4	0	4.6	3.9	3.99	8.6
La	73.4	52.2	0	53.4	48.7	0	36	37	51.2	75.4
Ce	105.3	115.2	0	120.4	109.4	0	70.4	69.4	113.8	121.7
Nd	54.2	42.3	0	46.4	39.7	0	25.7	25.8	43.4	63.9
Sm	13.1	11.2	0	12.2	11	0	5.4	5.1	9.2	16.7
Eu	0.131	0.056	0	0.054	0.025	0	0.846	0.879	0.094	0.182
Tb	3.42	2.71	0	2.79	2.5	0	0.88	0.71	1.58	3.47
Yb	12.22	11.4	0	10.8	9.8	0	3.05	2.36	5.66	11.96
Lu	1.77	1.67	0	1.62	1.45	0	0.47	0.37	0.87	1.7
Hf	14	14.2	0	13	11.9	0	6.42	6.28	8.65	13.2
Ta	10.8	10.7	0	9.6	9.3	0	3.3	2	6	9.1
Th	33.2	33	0	31.4	28.6	0	10	7.7	19.5	30.4
U	12.1	12	0	11.6	10	0	3.2	2.2	5.8	10.2

Sample	20-04i	20-04	20-08	20-11	20-14	20-20	20-22	20-25	20-27	20-31
Unit	UBT	UBT	UBT	UBT	UBT	UBT	UBT	UBT	UBT	UBT
Pb	45.18	43.68	137.51	54.34	53.2	50.42	103.62	113.47	28.65	37.88
Rb	250.13	252.22	151.39	166.02	165.83	163.74	234.28	152.23	163.53	227.2
Sr	9.43	11.45	11.36	12.26	11.5	10.5	31.55	19.09	35.78	78.17
Y	116.94	115.7	81.97	84.07	81.76	82.95	128.25	80.74	76.03	103.29
Zr	243.4	244.48	224.82	215.83	213.08	211.7	230.79	202.83	212.08	269.71
Nb	120.3	121.68	80.41	79.34	78.18	74.85	110.69	74.2	76.42	114.46
Ga	0	26.29	24.87	22.09	22.02	22.81	26.41	22.86	21.02	24.79
Zn	0	108.18	92.3	119.38	118.21	135.99	109.45	90.06	84.49	104.92
Ba	65.78	94	82	46	46	53	37	62	33	173
Sc	0	0	1	1	1	1	1	0	1	1
Cr	0	-0.2	-1	-2	-1	-1	-1	-2	-1	2
As	6.2	6.1	3.5	6.1	6	3.5	9.8	8	5	10
Sb	0.24	0.42	0.26	0.15	0.22	0.23	0.33	0.26	0.24	0.45
Cs	7.9	8.6	5.1	5.3	4.9	4.9	7.6	4.5	3.9	7.3
La	65.3	62.2	60.9	68.3	71	69.3	67.4	61.8	57.8	58.2
Ce	121.5	120.5	122.1	112.2	131.1	119.5	121.3	116.1	113.6	114.1
Nd	56.8	48.6	52	60.2	55.8	61.5	67.2	55.4	47.8	47.7
Sm	13.8	13.5	11	13.9	13.1	13.5	15.8	12.2	10.6	11.5
Eu	0.117	0.132	0.136	0.42	0.243	0.35	0.257	0.223	0.168	0.324
Tb	2.76	3.01	2.1	2.59	2.45	2.5	3.39	2.32	1.91	2.5
Yb	9.8	10.08	6.78	7.31	6.93	7.04	10.47	7.06	6.08	9.54
Lu	1.44	1.47	0.98	1.06	1.04	1.04	1.54	1.05	0.91	1.39
Hf	11.8	12.1	9.1	9	9.2	8.9	11.02	8.3	7.46	12.09
Ta	8.5	8.8	5.2	4.9	5.3	5	7.8	4.8	4.4	7.5
Th	28.1	28.7	20	18.5	19.9	19	26	18	17.2	26.2
U	9	10.2	5.6	5.6	6	5.6	9.4	5.3	5.5	9.1

Sample	20-35	20-39	20-40i	20-46	20-51	20-53	20-55i	20-56	20-60	20-63
Unit	UBT	UBT	UBT	UBT	UBT	UBT	UBT	UBT	UBT	UBT
Pb	22.57	24.94	21.32	27.38	85.94	53	36.36	71.1	39.14	375.08
Rb	88.06	145.66	159.86	159.46	108.83	158.35	160.02	156.22	140.09	142.72
Sr	225.34	12.17	13.36	18.31	210.13	15.16	19.59	17.59	23.71	17.64
Y	39.83	64.89	79.15	71.81	69.72	88.99	89.31	75.38	61.51	70.18
Zr	233.76	212.1	215.63	215.17	238.1	215.14	214.62	210.1	211.75	210.39
Nb	35.54	70.48	76.8	74.46	39.16	74.75	75.45	74.54	66.62	68.55
Ga	19.05	21.83	0	21.93	19.35	22.37	0	21.25	20.78	21.96
Zn	57.94	67.03	0	75.57	70.68	69.38	0	71.03	77.57	68.81
Ba	540	63	74.52	79	525	56	37.53	66	62	91
Sc	3	0	0	0	5	1	1	1	1	0
Cr	9	-1	-0.3	-1	13	19	-0.4	-1	2	-2
As	12.9	8.2	10	7.1	10.9	9.6	5.4	5.2	4.4	5.3
Sb	0.2	0.22	0.27	0.08	0.25	0.25	0.14	0.25	0.11	0.32
Cs	2.1	4	4.1	4.26	4	4.1	4.2	4.3	4	4.2
La	55	59.1	60.3	60.3	73.1	80.3	94.1	70.7	63	63.2
Ce	98.6	118.9	110.8	118	124.1	142	157.3	130.7	122.9	116.4
Nd	44.9	45.4	54.6	48.3	60.4	69.1	69.8	56.1	48.2	49.9
Sm	8.2	10	12	11.1	12	14.2	15.4	11.1	10.2	10.9
Eu	0.724	0.179	0.274	0.207	0.892	0.456	0.428	0.211	0.219	0.277
Tb	1.24	1.96	2.17	2.09	2.09	2.46	2.28	2.03	1.89	2.02
Yb	3.7	5.85	6.7	6.24	5.48	6.92	7.4	6.18	5.58	5.98
Lu	0.57	0.87	1.01	0.92	0.81	1.02	1.08	0.92	0.86	0.9
Hf	7.01	8.68	8.3	8.62	7.12	8.04	8.4	7.87	9.5	8.18
Ta	2.2	4.6	5.8	4.9	2.5	4.3	5.3	4.8	4.5	4.6
Th	9.8	17.9	19	18.6	12	18.3	20.2	18.8	17.7	17.8
U	3	5.4	5.8	5.8	2.9	5.3	5.5	5.6	5.5	5.2

Sample	20-67i	20-70	20-73	20-75	27-04	27-06i	27-07i	27-09i	27-09	27-10
Unit	UBT	UBT	UBT	UBT	UBT	UBT	UBT	UBT	UBT	UBT
Pb	35.61	113.35	73.72	24.04	49.44	41.65	47.21	49.17	44.27	42.09
Rb	158.49	147.29	141.14	220.17	287.83	242.52	285.85	306.52	295.64	270.57
Sr	19.4	17.59	52.5	42.84	8.75	13.8	11.59	56.66	47.04	7.02
Y	71.73	73.28	86.77	112.28	114.55	103.59	120.33	120.41	116.96	111.56
Zr	233.77	207.04	200.5	229.23	258.1	240.67	261.45	277.69	269.41	247.09
Nb	75.47	68.9	68.03	108.2	145.23	114.94	141.16	153.83	148.84	134.93
Ga	0	22.51	20.7	24.93	27.73	0	0	0	26.19	25.71
Zn	0	66.77	55.99	92.95	133.35	0	0	0	134.96	125.63
Ba	48.53	64	40	25	-20	27.11	17.33	8.54	-20	-20
Sc	1	1	0	0	0	0	0	0	0	0
Cr	-1.6	-2	-1	-1	-1	-0.2	-0.5	-1.3	-1	-1
As	2.8	3.7	8	5.5	3.7	2.3	3.5	3	3.6	3.4
Sb	0.24	0.3	0.29	0.38	0.48	0.35	0.42	0	0.47	0.39
Cs	4.1	4.3	3.8	7.8	9.9	7	8.8	9.6	9.38	8.8
La	63.4	69.6	70.4	57	52	51.3	55.2	51.8	51.2	53.7
Ce	123.7	122	128.1	113.7	116.5	114.9	121.5	113.2	113.1	121.5
Nd	51.1	58.3	44.4	54.7	44.9	47.3	47.7	43.6	40.3	44.6
Sm	11.1	12	11.9	14.1	11.2	11.9	12.2	10.8	11.1	12.2
Eu	0.197	0.365	0.41	0.282	0.042	0.062	0.056	0.021	0.054	0.138
Tb	1.91	2.19	2.18	3.22	2.81	2.59	2.78	2.63	2.68	2.81
Yb	6.3	6.3	6.7	10.04	11.16	9.2	11	11	10.92	10.7
Lu	0.92	0.93	1.02	1.5	1.65	1.36	1.63	1.67	1.6	1.58
Hf	8.63	8.33	8.14	11.08	14.39	11.5	12.9	14.2	13.47	12.85
Ta	5.5	4.6	4.5	7.8	10.7	7.8	10.2	10.6	9.8	9.2
Th	18.7	18.2	19	26.3	33.2	26.5	31.6	33.2	32.4	31.5
U	5.6	5.3	5.8	10	12.7	9.2	11	11.8	12.4	12

Sample	27-14	27-16	27-18i	27-22i	27-23	27-24i	27-25i	27-26Ai	27-28	27-31	28-02
Unit	UBT	UBT	UBT	UBT	UBT	UBT	UBT	UBT	UBT	UBT	UBT
Pb	44.43	38.79	42.72	32.39	44.37	45.54	167.47	28.63	35.58	39.52	54.81
Rb	279.31	277.03	315.15	127.48	286.21	298.21	79.49	166.77	240.95	271.99	352.71
Sr	8.61	12.83	13.07	393.4	13.75	7.58	411.28	391.19	14.1	4.93	17.67
Y	111.1	113.79	126.66	23.65	114.43	120.74	25.67	27.72	103.22	110.33	127.8
Zr	251.83	245.65	284.18	227.96	252.27	260.1	234.82	213.6	234.06	247.05	287.74
Nb	139.37	136.02	156.45	25.18	134.02	139.99	23.43	27.77	114.19	132.98	154.78
Ga	26.88	26.25	0	0	27.26	0	0	0	24.95	27.75	28
Zn	127.75	127.24	0	0	84.91	0	0	0	111.76	124.2	142
Ba	-20	-20	12.97	852.49	29	14.72	949.56	778.12	49	25	41.73
Sc	0	0	0	0	0	0	0	5	0	0	0
Cr	-1	-1	-2.6	0	-2	0	0	18.5	-1	-1	0
As	2.9	3.2	2.5	0	3.5	0	0	15.7	2.4	2.8	3.8
Sb	0.44	0.42	0.48	0	0.48	0	0	0.08	0.34	0.44	0.52
Cs	9.3	8.5	9.6	2.5	10.7	0	0	4.4	9.7	8.8	15.2
La	54.6	49.8	53.3	44.3	53.4	0	0	38.1	52.6	49.6	58.2
Ce	122	112.3	117.8	83	121.6	0	0	74.2	118.4	113.3	110.5
Nd	45	42	41.6	0	45.4	0	0	25.4	48	39.7	43.3
Sm	11.6	11.6	11.4	5.5	12.2	0	0	5.3	12.1	11.2	10.9
Eu	0.057	0.045	0.053	0.946	0.062	0	0	0.816	0.078	0.047	0.066
Tb	2.84	2.74	2.76	0.64	2.84	0	0	0.76	2.64	2.66	2.74
Yb	11.13	10.25	11.6	2.62	10.66	0	0	2.47	9.35	10.23	11.7
Lu	1.62	1.54	1.72	0.308	1.57	0	0	0.37	1.36	1.53	1.73
Hf	13.36	12.13	14.2	6.69	12.52	0	0	5.9	11.08	12.76	14.3
Ta	9.8	8.9	10.8	2.33	9	0	0	2.2	7.6	9.1	11.1
Th	32.6	30	33.6	7.95	30.9	0	0	7.8	27.2	30.3	34.6
U	12.6	11.4	12.8	1.94	11.6	0	0	2.7	10	11.6	11.9

Sample	20-51X	20-35X	20-22X	20-53X	20-04X	20-31X	27-09X	08-12gl	08-27gl
Unit	UBT	UBT	UBT	UBT	UBT	UBT	UBT	UBT	UBT
Pb	0	0	0	0	0	0	0	0	0
Rb	0	0	0	0	0	0	0	0	0
Sr	0	0	0	0	0	0	0	0	0
Y	0	0	0	0	0	0	0	0	0
Zr	0	0	0	0	0	0	0	0	0
Nb	0	0	0	0	0	0	0	0	0
Ga	0	0	0	0	0	0	0	0	0
Zn	80	105	9.7	9.3	5.6	26	45	130	114
Ba	0	0	0	0	0	0	0	0	0
Sc	5.86	8.85	0.18	0.092	0.333	2.325	1.576	0.981	0.852
Cr	32.6	36.1	15.9	14.6	19.4	15.4	12	2.4	5.5
As	0	8	3.07	0	3.9	2.1	0	3.3	4
Sb	-0.07	-0.06	-0.06	-0.05	0.062	-0.045	-0.045	0.58	0.49
Cs	2.04	0.48	0.424	0.145	0.575	0.73	0.56	12.45	15.6
La	44.6	65.1	24.05	8.62	72.51	47.4	55.1	99.6	57.9
Ce	85.2	124.6	46.3	17.4	47.4	94.7	118.3	129.4	117.4
Nd	39.4	47	15.9	7.3	51.2	32.3	47.8	53.2	41.3
Sm	6.82	8.41	3.19	1.07	8.35	5.38	11.42	16.4	12.36
Eu	0.746	1.07	0.07	0.153	0.079	0.344	0.071	0.128	0.072
Tb	0.99	0.98	0.349	0.139	0.84	0.6	1.72	4.3	2.98
Yb	3.16	2.9	1.04	0.47	2.1	2	3.76	16.6	12.5
Lu	0.461	0.446	0.177	0.078	0.347	0.29	0.545	2.221	1.84
Hf	10.45	17.98	2.89	2.64	6	7.52	2.98	7.56	14.67
Ta	0.556	0.936	0.6	0.215	1.14	1.056	1.029	12.37	10.53
Th	4.25	6.52	4.38	1.45	11.16	7.53	10.07	41.88	36.03
U	1	1.76	0.98	0.38	1.2	1.53	1.88	13.9	13.4

Appendix 3B: Major element chemistry

Sample	13-02	13-06	13-11	11-01	11-04	11-07	11-10	11-14	11-16
Unit	LBT	LBT	LBT	LBT	LBT	LBT	LBT	LBT	LBT
SiO_2	76.748	77.139	77.021	77.172	77.295	77.191	77.191	76.948	77.29
TiO_2	0.047	0.04	0.046	0.044	0.041	0.044	0.04	0.052	0.037
Al_2O_3	12.364	12.076	12.13	12.177	12.101	12.139	12.067	12.326	12.136
Fe_2O_3	1.477	1.453	1.508	1.512	1.49	1.425	1.465	1.459	1.467
MnO	0.086	0.082	0.083	0.084	0.083	0.084	0.085	0.084	0.082
MgO	0.15	0.123	0.08	0.09	0.099	0.056	0.076	0.141	0.015
CaO	0.304	0.307	0.309	0.292	0.283	0.281	0.285	0.296	0.275
Na_2O	3.888	3.91	4.031	4.257	4.219	4.387	4.194	4.298	4.304
K_2O	4.927	4.863	4.786	4.367	4.381	4.386	0.419	4.388	4.388
P_2O_5	0.005	0.006	0.007	0.004	0.007	0.006	0.007	0.005	0.006
LOI	4.856	4.295	4.565	4.656	5.078	4.332	4.3	4.531	4.246

Sample	11-20	11-23	11-25	11-28	11-31	11-33	11-36	11-C	11-G
Unit	LBT	LBT	LBT	LBT	LBT	LBT	LBT	LBT	LBT
SiO_2	77.151	77.193	76.625	77.097	77.055	76.98	77.17	77.036	77.125
TiO_2	0.05	0.043	0.045	0.046	0.048	0.045	0.046	0.046	0.044
Al_2O_3	12.135	12.181	12.336	12.148	12.122	12.226	12.097	12.124	12.077
Fe_2O_3	1.511	1.504	1.352	1.474	1.403	1.793	1.471	1.431	1.457
MnO	0.085	0.083	0.081	0.085	0.08	0.078	0.083	0.086	0.081
MgO	0.016	0.029	0.086	0.025	0.049	0.09	0.024	0.089	0.146
CaO	0.281	0.273	0.269	0.264	0.282	0.272	0.272	0.271	0.263
Na_2O	4.406	4.322	4.442	4.467	4.585	4.384	4.366	4.447	4.381
K_2O	4.354	4.371	4.379	4.387	4.373	4.424	4.469	4.462	4.424
P_2O_5	0.009	0.003	0.008	0.008	0.006	0.008	0.007	0.008	0.004
LOI	4.033	4.165	5.144	3.89	3.714	3.742	3.625	3.837	3.475

Sample	11-H	17-03	17-04	17-15	17-18	17-21	17-24	17-29	17-30
Unit	LBT	LBT	LBT	LBT	LBT	LBT	LBT	LBT	LBT
SiO_2	77.315	77.655	76.831	77.205	77.797	77.45	77.287	77.178	77.446
TiO_2	0.045	0.06	0.065	0.064	0.058	0.083	0.069	0.055	0.058
Al_2O_3	12.233	11.836	12.182	12.262	11.857	12.018	12.041	11.998	12.076
Fe_2O_3	1.394	1.288	1.309	1.332	1.32	1.268	1.306	1.453	1.296
MnO	0.078	0.052	0.059	0.059	0.061	0.049	0.052	0.068	0.061
MgO	0.102	0.167	0.204	0.059	0.122	0.081	0.028	0.03	0.027
CaO	0.293	0.403	0.773	0.325	0.367	0.346	0.292	0.278	0.29
Na_2O	4.033	3.847	3.921	4.041	3.908	3.907	4.009	4.106	3.919
K_2O	4.48	4.673	4.632	4.704	4.492	4.787	4.906	4.827	4.824
P_2O_5	0.025	0.018	0.025	0.009	0.018	0.013	0.009	0.008	0.006
LOI	3.734	3.276	3.761	2.921	3.168	2.691	2.806	2.849	2.414

Sample	17-31	17-37	27-39	27-53	27-56	27-59	27-63	27-70	27-75
Unit	LBT	LBT	LBT	LBT	LBT	LBT	LBT	LBT	LBT
SiO_2	77.63	77.537	77.001	77.224	77.515	77.614	77.943	77.545	77.174
TiO_2	0.092	0.055	0.078	0.071	0.068	0.074	0.11	0.092	0.068
Al_2O_3	11.985	12.033	12.336	12.033	11.905	11.869	11.669	11.996	12.086
Fe_2O_3	1.268	1.267	1.321	1.254	1.328	1.281	1.346	1.29	1.341
MnO	0.044	0.064	0.052	0.049	0.054	0.046	0.047	0.045	0.058
MgO	0.068	0.051	0.116	0.133	0.088	0.043	0.057	0.12	0.121
CaO	0.295	0.271	0.31	0.412	0.292	0.238	0.304	0.294	0.319

Na_2O	3.646	3.968	3.984	4.138	4.04	4.038	3.77	3.792	3.914
K_2O	4.964	4.747	4.793	4.675	4.705	4.738	4.741	4.818	4.908
P_2O_5	0.01	0.007	0.007	0.01	0.007	0.008	0.012	0.01	0.012
LOI	2.257	2.809	2.31	2.357	2.417	2.463	2.449	2.457	2.803

Sample	27-77	18-05	18-08	18-10	18-13	18-18	18-21	18-22	18-25
Unit	LBT	LBT	LBT	LBT	LBT	LBT	LBT	LBT	LBT
SiO_2	77.175	77.096	77.106	77.121	77.288	76.171	66.026	77.319	77.726
TiO_2	0.062	0.05	0.046	0.068	0.056	0.076	0.691	0.064	0.07
Al_2O_3	12.069	12.415	12.125	12.41	12.081	13.277	15.864	12.153	12.088
Fe_2O_3	1.328	1.594	1.442	1.462	1.333	1.411	4.414	1.266	1.325
MnO	0.058	0.103	0.08	0.045	0.053	0.038	0.074	0.043	0.047
MgO	0.08	0.074	0.032	0.096	0.086	0.08	1.875	0.023	0.048
CaO	0.304	0.24	0.27	0.271	0.219	0.151	3.846	0.247	0.233
Na_2O	3.863	3.051	3.552	2.983	2.733	2.966	3.762	3.036	2.642
K_2O	5.039	5.367	5.342	5.537	6.145	5.817	3.198	5.841	5.814
P_2O_5	0.022	0.01	0.006	0.008	0.006	0.012	0.252	0.006	0.008
LOI	2.603	3.683	3.653	2.819	2.494	3.055	2.306	2.789	2.674

Sample	18-25	18-28	18-38	18-42	177-01	177-02	177-03	177-05	177-07
Unit	LBT	LBT	LBT	LBT	LBT	LBT	LBT	LBT	LBT
SiO_2	77.726	77.373	77.267	75.853	76.441	77.218	77.235	77.304	77.456
TiO_2	0.07	0.064	0.078	0.084	0.055	0.057	0.059	0.081	0.073
Al_2O_3	12.088	12.233	12.418	13.726	12.339	12.277	12.179	12.181	12.108
Fe_2O_3	1.325	1.296	1.328	1.555	1.496	1.399	1.414	1.277	1.298
MnO	0.047	0.044	0.04	0.034	0.087	0.077	0.059	0.055	0.051
MgO	0.048	0.05	0.068	0.117	0.344	0.166	0.132	0.168	0.105
CaO	0.233	0.23	0.136	0.144	0.627	0.307	0.566	0.207	0.211
Na_2O	2.642	3.179	2.932	2.646	3.81	3.757	3.717	3.134	3.183
K_2O	5.814	5.525	5.724	5.83	4.762	4.738	4.619	5.579	5.508
P_2O_5	0.008	0.005	0.008	0.01	0.039	0.006	0.02	0.011	0.008
LOI	2.674	2.572	2.759	3.903	3.95	3.2	4.32	2.78	2.7

Sample	22-32	22-33	22-35	22-43	22-48	22-03	22-08	22-09	22-19
Unit	LBT	LBT	LBT	LBT	LBT	LBT	LBT	LBT	LBT
SiO_2	77.62	77.051	76.586	77.032	76.908	76.802	76.862	77.344	76.838
TiO_2	0.05	0.043	0.048	0.45	0.054	0.037	0.047	0.051	0.051
Al_2O_3	12.12	12.05	12.26	12	12.18	12.19	12.111	11.921	12.041
Fe_2O_3	1.396	1.437	1.432	1.36	1.392	1.467	1.471	1.487	1.433
MnO	0.076	0.075	0.085	0.072	0.066	0.076	0.084	0.081	0.078
MgO	0.113	1.22	0.134	0.086	0.113	0.11	0.07	0.096	0.122
CaO	0.253	0.291	0.232	0.224	0.292	0.254	0.204	0.295	0.363
Na_2O	3.664	3.562	3.418	3.62	3.795	3.775	3.773	3.317	3.357
K_2O	5.747	5.361	5.798	5.551	5.19	5.279	5.371	5.442	5.709
P_2O_5	0.006	0.008	0.008	0.01	0.011	0.009	0.007	0.01	0.009
LOI	3.511	3.24	2.815	2.674	3.008	4.007	3.084	3.335	2.803

Sample	22-23	22-28
Unit	LBT	LBT
SiO_2	76.912	76.917
TiO_2	0.052	0.052
Al_2O_3	12.056	12.013
Fe_2O_3	1.407	1.364
MnO	0.07	0.067
MgO	0.153	0.142
CaO	0.318	0.346
Na_2O	3.741	3.496
K_2O	5.285	5.7
P_2O_5	0.01	0.006
LOI	3.071	2.74

Sample	08-09	08-15	08-18	08-20	08-12	08-23	08-27	08-31	08-34
Unit	UBT	UBT	UBT	UBT	UBT	UBT	UBT	UBT	UBT
SiO_2	76.452	76.579	76.991	76.339	76.168	76.525	76.495	76.852	76.722
TiO_2	0.065	0.065	0.065	0.062	0.067	0.069	0.076	0.066	0.064
Al_2O_3	12.556	12.272	12.028	12.413	13.044	12.209	12.237	12.105	12.202
Fe_2O_3	1.814	1.692	1.704	1.717	1.776	1.803	1.781	1.677	1.707
MnO	0.085	0.085	0.084	0.082	0.09	0.084	0.086	0.085	0.083
MgO	0.041	0.095	0.104	0.098	0.08	0.231	0.122	0.062	0.048
CaO	0.312	0.364	0.336	0.33	0.312	0.355	0.352	0.302	0.328
Na_2O	3.417	3.481	3.39	3.536	3.396	3.409	3.402	3.497	3.535
K_2O	5.247	5.354	5.291	5.352	5.058	5.303	5.436	5.342	5.247
P_2O_5	0.009	0.012	0.008	0.01	0.008	0.011	0.013	0.012	0.013
LOI	4.429	2.818	3.343	3.952	4.55	3.452	3.271	3.327	2.977

Sample	08-38	08-40A	22-50	22-53	22-55	22-60	22-65	22-69A	22-70
Unit	UBT	UBT	UBT	UBT	UBT	UBT	UBT	UBT	UBT
SiO_2	76.973	76.211	76.837	76.873	77.395	77.178	77.234	68.938	68.051
TiO_2	0.054	0.087	0.055	0.057	0.051	0.055	0.055	0.408	0.42
Al_2O_3	12.125	12.549	11.958	11.997	11.805	11.839	11.713	14.757	14.959
Fe_2O_3	1.503	1.841	1.706	1.586	1.629	1.622	1.656	3.403	3.397
MnO	0.082	0.086	0.09	0.087	0.085	0.086	0.085	0.07	0.07
MgO	0.072	0.127	0.099	0.059	0.05	0.082	0.065	1.31	1.362
CaO	0.253	0.469	0.331	0.345	0.284	0.276	0.283	2.997	2.988
Na_2O	3.833	3.111	4.342	3.959	3.748	3.777	3.597	4.865	4.849
K_2O	5.094	5.503	4.574	5.028	4.946	5.079	5.305	3.104	3.29
P_2O_5	0.01	0.018	0.008	0.009	0.006	0.006	0.007	0.148	0.154
LOI	2.822	3.997	3.352	2.941	2.697	2.685	2.66	1.461	1.28

Sample	UBT SU IV	20-02	20-04i	20-04	20-08	20-11	20-14	20-20	20-22
Unit	UBT	UBT	UBT	UBT	UBT	UBT	UBT	UBT	UBT
SiO_2	77.926	77.166	77.933	77.809	77.04	78.22	78.418	79.025	77.574
TiO_2	0.081	0.153	0.063	0.056	0.079	0.079	0.084	0.075	0.055
Al_2O_3	12.246	13.081	12.438	12.368	13.193	12.21	12.011	11.918	12.328
Fe_2O_3	1.591	1.641	1.58	1.741	1.533	1.398	1.463	1.183	1.226
MnO	0.05	0.045	0.054	0.057	0.041	0.035	0.04	0.04	0.04
MgO	0.002	0.133	0.077	0.114	0.162	0.27	0.201	0.153	0.186
CaO	0.153	0.328	0.384	0.446	0.325	0.48	0.333	0.33	1.092
Na_2O	3.059	2.822	2.598	2.627	2.944	2.764	2.933	2.768	2.767
K_2O	4.883	4.712	4.86	4.768	4.668	4.526	4.506	4.495	4.716
P_2O_5	0.007	0.019	0.012	0.015	0.015	0.018	0.011	0.013	0.017
LOI	2.89	2.557	2.941	2.484	2.4	2.885	2.399	2.628	4.949

Sample	20-25	20-27	20-31	20-35	20-39	20-40i	20-46	20-51	20-53
Unit	UBT	UBT	UBT	UBT	UBT	UBT	UBT	UBT	UBT
SiO_2	78.297	78.139	75.891	72.916	78.718	78.757	77.994	72.108	78.031
TiO_2	0.068	0.068	0.12	0.283	0.083	0.072	0.07	0.272	0.082
Al_2O_3	12.039	11.743	13.062	13.966	11.773	11.861	11.776	14.753	12.163
Fe_2O_3	1.428	1.343	1.858	2.532	1.408	1.552	1.36	2.829	1.54
MnO	0.041	0.039	0.063	0.049	0.043	0.039	0.052	0.044	0.036
MgO	0.286	0.32	0.405	0.774	0.236	0.101	0.387	1.068	0.346
CaO	0.759	1.071	1.122	2.226	0.31	0.307	0.692	1.802	0.396
Na_2O	2.752	2.877	3.09	3.466	3.149	3.011	3.063	3.278	2.902
K_2O	4.297	4.387	4.36	3.712	4.267	4.285	4.576	3.778	4.479
P_2O_5	0.033	0.013	0.03	0.076	0.013	0.013	0.031	0.069	0.024
LOI	3.489	5.554	3.168	4.122	1.836	3.142	2.689	5.267	3.048

Sample	20-55i	20-56	20-60	20-63	20-67i	20-70	20-73	20-75	27-04
Unit	UBT	UBT	UBT	UBT	UBT	UBT	UBT	UBT	UBT
SiO_2	78.747	79.178	77.822	79.176	78.006	76.151	78.525	76.584	76.982
TiO_2	0.073	0.058	0.081	0.087	0.075	0.078	0.074	0.057	0.052
Al_2O_3	11.608	11.445	11.842	11.467	11.683	11.26	11.464	11.991	12.086
Fe_2O_3	1.41	1.422	1.577	1.481	1.571	1.417	1.34	1.425	1.51
MnO	0.043	0.042	0.038	0.047	0.048	0.046	0.042	0.054	0.081
MgO	0.2	0.151	0.365	0.214	0.382	0.249	0.23	0.354	0.143
CaO	0.663	0.4	0.94	0.406	0.516	0.349	1.134	1.145	0.289
Na_2O	2.696	2.727	2.88	2.767	3.008	2.584	2.736	3.504	4.346
K_2O	4.537	4.55	4.43	4.324	4.39	4.313	4.439	4.865	4.502
P_2O_5	0.023	0.026	0.025	0.03	0.021	0.022	0.017	0.021	0.009
LOI	4.048	3.534	4.217	3.117	3.712	3.307	5.351	3.104	2.404

Sample	27-06i	27-07i	27-09i	27-09	27-10	27-14	27-16	27-18i
Unit	UBT	UBT	UBT	UBT	UBT	UBT	UBT	UBT
SiO_2	77.3	77.407	76.419	76.712	77.288	77.234	76.949	76.976
TiO_2	0.066	0.052	0.05	0.048	0.047	0.045	0.057	0.056
Al_2O_3	11.847	11.755	11.994	11.848	11.874	11.94	11.898	11.992
Fe_2O_3	1.561	1.568	1.554	1.583	1.528	1.515	1.591	1.652
MnO	0.075	0.079	0.085	0.08	0.085	0.086	0.082	0.094
MgO	0.118	0.047	0.108	0.163	0.069	0.084	0.243	0.113
CaO	0.464	0.34	0.649	0.541	0.316	0.378	0.351	0.446
Na2O	4.068	4.24	4.675	4.6	4.341	4.217	4.387	4.125
K2O	4.49	4.5	4.454	4.419	4.445	4.493	4.435	4.535
P2O5	0.009	0.01	0.008	0.006	0.007	0.007	0.006	0.011
LOI	2.942	2.864	5.152	5.624	2.088	2.251	3.088	2.98

Sample	27-23	27-24i	27-25i	27-26Ai	27-28	27-31	27-33
Unit	UBT	UBT	UBT	UBT	UBT	UBT	UBT
SiO_2	76.301	77.01	68.464	68.484	77.159	77.429	76.578
TiO_2	0.06	0.053	0.415	0.421	0.057	0.048	0.066
Al_2O_3	12.031	11.839	14.981	14.72	11.944	11.874	12.269
Fe_2O_3	1.669	1.566	3.382	3.305	1.516	1.461	1.731
MnO	0.077	0.077	0.068	0.08	0.075	0.076	0.082
MgO	0.28	0.026	1.404	1.285	0.202	0.156	0.138
CaO	0.475	0.296	3.293	3.042	0.368	0.281	0.329
Na_2O	3.465	3.331	4.265	4.764	4.235	4.202	3.428
K_2O	5.627	5.773	3.574	3.744	4.438	4.466	5.365
P_2O_5	0.016	0.029	0.153	0.155	0.006	0.006	0.01
LOI	2.396	2.425	2.523	1.832	1.888	2.144	3.66

Appendix 4: Microprobe Analyses of Feldspars

Lower Bandelier Tuff: Alkali Feldspars

Sample	Na_2O	Al_2O_3	SiO_2	K_2O	CaO	BaO	Fe_2O_3	Total
11-14/1 B	6.38	18.94	67.40	6.59	0.10	0.00	0.16	99.64
11-14/2 B	6.32	18.95	67.36	7.04	0.10	0.24	0.16	100.16
11-14/3 B	6.07	19.30	67.60	7.38	0.11	0.08	0.15	100.69
11-14/4 B	7.05	18.89	67.97	5.68	0.12	0.00	0.23	99.95
11-14/5 B	6.45	19.04	66.64	6.86	0.15	0.00	0.16	99.36
11-14/6 B	6.71	19.00	66.59	6.62	0.17	0.00	0.11	99.21
11-14/7 B	6.63	19.17	67.33	6.03	0.15	0.22	0.15	99.70
11-14/8 B	6.48	19.16	67.49	6.22	0.13	0.05	0.16	99.70
11-14/9 B	6.58	19.09	67.90	6.49	0.13	0.07	0.18	100.44
11-14/10 B	6.59	19.17	67.58	6.61	0.13	0.08	0.18	100.34
11-14/11 B	6.57	19.02	67.62	6.41	0.11	0.00	0.14	99.86
average	6.54	18.82	67.36	6.87	0.21	0.03	0.20	100.10
18-13/1a	6.68	19.09	66.53	7.04	0.19	0.09	0.16	99.77
18-13/1b	6.70	18.93	67.52	7.09	0.20	0.00	0.21	100.78
18-13/1c	6.80	18.64	67.93	6.93	0.21	0.00	0.21	100.78
18-13/2a	6.87	18.94	68.21	6.54	0.21	0.00	0.16	100.93
18-13/2b	6.86	19.25	67.76	6.72	0.21	0.29	0.17	101.27
18-13/2c	7.21	19.07	67.04	5.79	0.28	0.06	0.22	99.69
18-13/2d	6.75	18.46	67.36	6.92	0.21	0.00	0.16	99.87
18-13/3a	7.66	19.48	67.84	5.57	0.34	0.07	0.19	101.21
18-13/3b	7.12	19.25	68.27	6.72	0.21	0.07	0.18	101.82
18-13/3c	6.72	18.81	67.25	6.43	0.18	0.00	0.21	99.60
18-13/4a	6.88	18.57	66.32	7.02	0.20	0.09	0.19	99.29
18-13/4b	6.80	18.82	66.77	6.76	0.22	0.13	0.17	99.67
18-13/5a	6.79	19.31	68.05	6.29	0.17	0.21	0.13	100.94
18-13/5b	7.05	19.13	66.51	6.42	0.24	0.00	0.16	99.52
18-13/5c	7.02	19.25	67.79	6.45	0.23	0.18	0.17	101.09
average	6.93	19.00	67.41	6.58	0.22	0.08	0.18	100.41

Sample	Na_2O	Al_2O_3	SiO_2	K_2O	CaO	BaO	Fe_2O_3	Total
17-03/1a	6.51	18.83	67.72	7.31	0.20	0.10	0.15	100.83
17-03/1b	6.56	18.62	67.54	7.27	0.22	0.00	0.18	100.48
17-03/2a	6.69	18.73	66.71	7.14	0.25	0.00	0.16	99.74
17-03/2b	7.12	18.57	65.02	6.52	0.36	0.00	0.15	97.75
17-03/2c	6.93	18.65	67.70	6.87	0.28	0.00	0.18	100.61
17-03/3a	6.76	18.66	67.69	7.11	0.24	0.00	0.19	100.68
17-03/3b	6.81	19.06	67.39	7.14	0.23	0.00	0.19	100.92
17-03/4a	6.78	18.56	67.04	7.45	0.17	0.05	0.20	100.36
17-03/4b	6.5	18.50	67.15	7.64	0.19	0.06	0.14	100.25
17-03/4c	6.59	18.78	67.15	7.31	0.19	0.07	0.18	100.29
17-03/4d	6.33	18.12	66.87	7.71	0.16	0.00	0.16	99.36
17-03/5a	7.18	18.85	66.20	6.4	0.37	0.00	0.19	99.18
17-03/5b	7.16	18.51	66.29	6.74	0.34	0.00	0.13	99.16
17-03/6a	6.63	18.51	67.04	7.50	0.18	0.00	0.17	100.12
17-03/6b	6.70	18.85	66.66	7.04	0.22	0.07	0.16	99.74
17-03/6c	6.66	18.84	65.27	7.38	0.20	0.06	0.22	98.63
17-03/6d	7.32	19.08	64.25	5.89	0.36	0.05	0.14	97.08
17-03/7	6.82	18.56	66.86	6.91	0.25	0.00	0.19	99.59
17-03/8	6.76	19.03	67.38	7.09	0.24	0.05	0.17	100.72
17-03/9	6.93	18.55	67.45	6.61	0.20	0.11	0.21	100.06
17-03/10a	8.60	20.30	64.18	3.24	1.14	0.21	0.17	98.54
17-03/10b	8.73	20.13	65.81	3.19	1.20	0.09	0.18	99.70
average	6.96	18.83	66.61	6.70	0.33	0.04	0.17	99.71

Sample	Na_2O	Al_2O_3	SiO_2	K_2O	CaO	BaO	Fe_2O_3	Total
11- /1	6.77	18.66	67.75	7.17	0.14	0.00	0.17	100.67
11- /2a	6.47	18.46	65.16	6.87	0.09	0.09	0.23	97.55
11- /2b	6.53	18.90	66.74	7.15	0.12	0.09	0.21	99.74
11- /3a	6.70	18.61	67.40	7.17	0.14	0.04	0.16	100.25
11- /3b	6.80	18.82	66.36	6.97	0.15	0.00	0.17	99.27
11- /3c	6.64	18.66	67.21	6.65	0.13	0.00	0.15	99.44
11- /3d	6.69	19.16	66.50	7.07	0.12	0.06	0.21	99.81
11- /3e	6.52	18.49	66.80	7.06	0.12	0.00	0.23	99.23
11- /4a	6.78	18.60	66.84	6.94	0.17	0.05	0.19	99.61
11- /4b	6.82	18.82	67.29	6.98	0.15	0.11	0.23	100.48
11- /5a	6.88	18.63	66.14	6.81	0.17	0.00	0.17	98.80
11- /5b	6.68	18.82	66.55	6.82	0.16	0.00	0.19	99.22
11- /6	6.52	18.84	66.08	6.80	0.15	0.07	0.23	98.69
11- /7a	6.55	18.40	65.71	6.89	0.10	0.00	0.18	97.85
11- /7b	6.59	18.74	66.97	7.21	0.10	0.00	0.20	99.84
11- /8	6.54	18.71	67.20	7.31	0.10	0.02	0.18	100.05
11- /9a	6.52	18.66	66.39	7.17	0.10	0.12	0.23	99.24
11- /9b	6.66	18.74	66.59	7.16	0.11	0.07	0.26	99.60
11- /10	6.52	17.99	67.23	6.61	0.12	0.09	0.21	98.78
11- /11a	6.55	18.66	67.17	7.11	0.10	0.11	0.20	99.89
11- /11b	6.56	18.56	66.74	7.01	0.12	0.00	0.19	99.18
11- /12a	6.36	17.86	66.28	7.04	0.13	0.00	0.21	97.93
11- /12b	6.68	18.49	66.16	7.01	0.10	0.15	0.20	98.80
11- /13a	6.70	18.91	67.38	6.62	0.14	0.18	0.18	100.11
11- /13b	6.61	18.88	67.05	6.64	0.14	0.00	0.27	99.63
11- /13c	6.81	18.68	67.33	6.59	0.16	0.00	0.20	99.78
average	6.63	18.64	66.73	6.96	0.13	0.05	0.20	99.36

Upper Bandelier Tuff: Alkali Feldspars

Sample	Na_2O	Al_2O_3	SiO_2	K_2O	CaO	BaO	Fe_2O_3	Total
UBT high silica rhyolite								
20-4/1	6.38	18.89	67.79	7.41	0.17	0.08	0.19	100.92
20-4/2	6.52	18.95	67.62	7.08	0.16	0.03	0.18	100.59
20-4/3	6.34	18.8	66.86	7.42	0.13	0.00	0.19	99.73
20-4/4a	6.44	18.61	66.30	7.11	0.17	0.05	0.22	98.91
20-4/4b	6.41	18.96	67.04	7.25	0.17	0.08	0.18	100.11
20-4/5	6.37	19.10	68.36	7.22	0.18	0.09	0.18	101.49
20-4/6	6.58	18.91	66.57	7.11	0.19	0.01	0.15	99.52
20-4/7	6.51	19.04	67.01	7.33	0.16	0.00	0.17	100.42
20-4/8	6.34	19.16	68.02	6.85	0.14	0.00	0.14	100.68
20-4/9	6.38	18.47	67.52	7.19	0.22	0.15	0.17	100.09
average	6.43	18.89	67.31	7.20	0.17	0.05	0.18	100.24
20-53/1	6.31	19.15	68.09	7.58	0.23	0.15	0.21	101.73
20-53/2	6.67	19.09	65.01	6.22	0.36	0.09	0.14	97.59
20-53/3	6.73	19.20	67.51	6.60	0.32	0.01	0.16	100.65
20-53/4	6.41	19.02	67.77	6.79	0.19	0.07	0.18	100.46
20-53/5	6.47	19.06	67.64	6.30	0.23	0.00	0.16	99.92
20-53/6	6.85	19.37	67.32	6.52	0.36	0.09	0.14	100.66
20-53/7	6.50	18.92	67.12	6.73	0.23	0.07	0.17	99.76
20-53/8	6.35	18.63	67.07	6.72	0.15	0.09	0.19	99.27
20-53/9	6.27	18.80	66.38	7.08	0.20	0.00	0.18	98.91
20-53/10	6.47	18.95	67.57	7.00	0.23	0.24	0.14	100.73
average	6.50	19.02	67.15	6.75	0.25	0.08	0.17	99.97
grey hb pumice								
27-21/1	8.51	20.47	65.87	3.05	1.09	0.14	0.18	99.89
27-21/1oga	6.71	18.82	67.69	6.77	0.14	0.07	0.18	100.38
27-21/1ogb	6.96	18.83	66.82	6.48	0.16	0.11	0.19	99.54
27-21/4	6.23	17.93	67.68	6.18	0.43	0.05	0.21	98.78
27-21/5	7.09	19.04	68.26	5.98	0.17	0.00		
27-21/6	5.60	17.66	69.09	7.06	0.08	0.00	0.35	99.84
27-21/7	6.84	19.06	68.04	6.36	0.14	0.18	0.17	100.84
27-21/8	6.67	19.71	66.11	5.67	0.75	0.45	0.20	99.66
27-21/9	6.62	18.88	67.39	6.77	0.13	0.12	0.15	100.05
27-21/10	6.88	18.88	66.66	5.93	0.14	0.00	0.21	98.60
27-21/11a	6.84	19.14	66.17	6.05	0.14	0.18	0.20	98.79
27-21/11b	6.50	22.12	65.14	3.82	3.02	0.11	0.19	100.90
27-21/12	7.04	19.08	65.24	5.76	0.19	0.00	0.19	97.59
27-21/13a	6.48	18.64	67.60	6.32	0.32	0.00	0.21	99.57
27-21/13b	6.63	19.10	66.57	6.33	0.16	0.26	0.13	99.22
average	6.77	19.16	66.96	5.90	0.47	0.13	0.19	99.64

Sample	Na_2O	Al_2O_3	SiO_2	K_2O	CaO	BaO	Fe_2O_3	Total
UBT Low silica rhyolite								
20-35/1a	6.50	18.85	66.80	6.76	0.24	0.00	0.19	99.34
20-35/1b	6.48	18.20	66.81	6.88	0.27	0.00	0.13	98.77
20-35/2	6.91	18.99	66.80	6.24	0.30	0.00	0.17	99.49
20-35/3	8.14	20.03	66.64	3.79	1.14	0.28	0.18	100.24
20-35/4	6.75	19.01	66.81	6.54	0.38	0.02	0.19	99.69
20-35/5	7.08	19.18	67.44	5.21	0.62	0.03	0.17	99.74
20-35/6	7.04	18.83	66.55	5.72	0.47	0.11	0.16	99.00
20-35/7	7.15	19.35	66.68	5.85	0.52	0.00	0.18	99.72
20-35/8	6.36	18.90	66.27	6.86	0.23	0.03	0.19	99.08
20-35/9	8.07	20.54	65.21	3.2	1.73	0.47	0.14	99.35
20-35/10	6.15	18.31	67.18	7.53	0.23	0.00	0.18	99.60
20-35/11	7.65	19.80	65.87	4.44	0.85	0.25	0.19	99.05
20-35/12	7.24	19.52	67.48	5.17	0.71	0.13	0.21	100.46
20-35/13	6.54	18.85	67.14	6.05	0.28	0.27	0.23	99.46
average	7.00	19.16	66.69	5.73	0.56	0.11	0.17	99.49
20-51/2	7.22	19.77	67.27	5.24	0.75	0.17	0.17	100.59
20-51/3	6.66	19.17	66.96	6.35	0.34	0.12	0.18	99.78
20-51/4	7.24	19.44	67.54	5.00	0.64	0.15	0.18	100.29
20-51/5	7.15	19.43	67.59	5.19	0.63	0.02	0.25	100.34
20-51/6	6.54	19.12	67.54	6.54	0.27	0.02	0.14	100.16
20-51/7	7.70	20.07	67.21	4.23	0.88	0.15	0.19	100.53
20-51/8	7.77	19.93	66.69	4.03	0.91	0.32	0.17	99.91
20-51/9	7.00	19.66	67.29	5.26	0.47	0.13	0.17	99.97
20-51/10	6.62	19.23	67.34	6.14	0.28	0.04	0.23	99.50
20-51/11	6.24	18.70	66.71	6.84	0.29	0.11	0.21	99.17
20-51/12	7.38	19.78	66.49	4.80	0.80	0.05	0.23	99.56
20-04/9	6.38	18.47	67.52	7.19	0.22	0.15	0.17	100.09
average	6.99	19.40	67.18	5.57	0.54	0.12	0.19	100.03
UBT grey hornblende pumice								
22-69/2	8.07	19.39	66.75	4.26	0.59	0.48	0.18	99.77
22-69/3	8.76	20.72	66.10	2.20	1.89	0.25	0.14	100.13
22-69/4	7.55	19.05	67.41	5.32	0.39	0.22	0.12	100.10
22-69/6	7.81	18.79	66.39	4.10	1.85	0.26	0.16	99.51
22-69/7	8.26	19.34	67.45	4.12	0.63	0.47	0.13	100.46
22-69/8	7.39	18.25	67.03	5.54	0.39	0.29	0.14	99.14
22-69/9	7.56	19.26	67.17	4.73	0.59	0.50	0.08	99.91
22-69/10a	8.86	21.70	64.33	1.15	2.79	0.13	0.21	99.20
22-69/10b	6.45	19.19	66.16	6.52	0.27	1.04	0.15	99.77
22-69/11	7.11	19.00	66.62	5.54	0.61	0.60	0.19	99.78
average	7.78	19.47	66.54	4.35	1.00	0.42	0.15	99.78

Upper Bandelier Tuff: Plagioclases

Sample	Na_2O	Al_2O_3	SiO_2	SrO	K2O	CaO	BaO	Fe_2O_3	Total
UBT grey hornblende pumice									
22-69/5	6.65	25.62	58.07	0.14	0.37	6.84	0.12	0.30	98.10
22-69/1	6.09	26.60	57.60	0.24	0.29	8.66	0.07	0.40	99.95
22-69/1e B	7.73	21.54	63.88	0.13	2.87	3.11	N/A	0.25	99.52
22-69/1c B	6.66	25.78	57.68	0.25	0.34	7.79	N/A	0.29	98.78
22-69/2 B	8.11	21.19	63.68	0.15	1.37	3.34	N/A	0.27	98.10
22-69/3 B	6.98	22.74	61.97	0.14	2.70	4.21	N/A	0.23	98.98
22-69/4a B	9.32	21.61	63.65	0.00	0.94	2.98	N/A	0.20	98.71
22-69/4b B	8.60	19.48	66.20	0.05	3.42	0.80	N/A	0.17	98.72
22-69/5c B	6.45	25.77	56.66	0.33	0.5	7.21	N/A	0.30	97.21
22-69/5e B	6.18	26.30	56.75	0.11	0.28	7.82	N/A	0.31	97.75
22-69/6 B	6.84	25.62	57.87	0.14	0.31	6.82	N/A	0.26	97.86
22-69/7c1 B	5.84	27.25	55.20	0.06	0.19	9.19	N/A	0.30	98.04
22-69/7e1 B	9.34	20.38	64.95	0.01	1.50	1.66	N/A	0.13	97.97
22-69/7e2 B	7.81	18.96	65.98	0.00	4.31	0.50	N/A	0.11	97.67
22-69/7c2 B	5.98	27.01	56.03	0.25	0.25	8.03	N/A	0.32	97.88
22-69/8a B	5.73	27.09	55.34	0.05	0.25	10.18	N/A	0.33	98.98
22-69/8b B	5.90	27.01	55.54	0.05	0.26	9.69	N/A	0.32	98.77
22-69/8c B	5.97	27.16	56.01	0.08	0.26	9.63	N/A	0.32	99.42
22-69/8d B	5.76	27.25	55.30	0.18	0.24	9.74	N/A	0.36	98.82
22-69/8e B	5.77	27.46	55.01	0.15	0.25	9.90	N/A	0.30	98.84
22-69/8f B	5.83	27.46	55.14	0.14	0.27	9.80	N/A	0.38	99.01
22-69/8g B	5.82	26.89	54.97	0.15	0.23	9.73	N/A	0.35	98.14
22-69/8h B	6.18	26.89	56.05	0.19	0.27	9.43	N/A	0.29	99.28
22-69/8i B	6.66	26.07	57.11	0.19	0.28	8.30	N/A	0.25	98.86
22-69/8j B	6.32	26.14	55.69	0.18	0.25	8.72	N/A	0.29	97.58
22-69/8k B	6.41	26.29	57.27	0.18	0.25	8.42	N/A	0.29	99.12
22-69/8L B	6.38	26.98	57.13	0.16	0.26	8.98	N/A	0.25	100.14
22-69/9c B	6.90	25.86	57.96	0.31	0.33	7.55	N/A	0.25	99.17
27-69/9e B	6.75	24.66	59.43	0.13	0.80	6.84	N/A	0.32	98.94
22-69/10c B	6.40	26.80	57.20	0.18	0.27	8.64	N/A	0.25	99.73
22-69/10e B	5.93	27.07	55.76	0.12	0.27	9.45	N/A	0.31	98.91
22-69/11 B	6.24	26.82	56.49	0.13	0.26	8.83	N/A	0.37	99.14
22-69/12 B	6.53	26.67	57.30	0.27	0.30	8.82	N/A	0.45	100.35
22-69/13 B	6.71	26.24	57.33	0.43	0.32	7.96	N/A	0.34	99.35
22-69/14 B	5.53	28.25	54.60	0.08	0.21	10.05	N/A	0.37	99.10
22-69/15c B	6.06	26.65	55.18	0.33	0.29	9.21	N/A	0.37	98.09
22-69/15e B	6.16	27.00	55.51	0.21	0.25	8.86	N/A	0.30	98.30
22-69/16c B	6.00	27.21	55.84	0.17	0.27	9.39	N/A	0.35	99.23
22-69/16e B	6.27	26.61	56.48	0.25	0.33	9.15	N/A	0.27	99.36
22-69/17 B	6.21	26.04	56.71	0.21	0.32	8.77	N/A	0.34	98.60
22-69/18 B	5.56	27.54	54.31	0.27	0.26	10.40	N/A	0.36	98.70
22-69/19c B	5.36	27.47	53.95	0.29	0.24	10.24	N/A	0.37	97.91
22-69/19e B	8.02	20.25	64.64	0.07	3.42	2.00	N/A	0.17	98.56
average	6.56	25.57	57.80	0.17	0.72	7.62	N/A	0.30	98.73

Sample	Na_2O	Al_2O_3	SiO_2	SrO	K_2O	CaO	BaO	Fe_2O_3	Total
UBT ~~high silica rhyolite~~ grey hb pumice									
27-21/1c	5.32	27.59	55.16	0.27	0.27	10.80	N/A	0.41	99.82
27-21/1e	6.45	26.54	57.09	0.32	0.34	8.64	N/A	0.30	99.70
27-21/2c	5.36	28.21	54.55	0.20	0.25	10.40	N/A	0.36	99.34
27-21/2e	6.50	18.51	65.93	0.10	7.09	0.18	N/A	0.14	98.46
27-21/3a	6.27	27.20	56.86	0.25	0.28	9.31	N/A	0.32	100.49
27-21/3b	6.70	19.11	66.21	0.10	6.42	0.64	N/A	0.16	99.33
27-21/4a	6.04	26.99	56.10	0.14	0.31	9.68	N/A	0.43	99.65
27-21/4b	6.03	27.18	56.23	0.25	0.27	9.48	N/A	0.35	99.78
27-21/5c	5.45	27.63	55.27	0.25	0.22	10.19	N/A	0.36	99.35
27-21/5e	5.41	27.79	54.50	0.13	0.27	10.80	N/A	0.37	99.25
27-21/6c	6.18	27.20	56.21	0.31	0.33	9.29	N/A	0.29	99.82
27-21/6e	6.07	18.92	65.79	0.05	7.82	0.16	N/A	0.16	98.96
27-21/7a	5.61	26.07	52.91	0.24	0.26	12.03	N/A	0.52	97.64
27-21/7b	5.70	27.09	55.75	0.23	0.27	10.20	N/A	0.42	99.66
27-21/8c	6.06	27.04	55.85	0.27	0.27	8.90	N/A	0.34	98.73
27-21/8e	5.65	27.34	55.08	0.21	0.25	9.45	N/A	0.32	98.29
27-21/9a	5.79	27.43	55.50	0.30	0.28	9.98	N/A	0.30	99.60
27-21/9b	5.52	27.97	54.95	0.19	0.27	10.11	N/A	0.36	99.36
average	5.90	25.88	57.22	0.21	1.42	8.35	N/A	0.33	99.29
27-25/1	6.94	26.18	58.01	0.15	0.36	7.14	N/A	0.36	99.14
27-25/2	4.98	28.8	54.42	0.19	0.19	9.91	N/A	0.45	98.94
27-25/3	5.05	28.89	53.77	0.12	0.16	9.96	N/A	0.52	98.46
27-25/4	5.04	28.72	54.73	0.17	0.2	10.75	N/A	0.57	100.18
27-25/5	5.76	27.5	55.54	0.25	0.25	9.33	N/A	0.45	99.08
27-25/6	5.97	26.97	56.33	0.33	0.27	8.55	N/A	0.45	98.88
27-25/7	8.17	24.27	61.4	0.17	0.52	5.12	N/A	0.26	99.91
27-25/8	5.33	28.55	54.63	0.21	0.24	9.53	N/A	0.47	98.96
27-25/9	6.28	27	57.37	0.21	0.27	7.89	N/A	0.34	99.37
27-21/9c	5.35	28.02	54.97	0.04	0.25	10.82	N/A	0.34	99.77
average	5.89	27.49	56.12	0.18	0.27	8.90	N/A	0.42	99.27

Sample	Na_2O	Al_2O_3	SiO_2	SrO	K_2O	CaO	BaO	Fe_2O_3	Total
UBT Low silica rhyolite									
20-35/1	8.79	21.25	64.46	0.10	2.32	2.33	N/A	0.11	99.36
20-35/2	5.39	27.65	54.74	0.11	0.26	10.53	N/A	0.43	99.11
20-35/3c	6.71	26.34	58.22	0.24	0.35	7.62	N/A	0.23	99.71
20-35/3e	5.74	27.98	56.22	0.29	0.24	9.31	N/A	0.29	100.07
20-35/4	6.02	27.04	56.42	0.20	0.27	9.27	N/A	0.33	99.53
20-35/5	8.13	20.46	64.28	0.14	3.38	1.62	N/A	0.20	98.20
20-35/6	5.47	27.78	54.84	0.18	0.22	10.05	N/A	0.39	98.92
20-35/7	6.71	26.57	58.54	0.16	0.33	7.68	N/A	0.20	100.18
20-35/8	5.85	27.71	56.38	0.19	0.27	10.05	N/A	0.39	100.84
20-35/9	5.73	27.52	55.96	0.22	0.27	9.25	N/A	0.42	99.35
20-35/10	5.45	28.16	55.66	0.25	0.21	10.85	N/A	0.40	100.98
20-35/11	5.55	28.19	55.20	0.15	0.22	10.38	N/A	0.38	100.07
average	6.30	26.39	57.58	0.19	0.70	8.25	N/A	0.31	99.70
20-51/1c	5.25	28.57	54.80	0.30	0.21	10.59	N/A	0.33	100.06
20-51/1e	5.24	28.26	54.85	0.26	0.21	9.75	N/A	0.48	99.05
20-51/2	5.84	27.70	56.30	0.16	0.25	9.64	N/A	0.32	100.21
20-51/3	6.43	26.94	57.42	0.32	0.33	8.11	N/A	0.29	99.84
20-51/4	6.10	27.26	56.27	0.25	0.26	8.64	N/A	0.35	99.13
20-51/5	6.6	25.99	56.74	0.22	0.32	7.81	N/A	0.2	97.88
20-51/6	6.59	26.46	57.36	0.21	0.29	7.66	N/A	0.21	98.79
20-51/7	6.00	27.39	56.16	0.08	0.26	8.65	N/A	0.43	98.98
20-51/8	6.31	26.95	57.04	0.15	0.30	8.93	N/A	0.35	100.04
20-51/9	9.03	21.81	64.97	0.07	1.56	2.85	N/A	0.25	100.54
20-51/10	5.82	27.94	56.24	0.21	0.25	9.76	N/A	0.37	100.59
20-51/11	8.11	24.76	60.92	0.21	0.43	5.64	N/A	0.17	100.24
20-51/12	8.73	22.47	62.82	0.03	1.16	4.02	N/A	0.23	99.46
20-51/13	5.84	27.99	56.35	0.26	0.26	8.95	N/A	0.32	99.97
20-51/14	7.32	25.79	59.22	0.18	0.46	6.89	N/A	0.36	100.21
average	6.61	26.42	57.83	0.19	0.44	7.86	N/A	0.36	99.66

APPENDIX 5: Theses produced from the grant

Balsley SD (1988) The petrology and geochemistry of the Tshirege Member of the Bandelier Tuff, Jemez Mountains volcanic field, New Mexico, USA. Unpubl. M.S. thesis, Univ. of Texas at Arlington, 158 pp. [partial support]

Duncker KE. (1988) Trace element geochemistry and stable isotope constraints on petrogenesis of Cerros del Rio lavas, Jemez Mountains, New Mexico. Unpubl. MS thesis, Univ. of Texas at Arlington, 109 pp. [partial support]

Skuba CE (1990) Sr, Nd, Pb, and O isotopic constraints on the genesis and evolution of the Bandelier Tuff. Unpubl. MS thesis, Univ. of Texas at Arlington, 98 p.

APPENDIX 6: Publications resulting from the grant

Journal articles

Duncker KE, JA Wolfl, RS Harmon, PT Leat, AP Dickin and RN Thompson (1991) Diverse mantle and crustal components in lavas of the NW Cerros del Rio volcanic field, Rio Grande rift, New Mexico. Contrib. Mineral. Petrol. 108, 331-345.

Self S, JA Wolff, TL Spell, CE Skuba, MM Morrissey (1991) Revisions to the stratigraphy and volcanology of the post-0.5 Ma units and the volcanic section of VC-1 Core Hole, Valles Caldera, New Mexico. J. Geophys. Res. 96, 4107-4116.

Self S, Kircher DE, Wolff JA (1988) The El Cajete Series, Valles Caldera, New Mexico. J Geophys Res 93, 6113-6127

Skuba CE, Wolff JA, Harmon RS (1991) Sr, Nd, Pb and O isotope variations in the Bandelier Tuff. Geology, to be submitted.

Spell TL, TM Harrison, JA Wolff (1990) $^{40}Ar/^{39}Ar$ dating of the Bandelier Tuff and San Diego Canyon ignimbrites, Jemez Mountains, New Mexico: Temporal constraints on magmatic evolution. J. Volcanol. Geotherm. Res. 43, 175-193.

In preparation

Wolff JA and 6 others (in prep) Petrology of the Bandelier Tuffs, I. Differentiation and zonation of the Otowi Member magma. J Petrol.

Self S and ML Sykes (in prep) Deposition of intra-caldera facies of the Bandelier Tuff. J. Geophys. Res.

Abstracts

Balsley, SD, JA Wolff, DC Kuentz, PR Kyle and JN Gardner (1987) The inter-relationship of the Upper and Lower Bandelier Tuffs: evidence from incompatible trace elements. Eos 68, p. 1512.

Duncker KE, JA Wolff, RS Harmon, PT Leat, RN Thompson and WS Baldridge (1987) Stable isotope constraints on the petrogenesis of Cerros del Rio magmas. Eos 68, p. 1532.

Duncker KE, JA Wolff, RS Harmon, PT Leat, RN Thompson, AP Dickin (1989) Diverse mantle and crustal components in lavas of the NW Cerros del Rio volcanic field. Geol Soc Amer abs w progs 21, p.9

Duncker KE, JA Wolff, RS Harmon, PT Leat, RN Thompson, AP Dickin (1989) Mantle and crustal components in mafic to intermediate lavas of the Cerros del Rio volcanic field, Rio Grande Rift, New Mexico. NM Bur Mines Miner Resources Bull 131, p. 77

Duncker, KE, JA Wolff, RS Harmon, PT Leat, RN Thompson and AP Dickin (1989) Mantle and crustal components in mafic to intermediate lavas of the Cerros del Rio volcanic field, Rio Grande rift, New Mexico. IAVCEI mtg, Santa Fe, New Mexico, abstracts.

Self S, JA Wolff, TL Spell TL (1990) Stratigraphic and volcanological significance of the volcanic section of the CSDP VC- 1 core hole, Valles Caldera, New Mexico. Eos 71, p. 1693.

Skuba CE and JA Wolff (1989) Trace element and radiogenic isotope constraints on the genesis and evolution of rhyolitic magmas beneath Valles Caldera. IAVCEI meeting abstracts, Santa Fe, NM.

Skuba CE and JA Wolff JA (1989) Trace element and radiogenic isotope constraints on the genesis and evolution of rhyolitic magmas beneath Valles Caldera. NM Bur Mines Miner Resources Bull 131, p. 245.

Skuba CE, Wolff JA (1990) Sr, Nd, Pb and O isotopic variations in the Bandelier Tuff: Implications for petrogenesis. Geol. Soc. Abst. and Prog. 22-7, p. 243.

Skuba, CE, JA Wolff, and SD Balsley (1989) Trace element evidence for the origin of the Bandelier Tuff and associated rhyolites of the Valles caldera, Jemez Mountains, New Mexico. GSA Abst. Programs 21 (1), p. 41.

Spell TL, TM Harrison and JA Wolff (1989) $^{40}Ar/^{39}Ar$ dating of the Bandelier Tuffs and associated ignimbrites: Constraints on evolution of the Bandelier magma system. Eos 70, p. 1413.

Sykes ML and S Self (1990) Deposition of intracaldera facies of the Bandelier Tuffs, Jemez Mountains, New Mexico, based on data from CSDP drill hole VC-2A. Eos 71, p. 1684.

Wolff JA, K Duncker, Leat, Thompson, Dickin and Harmon (1991) Low-K, Rb, Nd, Ta lavas in the Cerros del Rio volcanic field: Products of Cenozoic regional tectonic history. Geol. Soc. Amer. Abstr. and Progr. 23, p. 107.

Wolff, JA, S Self, PR Kyle and JN Gardner (1987) Petrology of the El Cajete-Battleship Rock-Banco Bonito sequence, Valles Caldera, New Mexico. EOS AGU Fall mtg abst.

END

DATE
FILMED
12/02/93